Photocopy and Use Authorization

Minimum Detectable Concentration of Selenium Isotopes in Soil Using Photon Activation Analysis

by

Leyton Brenner

A thesis
submitted in partial fulfillment
of the requirements for the degree of
Master of Science in the Department of Physics

Idaho State University

Fall 2018

To the Graduate Faculty:

The members of the committee appointed to examine the thesis of Leyton Brenner find it satisfactory and recommend that it be accepted.

Dr. Tony Forest,
Major Advisor

Dr. Dan Dale,
Committee Member

Dr. Robert Fisher,
Graduate Faculty Representative

Dedicated to Ruth Dorothea Maul and Theodore Brenner

Acknowledgements

I would like to thank Dr. Tony Forest, and the rest of the Idaho State University Physics and Math faculty for helping me succeed and constantly pushing me to become a better physicist. I would also like to thank Jeff Burggraff and Kevin Tsai for the encouragement and insight they provided. Finally I would like to thank Ralph and Carolyn Brenner for providing me with the opportunity to study physics at a collegiate level.

Contents

List of Figures

List of Tables

Abbreviations

PAA	**P**hoton **A**ctivation **A**nalysis
HpGe	**H**igh **p**urity **G**ermanium
ADC	**A**nalog **D**igital **C**onverter
CFD	**C**onstant **F**raction **D**iscriminator
SNR	**S**ignal **N**oise **R**atio
MPA	**M**ulti**P**arameter **A**cquisition System
DAQ	**D**ata **A**c**Q**uisition System

Physical Constants

Speed of Light	c	=	$2.997\ 924\ 58 \times 10^{8}$ ms^{-S} (exact)
Half Life of Se-81m	$t_{\frac{1}{2}}^{Se-81m}$	=	57.28 ± 0.02 minutes
Half Life of Se-75	$t_{\frac{1}{2}}^{Se-75}$	=	119.779 ± 0.004 days
Half Life of Ni-57	$t_{\frac{1}{2}}^{Ni-57}$	=	35.60 ± 0.06 hours
Mass of electron	m_e	=	9.11×10^{-31} kg
Plank's Constant	h	=	$6.63 \times 10^{-34} \frac{m^2 kg}{s}$
Classical Electron Radius	r_e	=	2.82×10^{-15} m

Symbols

m_F^{Ni}	mass of front inner nickel foil	g
m_R^{Ni}	mass of rear inner nickel foil	g
M_F^{Ni}	mass of front outer nickel foil	g
M_R^{Ni}	mass of rear outer nickel foil	g
m_o^{Se}	mass of outer selenium	g
m_i^{Se}	mass of inner selenium	g
m_s	mass of soil	g
v_F^{Ni}	volume of front inner nickel foil	cm^3
v_R^{Ni}	volume of rear inner nickel foil	cm^3
V_F^{Ni}	volume of front outer nickel foil	cm^3
V_R^{Ni}	volume of rear outer nickel foil	cm^3
V_o^{Se}	volume of outer selenium	cm^3
V_i^{Se}	volume of inner selenium	cm^3
V_s	Volume of soil	cm^3

Abstract

Photon Activation Analysis (PAA) is a technique used to measure radioactive elemental activities by observing the characteristic gamma decay of a sample of interest post-irradiation and quantify the parent nuclei present in the sample. The photons used to irradiate a sample were produced by accelerating electrons to an energy of 32 MeV at the Idaho Accelerator Center and impinging those electrons onto a tungsten/aluminium converter to create bremsstrahlung radiation. Four soil samples with varying concentrations of selenium by mass were irradiated. The purpose of the experiment was to determine the minimum concentration in which selenium can be accurately identified when embedded in soil. This minimum observable concentration was measured in terms of the signal to noise ratios of two daughter nuclei (Se-81m and Se-75). The detection limit of selenium in soil using PAA will be reported.

Minimum Detectable Concentration of Selenium Isotopes in Soil Using Photon Activation Analysis

Thesis Abstract–Idaho State University (2018)

Key Words: Photon Activation Analysis (PAA), detection limit, selenium

Chapter 1

Introduction

Photon Activation Analysis (PAA) exploits nuclear reactions to identify the isotopes within a sample. If the isotope of interest is embedded in some matrix, then a natural question arises: "What concentration of the isotope must be present within the matrix to detect it?". The answer can be quantified by studying the signal to noise ratio of characteristic gamma decay lines of the activation products of interest. The signal to noise ratio is defined as the number of background subtracted counts divided by the background. Plots of this ratio against the total concentration of selenium were constructed and fit with a line. The expectation is that the signal should be zero when the total concentration of selenium is zero within the soil sample. The uncertainty in the y-intercept of the above fit was used to define a detection limit. A concentration corresponding to a signal to noise ratio that is increased by twice the error in the y-intercept represents the minimum detectable concentration.

The purpose of this experiment was to quantify the minimum detectable concentrations of selenium in soil. Se-82 and Se-76 are naturally occurring isotopes with abundances of 8.73% and 9.37% respectively. Using high energy photons to eject a neutron from either isotope leaves the isotope in an excited state that will eventually de-excite by emitting characteristic gamma radiation that can be detected by a High Purity germanium (HpGe) detector. The goal of this work is to determine if the minimum detectable concentration of selenium in soil.

Chapter 2

Theory

Photon activation analysis (PAA) is a method used to determine the elemental composition of a sample based on the characteristic photon energies emitted by gamma decays from the nucleus of radioactive isotopes that have been activated by bremsstrahlung photons or their β delayed daughter nuclei. Bremsstrahlung photons are produced with sufficient energy to free nucleons from the target nuclei in the sample of interest. The resulting nucleus tends to be in an excited state after the interaction. Photons with characteristic energies corresponding to the nucleus are emitted when the nucleus de-excites. The energy of these photons can be measured using a high purity germanium (HpGe) detector. Isotopes of interest are uniquely identified by measuring the decay rates of their characteristic energy lines over time and comparing them to their expected values. A theoretical description of each of the above steps is given below.

2.1 Bremsstrahlung Radiation

A charged particle emits bremsstrahlung (braking radiation) if it decelerates due to its interaction with the electric field of an atom in a material. Consider an electron from an accelerator that has travelled into a tungsten/aluminium radiator. As the electron travels, there is a probability that it will be deflected by the electric field of either electrons or nuclei within the material and emit a photon. The cross section for the nuclear process is given by the Bethe-Heitler equation [1]:

$$d\sigma_{Brem} = 4Z^2 r_e^2 \frac{d\nu}{\nu}[(1+(\frac{E}{E_0})^2)[\frac{\phi_1(\gamma)}{4}-\frac{1}{3}\ln Z - f(Z)] - \frac{2E}{3E_0}[\frac{\phi_2(\gamma)}{4}-\frac{1}{3}\ln Z - f(Z)]]$$

where

E_0 = initial energy of the electron

E = final energy of the electron

$\nu = \frac{E_0 - E}{h}$ = energy of the bremsstrahlung photon

Z = number of protons in the target material

$\gamma = \frac{100 m_e c^2 h\nu}{E_0 E Z^{\frac{1}{3}}}$

$f(Z) = (Z\alpha)^2 \Sigma_1^\infty \frac{1}{n[n^2 + (Z\alpha)^2]}$

It is important to note that $\phi_1(\gamma)$ and $\phi_2(\gamma)$ are screening functions that change based on the value of Z. Including the case where the incident electron is deflected by another electron, the cross section for the Bethe-Heitler formula becomes

$$d\sigma_{e^-} = \frac{Z(Z+1)}{Z^2} d\sigma_{Brem}$$

2.2 Minimum Neutron Knockout Energy in Selenium

Determining the most efficient irradiation of a target sample for PAA relies on knowing both the minimum nucleon knockout energy of the isotope of interest and the cross section for the reaction. The cross section expresses the probability of liberating a nucleon from the target. If a photon has insufficient energy to liberate a nucleon from a target, then the nucleus could still be put in an excited state, but this experiment focused on neutron removal. Both the incident photon energy and the cross section of the reaction of interest are used to determine the optimal irradiation conditions for the sample.

There are three important aspects for the efficient irradiation by the bremsstrahlung photons that escape the accelerator's radiator. The photons must have sufficient energy to overcome the binding energy and liberate nucleons from within the target. The energy of the photons impinging upon the target must also include as much of the cross section as possible to increase the probability of the reaction occurring. Finally, saturation requires 5 half lives worth of irradiation time. The samples in this experiment were not saturated, which means the production rate of the daughter nucleus of interest and its decay rate are approximately equal.

The minimum photon energy that may induce the nuclear reactions of interest is calculated using the binding energy of a nucleus. In this case, the reactions of interest are ${}^{76}_{34}Se(\gamma,n){}^{75}_{34}Se$ and ${}^{82}_{34}Se(\gamma,n){}^{81}_{34}Se$. The minimum neutron knockout energy for both reactions can be found by

$$E^{neutron}_{knockout} = |M_{Se76} - M_{Se75} - M_n| = |70718.2992 - 69789.8882 - 939.57| = 11.2MeV$$

$$E^{neutron}_{knockout} = |M_{Se82} - M_{Se81} - M_n| = |76304.9218 - 75374.6322 - 939.57| = 9.3MeV$$

Both reactions can be studied if the bremsstrahlung photon energy is at least 11.2 MeV.

Another important aspect to take into consideration when choosing the beam energy is the cross section for the specific reactions [2][3].

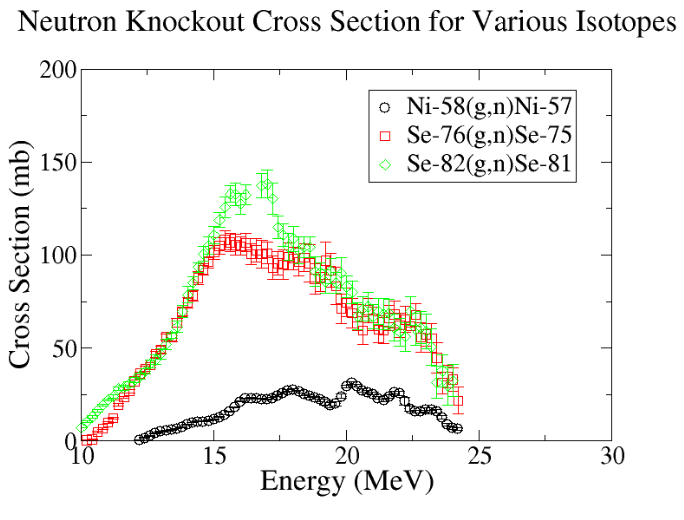

FIGURE 2.1: Neutron knockout cross section for selenium isotopes and nickel used in this work.

The maximum value of the cross section occurs between 15 MeV and 20 MeV.

This means that photons in that energy range will have the highest probability of liberating a neutron from a selenium nucleus.

The differential number of activated nuclei produced as a function of time ($\frac{dN}{dt}$) is given by [4]

$$\frac{dN}{dt} = N^{+} - \lambda N(t) \tag{2.1}$$

$$N(t) = \frac{N^{+}}{\lambda}(1 - e^{-\lambda t}) \tag{2.2}$$

where the production rate, N^{+}, is given by

$$N^{+} = n_T V_T \int \sigma(E)\phi(E)dE \tag{2.3}$$

Where n_T is the number of nucleons per unit volume within the target, V_T is the volume of the target, $\sigma(E)$ is the reaction cross section, $\phi(E)$ is the photon flux through the target, dE represents the energy range in which the cross section is non-zero, and λ is the decay constant for the isotope ($\ln 2/t_{1/2}$). The dependence of this equation on the half life means the net production will be lower for the isotopes of interest for this experiment (due to their similar cross sections, flux values, and natural abundances) with shorter half lives because the isotopes with longer half lives will not reach saturation as quickly, meaning the levelling off of the capacitive production rate curve would take longer to become apparent. Due to the large difference in half lives (57.28 minutes for Se-81m and 120 days for Se-75), the net production will be higher for Se-75 than Se-81m if they are irradiated at the same time.

2.3 HpGe Detector Physics

The class of detectors used to measure photon energies with high resolution are high purity germanium (HpGe) detectors. Germanium is a semiconductor, thus current flows if electrons are moved from the valence band to the conduction band. Unfortunately the "band gap" for germanium is such that, at room temperature, thermal excitations can move electrons from the valence band into the conduction band, creating a high amount of noise that could potentially make a signal ambiguous. The band gap energy in a material is given by

$$E_g(T) = E_g(0) - \frac{\alpha T^2}{T + \beta}$$

where $\alpha = \frac{\sqrt{2m(V_0 - E)}}{\hbar}$ and $\beta = \frac{\sqrt{2mE}}{\hbar}$ [5] . It is clear that as the temperature decreases, the band gap energy increases. The large amount of noise at room temperature can be remedied by cryogenically cooling the detector thereby increasing the band gap energy. This makes a signal produced by an incoming photon very obvious in the detector. A high voltage is applied across the semiconductor to accelerate electron-hole pairs to opposite sides of the semiconductor and increase the depletion region improving detection efficiency.

There are three main types of interactions that can create a signal within the detector. The first interaction is the photoelectric effect. This means that the incoming radiation has sufficient energy to liberate an electron within the material creating an electron-hole pair. The electric field created by the applied high voltage will drift the electrons to one terminal and the holes to another producing a signal.

The second type of interaction that can occur is Compton scattering in which a photon scatters off of an electron losing energy. For the photon's remaining energy to contribute to a signal that is proportional to the original energy of the incoming photon, all Compton scattering events must occur inside the sensitive volume of the detector and subsequently liberate an electron via the photoelectric effect. This ensures that all of the energy of the incoming photon has been measured by the detector. It is possible that the radiated photon from the decay process Compton scatters depositing a fraction of its energy inside the sensitive volume of the detector. If this happens then the detected signal does not accurately represent the total energy of the radiated photon, but instead will contribute to the Compton continuum. Inspecting the Compton scattering formula for the energy of the outgoing photon, it can be seen that there is a maximum energy that the photon can deposit.

$$E' = \frac{E}{1 + \frac{E}{m_e c^2}(1 - \cos\theta)}$$

where

E' is the final energy of the photon

E is the initial energy of the photon

θ is the deflection angle for the photon

It can be seen that the maximum energy loss occurs when the photon backscatters off of the electron ($\theta = 180°$), resulting in a Compton edge. An example of the Compton edge from a 1.1 MeV photon is shown in Figure 2.3.

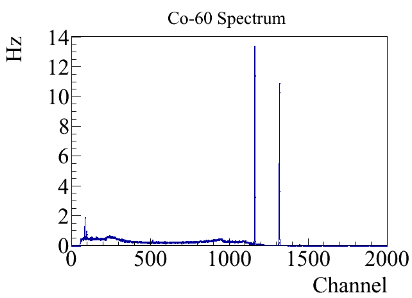

FIGURE 2.2: Co-60 spectrum.

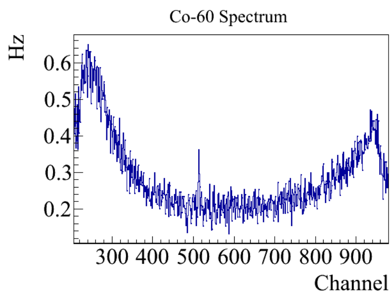

FIGURE 2.3: Compton continuum ranging from 294-906 keV.

The final interaction that can occur is pair production. If the incident photon has high enough energy (1.02 MeV), then the photon can fluctuate into an electron-positron pair. These can produce pulses within the detector. The size of the pulse is proportional to the energy of the electron and the positron. If the positron annihilates with an electron within the semiconductor, then two 511 keV photons are produced that can also create signals within the detector as outlined above.

Once the signals are produced, they are sent through a pre-amplifier, located close to the semiconductor, and then a post amplifier with two analog outputs. One is sent to a constant fraction discriminator (CFD), while the other signal is sent to an analog-to-digital converter (ADC) which converts the analog signal from the HpGe detector into a channel number. A sample histogram is shown in Figure 2.4

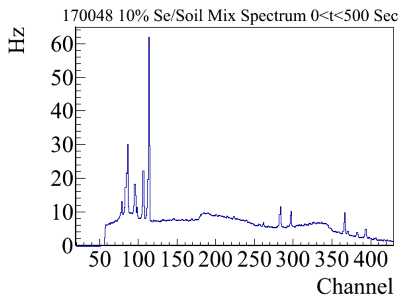

FIGURE 2.4: Sample energy spectrum.

It is easy to see that there could be lines produced by the selenium radioisotopes with competing energy lines produced by the matrix the selenium was embedded in, or from other radioactive materials within the lab.

2.4 Identifying Isotopes of Interest in a Gamma Spectrum

Identifying energy lines characteristic of an isotope of interest and measuring the decay rate of those energy lines to calculate a half life are the two steps taken to identify an isotope of interest. Isotopes can have several characteristic gamma decay lines. Consider an isotope of interest that has three prominent decay lines. If all of those lines are present in the spectrum, then that would be some indication that the isotope of interest may be in the sample. The more characteristic decay lines an isotope has, the easier it is to infer that it may be present in the sample. If an isotope of interest only has one characteristic decay line, then that could increase the chances for a false positive. Unfortunately, the presence of energy lines alone are not enough information to prove the observed energy lines were produced by the isotope of interest.

To strengthen the argument further, the lifetime of the energy line of interest is measured. The activity (A) of decaying isotopes will follow the standard radioactive decay equation

$$A(t) = A_0 e^{-\lambda t}$$

where λ is the decay constant for the isotope and t is the time that has passed since the irradiation. The decay constant is related to the half life via

$$\lambda = \frac{\ln 2}{t_{\frac{1}{2}}}. \tag{2.4}$$

By measuring the activity and plotting it as a function of time, the decay constant, and thus the half life can be found. A sample nickel decay curve which has been fitted with a line is shown in Figure 2.5.

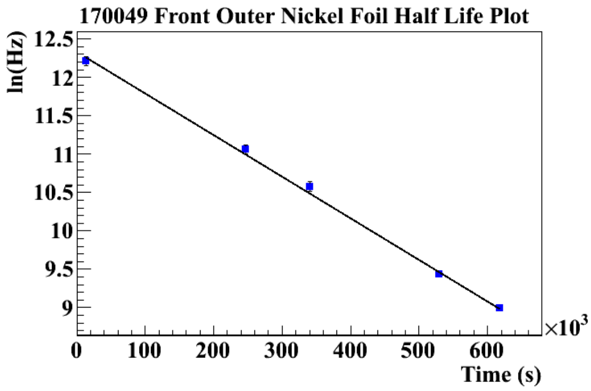

FIGURE 2.5: Example of a decaying Ni-57 1337 keV energy line with a half life of 35.60 hours.

It can be seen that the activity will decrease as time goes on due to decay. If both the characteristic energy lines of the isotopes and the half life are in agreement with the attributes of the isotope of interest, then the argument vastly strengthens as there aren't many isotopes with both similar half lives and energies. Usually these two pieces of information are sufficient to identify an isotope of interest within the irradiated sample. The argument may be strengthened further, for isotopes with several lines, by quantifying the branching ratios for the different energy lines. The activity of the energy lines should match the branching ratio, but an accurate measurement of the detector efficiency needs to be taken for each energy line.

2.5 Signal to Noise Ratio

The previous sections discussed how to produce and identify isotopes of interest within a certain sample, but these steps do not ensure that characteristic energy lines will be visible at all. One problem that may arise is the background signal from the matrix could be much more prominent than the characteristic energy lines of interest. If this is the case, then the signals will not be visible for data analysis. The signal to noise ratio is a quantity that may be used to quantify the minimum detectable concentration of selenium in soil. Irradiating the selenium and the soil in the same container and measuring them as a single target begs the question: "At what concentration of selenium in soil will the characteristic energy lines of selenium not be visible?". The signal to noise ratio (SNR) is given by

$$SNR = |\frac{I - B}{B}| \tag{2.5}$$

The signal to noise ratio can be plotted as a function of concentration to determine the concentration that corresponds to the ratio which is two standard deviations above the y-intercept, making the signal minimally measurable. It can also be plotted for a single measurement as a function of time to see how the background matrix signal decays during the measurement. This can be used to investigate an optimum measurement time delay after the beam has been turned off to determine an optimal time to measure.

Chapter 3

Experimental Setup

3.1 Target Information

On May 23, 2017 four targets were irradiated using 32 MeV electrons impinging on a 25.4 mm thick radiator. Aluminium cylinders were used to contain the samples. The cylinder had a 4.5 cm diameter, a height of 12 cm, and a thickness of 1 mm. The beam conditions were set to a pulse repitition frequency of 180Hz, a pulse width of 2.2 μs, and an average current of 0.15 μA. Figure 3.1 is a schematic of the sample configuration, while Figure 3.2 is a schematic of the tungsten/aluminium converter.

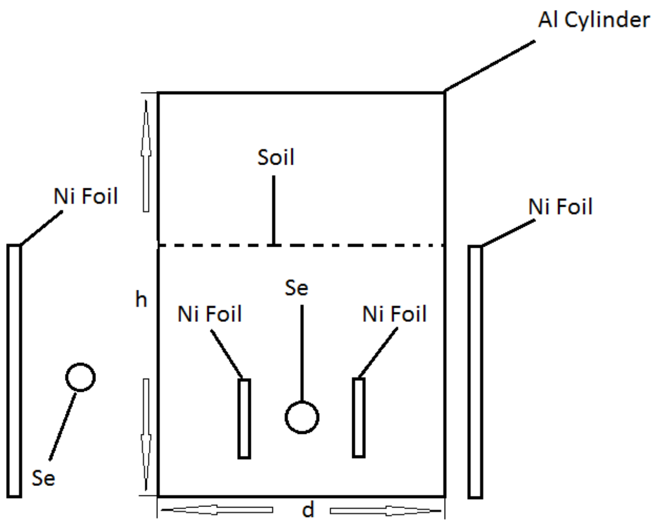

FIGURE 3.1: Target schematic, d = 4.5 cm, h = 12 cm, 1 mm thick.

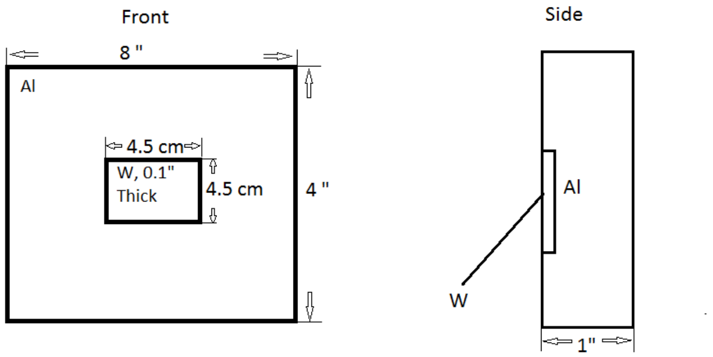

FIGURE 3.2: Schematic of tungsten/aluminium converter.

% Concentration of Se doping by Mass	Beam On	Beam Off	$\Delta t_{Measure}$ (s)
50%	08:47	09:19	1476
10%	09:55	10:55	1504
1%	11:07	12:07	1214
0.1%	16:09	16:39	2037

TABLE 3.1: Beam times for each sample.

Sample	m_s	m_i^{Se}	m_o^{Se}	M_F^{Ni}	M_R^{Ni}	m_F^{Ni}	m_R^{Ni}
50%	0.4921	0.5145	0.0900	1.5535	1.6140	0.3956	0.3050
10%	4.9921	0.5142	0.1245	1.3310	1.2196	0.3592	0.2768
1%	10.2403	0.0954	0.0914	3.4274	3.4887	1.8672	1.7220
0.1%	100.1242	0.1074	0.1042	1.3911	1.3804	0.4467	0.2548

TABLE 3.2: Masses of target components in grams, each mass has a reading error of 5 $\times 10^{-4}$ g. m_s = soil mass, m_i^{Se} = inner Se mass, m_o^{Se} = outer Se mass, M_F^{Ni} = mass of front outer foil, M_R^{Ni} = mass of rear outer foil, m_F^{Ni} = front inner foil mass, m_R^{Ni} = mass of rear inner foil.

Sample	V_s	V_i^{Se}	V_o^{Se}	V_F^{Ni}
50%	0.57 ± 0.1%	0.11 ± 0.09%	0.02 ± 0.52%	0.20 ± 0.03%
10%	5.82 ± 0.01%	0.11 ± 0.09%	0.03 ± 0.35%	0.17 ± 0.03%
1%	11.94 ± 0.01 %	0.02 ± 0.52%	0.02 ± 0.35%	0.44 ± 0.01%
0.1%	116.79 ± 0.01 %	0.02 ± 0.52%	0.02 ± 0.35%	0.18 ± 0.03%

Sample	V_R^{Ni}	v_F^{Ni}	v_R^{Ni}
50%	0.21 ± 0.03%	0.05 ± 0.11%	0.04 ± 0.14%
10%	0.16 ± 0.04%	0.05 ± 0.11%	0.04 ± 0.14%
1%	0.45 ± 0.01%	0.24 ± 0.02%	0.22 ± 0.03%
0.1%	0.18 ± 0.03%	0.06 ± 0.09%	0.03 ± 0.19%

TABLE 3.3: Volumes of target components in cubic centimeters, V_s = soil volume, V_i^{Se} = inner Se volume, V_o^{Se} = outer Se volume, V_F^{Ni} = volume of front outer foil, V_R^{Ni} = volume of rear outer foil, v_F^{Ni} = volume of front inner foil, v_R^{Ni} = volume of rear inner foil.

3.2 Data Acquisition System

Signals produced by photons from the radioactive target which travelled into the sensitive volume of the HpGe detector (as outlined in Section 1.3) were sent through a series of electronic units commonly referred to as a data acquisition system (DAQ). Specifically, after the signal was produced it was amplified by a pre-amplifier within the HpGe detector. The final two pieces of the DAQ were an ORTEC model 672 spectroscopy amplifier and a Canberra model 8701 peak sensing analog to digital converter (ADC) with an internal constant fraction discriminator (CFD). The high voltage source used was an ORTEC 659 5 kV power supply set to 4.5 kV in a reverse bias.

The constant fraction discriminator's purpose was to filter unwanted signals created within the HpGe detector's sensitive volume. The CFD duplicated the analog signal, inverted it, and scaled it by a constant value. Once this has been done the duplicate signal is time-delayed by an amount of time that is less than the rise time of the analog signal. The CFD then searched for a zero crossing point. If such a point was found then the signal was allowed to pass through the CFD. If not, then the signal was rejected. For the purpose of this experiment the lower limit setting resulted in measurements of 40 keV photons or lower being rejected.

The peak sensing analog to digital converter is a Wilkinson apparatus which operates by opening a gate for a select amount of time. While the gate is open, the conversion takes place. Assuming the gate is open, the analog pulse is sent through a differentiating circuit, which has an output proportional to the rate of change of the signal. Once the circuit finds a maximum, the voltage is held constant by a capacitor. If a larger signal were to appear while the gate was still open, then the capacitor would maintain the larger voltage as opposed to the smaller one. A comparitor was used to decide if a higher voltage appeared while the gate was open. After the gate closes, the capacitor discharges and voltage information is assigned a unique numerical channel.

Chapter 4

Data Analysis

4.1 Split Run Measurement Technique

The measured activity of a sample and its normalization target (outer witness Se pellet) were stored in the same data file along with a calibration source used as a marker to separate the measurements. Each sample was measured at the same position from the detector by switching samples after five minutes. This allows multiple measured samples to be written to the same file. Calibrated sources were used as a marker to indicate a change in the sample being measured by the HpGe detector. Several samples were measured during a single Multiparameter Data Acquisition System (MPA) run.

It is very important that the marker's energy spectrum be clearly distinguishable from the sample's energy spectrum. A Co-60 source was used as a marker because it has very strong energy lines at 1.173 MeV and 1.332 MeV, whereas the selenium/soil samples had no strong energy lines greater than 1 MeV. After a five minute measurement, the first sample was removed and the Co-60 flag was placed in front of the HpGe detector for one minute. This ensured that the signal produced by the flag was strong enough to adequately separate the runs. After the one minute measurement using the Co-60 flag, it was removed and the second selenium sample was placed in front of the detector and measured for five minutes. This process was repeated for the length of the entire run. It can be quite cumbersome to record all of the transition times while switching the samples, but this can be remedied by plotting the channel number vs. time on a 2D histogram as shown in Figure 4.1.

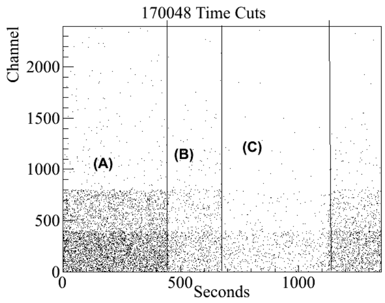

FIGURE 4.1: Sample split run where (A) is the Se/-soil Mix, (B) is the Co-60 marker, and (C) is the pure selenium.

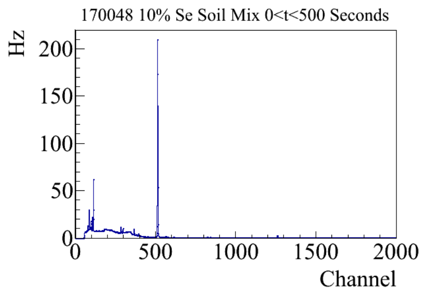

FIGURE 4.2: (A) Se/soil mixture for 0<t<500 s.

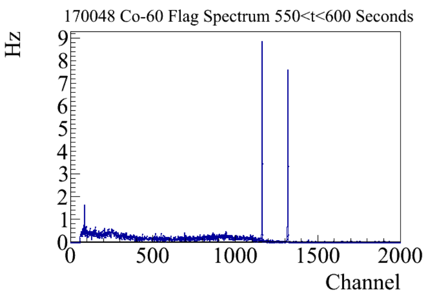

FIGURE 4.3: (B) Co-60 flag 550 <t<600 s.

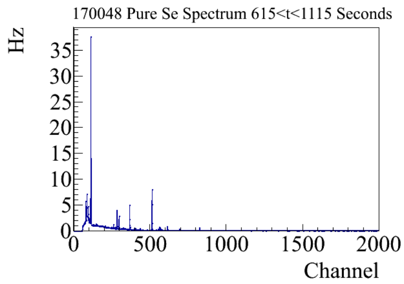

FIGURE 4.4: (C) Pure Se 615<t<1115 s.

Note the different runs are distinct and can be identified as long as one measurement is known. The larger peaks in Figure 4.3 are from the Co-60's 1.173 and 1.332 MeV lines.

4.2 Energy Spectrum Analysis Method

A detailed explanation of how to trace the isotope of interest's activity back to its original value is given below. The sample of interest here is #170048, which was a soil sample that had selenium added to the soil such that the mass of the added selenium was equal to 10% of the soil's mass. The measurement of the irradiated sample was made using Detector A at the Idaho Accelerator Center. A full description of Detector A is given in Appendix A. The measurement was a split run using a Co-60 flag to identify the change between a pure selenium sample and the Se/soil mixture. The target masses can be found below:

Soil	Mixed Se	Outer Se	Front Ni Foil	Rear Ni Foil
4.9921 g	0.5142 g	0.1245 g	1.3310 g	1.2196 g

4.2.1 Multi-Channel Histograms

"Multi-Channel Histograms" were named such because the analysis was performed in a one, three, or ten channel spectrum window. Each histogram had its number of counts weighted by the mass of the sample. Since the resolution of Detector A is about 1 keV, the window in which the signal is viewed can't be less than 1 keV. The function used to fit the energy lines was of the form

$$f(x) = C_1 + C_2 e^{\frac{(x-\overline{x})^2}{2\sigma^2}} \tag{4.1}$$

Here, the constant value (C_1) added to the Gaussian measures the value for the background that will be subtracted. Figure 4.5 shows typical "multi-channel" histogram cuts that were made for Sample #170048.

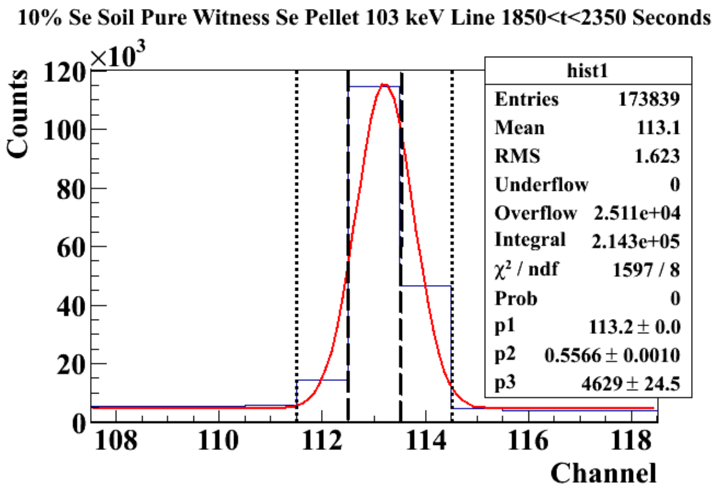

FIGURE 4.5: #170048 Pure Se witness pellet histogram with cuts representing a 3 channel (finer dots) window and a 1 channel window (coarser lines).

Channel 113 in Figure 4.5 is the value that corresponds to the 103 keV line of Se-81m once the calibration is applied. By looking at the statistics box in the desired window, the total number of counts can be found by the line labeled

"Integral". The intrinsic error in the signal was found by expanding the channel axis by half of the standard deviation of the fit on each side to see how the number of counts varied as the size of the window was varied. The purpose of the expansion was to see how inclusion of more channels affected the final result. Unfortunately in this situation the energy resolution is too small, so the window can only be expanded by one on both sides. The systematic error in the signal can be estimated by

$$e_I = |I_{Expanded} - I| \tag{4.2}$$

while the statistical error is given by

$$\sigma_I = \sqrt{I} \tag{4.3}$$

4.2.2 Background Subtraction

In the statistics box, the value labeled "background" corresponds to the constant value from Eq. 4.1 in the fitting function (C_1). To remove the background from the number of counts in the statistics box, the constant value must be integrated across the window of interest. In this case

$$Background = B = \int_{113}^{115} C_1 d(Chan) = nC_1 \tag{4.4}$$

where n is the width of the window (one, three, or ten). Since this reduces to multiplying the statistics box background value by a constant, the error can also be found by multiplying it by the same constant. In other words

$$\sigma_B = n\sigma_{C_1} \tag{4.5}$$

Now that the value for the signal and the background have been found, they can be subtracted from one another.

$$N = I - B \tag{4.6}$$

$$\sigma_N = \sqrt{I + \sigma_B^2} \tag{4.7}$$

This value can be divided by the runtime (t) of the measurement to find the activity.

$$A_{Measured} = \frac{N}{t} \tag{4.8}$$

Since the time interval for these measurements was recorded using a 20MHz clock, the error in the time is negligible compared to the error in the signal so it was not accounted for in this analysis. This means the error in the activity can be found by

$$\sigma_{A_{Measured}} = \frac{\sigma_N}{t} \tag{4.9}$$

4.2.3 Decay During Measurements

It is worth noting that the half life for Se-81 is rather short (57.28 min). For a 5 minute measurement, the activity decreases by

$$A(t) = A_0 e^{-\lambda_{Se-81m} 300} = 0.94 A_0. \tag{4.10}$$

The activity decreases by roughly 6% during the measurement. To remedy this, one can use the fact that the measurement being made is actually integrating the true value of the activity over the time of the measurement. In other words

$$A_{Measure} = \frac{\int_0^t A_{True} e^{-\lambda t} dt}{t} \tag{4.11}$$

By integrating this function and solving for the activity, the integral decay corrected activity can be found to be

$$A_{True} = \frac{e^{\lambda t} A_{Measure} t\lambda}{e^{\lambda t} - 1}. \tag{4.12}$$

The error can be found through standard error propagation methods to be

$$\sigma_{A_{True}} = \sqrt{\left(\frac{\lambda t e^{\lambda t} \sigma_{A_{Measured}}}{e^{\lambda t} - 1}\right)^2 + \left(\frac{A_{Measured} t e^{\lambda t}(e^{\lambda t} - 1 - t\lambda)}{(e^{\lambda t} - 1)^2}\right)^2 \sigma_\lambda^2}. \tag{4.13}$$

4.2.4 Dead Time

The fractional dead time is used to estimate the number of counts that may have been lost because the DAQ system was too busy recording the previous event. A count rate vs. the percent dead time plot is shown below:

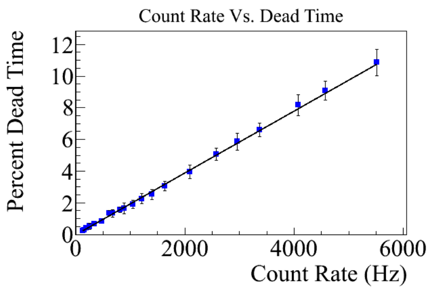

FIGURE 4.6: Detector A percent dead time, %D.T. = $(0.01 \pm 0.05) + (2.0 \pm 0.1) \times$(count rate).

To account for the fractional dead time, the total number of entries in the histogram was divided by the run time to get an average count rate. The plot was used to estimate the fractional dead time. Once the fractional dead time has been estimated, the correction is

$$A_{DTC} = \frac{A_{True}}{1 - DT} \tag{4.14}$$

Where DT is the fractional dead time of the measurement. The error is given by

$$\sigma_{A_{DTC}} = \sqrt{\left(\frac{A_{True}\sigma_{DT}}{(1-DT)^2}\right)^2 + \left(\frac{\sigma_{A_{True}}}{(1-DT)}\right)^2} \tag{4.15}$$

4.2.5 Efficiency Corrections

The HpGe detector has two types of efficiency: geometric and energy. Mathematically, the efficiency corrections can be made by dividing A_{DTC} by the efficiency (ϵ).

$$A_\epsilon = \frac{A_{DTC}}{\epsilon} \tag{4.16}$$

$$\sigma_{A_\epsilon} = A_\epsilon \sqrt{\left(\frac{\sigma_{A_{DTC}}}{A_{DTC}}\right)^2 + \left(\frac{\sigma_\epsilon}{\epsilon}\right)^2} \tag{4.17}$$

4.2.6 Consistency Check

In order to ensure the calculations outlined above were applied correctly, measured activities were corrected back to the time of the previous post-irradiation activity measurement using the known half life. Once all the corrections have been made, the radioactive decay equation was used to trace the rate back to the previous measurement. For example, consider a measurement taken 500 seconds after the first measurement of the sample is taken. After the corrections have been made, the signal was corrected back using a 500 second decay time and compared to the previous activity measurement.

$$A_{TC} = A_\epsilon e^{\lambda t} \tag{4.18}$$

$$\sigma_{A_{TC}} = \sqrt{\sigma_{A_\epsilon}^2 e^{2\lambda t} + \sigma_\lambda^2 A_\epsilon^2 t^2 e^{2\lambda t}} \tag{4.19}$$

Finally, the ratio of the first measurement and the time corrected measurement was taken to see if this number statistically agrees with unity.

4.2.7 Multi-Channel Method Applied

The multi-channel window method was applied in an attempt to trace the rate of the second and third measurements of the pure selenium sample #170048-001 back to the first measurement to determine if they are in agreement with each other. The calculations outlined above were used to create Figure 4.7. It was shown that the second and third measured values for the activity of the 103 keV line were in agreement with the initial activity measurement. The experimental half life was found by plotting the efficiency corrected data and using a fit of the form

$$A(t) = e^{\ln A_{\epsilon 0} - \lambda t} \tag{4.20}$$

Note that A_{ϵ_0} is the activity at the beginning of the measurement. This can be corrected back to t_{Off}^{Beam} using equations 4.18 and 4.19.

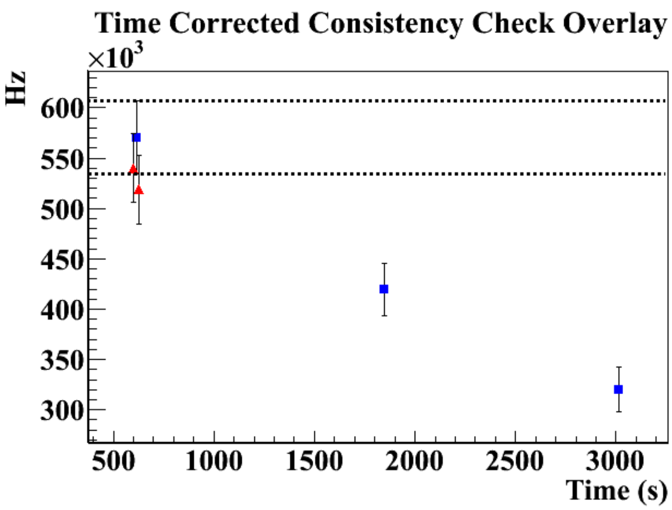

FIGURE 4.7: Overlay of the time corrected data (triangles) for the 10% pure selenium witness pellet's activity with the efficiency corrected data (squares).

4.3 Signal to Noise Ratio Calculations

The signal to noise ratio was determined using three steps. The first step was to determine a normalization constant that would re-scale each pure selenium witness pellet's specific activity, a_{Pure}, to a weighted average. The second step was to determine the linear dependence of the Se/soil mixtures' activity (A_{Mix}), normalized by the specific activity of the pure selenium witness pellets ($\frac{A_{Mix}}{a_{Pure}}$), with the concentration by mass of spikant. The resulting line used for the fitting function did not have an x-intercept of zero indicating that selenium was present in the sample prior to adding the spikant. An offset, representing the amount of this selenium present in the sample prior to addition of the selenium spikant, was added so the figure would indicate an activity of zero when no selenium in present in the sample. Finally the signal to noise ratio, $\frac{N}{B}$, was plotted as a function of the amount of Se spikant added plus the initial amount of selenium that was present in the soil to begin with in Figures 4.10 and 4.11. The minimum detectable limit was defined as being the selenium concentration that is two standard deviations above the y-intercepts in Figures 4.12 and 4.13.

The first step in the analysis was to find a normalization constant to make the specific activity of the pure witness selenium pellets the same. The specific activity, $a_{Pure}(\frac{Hz}{g})$, should be constant for samples with different spikant concentrations that received the same radiation exposure. Since this was not the case, a weighted average of the pure selenium witness pellets' specific activity was taken and used as the specific activity for all witness pellets to account for the differences in dose. The normalization factors are shown in Tables 4.1 and 4.2.

Sample	Uncorrected $a_{Pure}(\frac{Hz}{g})$	Normalization Factor	Corrected $\frac{A_Mix}{a_{Pure}}$ (g)
10%	6200 ± 190	0.25 ± 0.01	1.4 ± 0.08
1%	5400 ± 170	0.29 ± 0.01	0.16 ± 0.01
0.1%	1200 ± 37	1.3 ± 0.05	0.07 ± 0.004

TABLE 4.1: Table of Se-75 normalization corrections.

The second step in the analysis was to plot the activity ratio, $\frac{A_{Mix}}{a_{Pure}}$, as a function of the concentration by mass of spikant added to the soil. The initial

Sample	Uncorrected $a_{Pure}(\frac{Hz}{g})$	Normalization Factor	Corrected $\frac{A_Mix}{a_{Pure}}$ (g)
10%	(8.0 $\pm$ 0.3) $\times 10^5$	1.1 $\pm$ 0.04	0.17 $\pm$ 0.01
1%	(9.2 $\pm$ 0.3) $\times 10^5$	0.93 $\pm$ 0.04	0.04 $\pm$ 0.001

TABLE 4.2: Table of Se-81m normalization corrections.

concentration by mass of selenium in the soil was observed as the negative x-intercept in Figures 4.8 and 4.9. Unfortunately, the x-intercepts that resulted from these fits predicted concentrations that should have been observable in a pure soil sample but were not observed. The Se-75 had an x-intercept of (-0.44 $\pm$ 0.04)%, while the Se-81m had an x-intercept of (-1.75 $\pm$ 0.17)%. A pure soil sample was irradiated, but neither the 265 keV Se-75 line nor the 103 keV Se-81m line were observed.

As a result of this, a bounded fit to ensure that $\frac{b}{m} < 0.1\%$ was performed. Figures 4.10 and 4.11 represented the resulting fits with the $\frac{b}{m} < 0.1\%$ restriction. The restricted fit resulted in the x-intercepts of (-0.081 $\pm$ 0.003)% for the Se-75 and (-0.099 $\pm$ 0.005)% for the Se-81m samples. The x-intercepts correspond to an initial concentration of selenium present in the sample before the addition of any spikant.

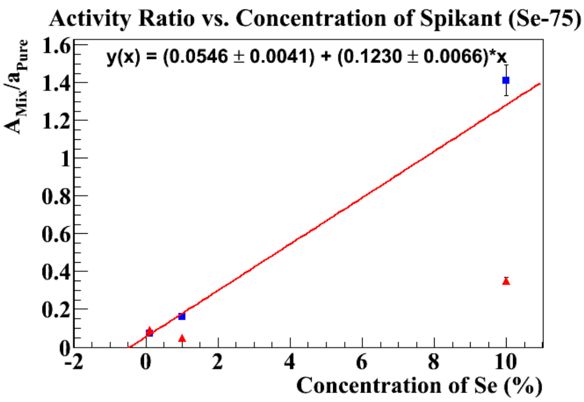

FIGURE 4.8: Uncorrected activity ratios (triangles) and corrected activity ratios (squares) for Se-75. Only the blue points were fit.

The final step was to plot the signal to noise ratio, $\frac{N}{B}$, as a function of the absolute selenium concentration by mass within the sample by adding the initial concentration of selenium in the soil to the amount of spikant introduced to the

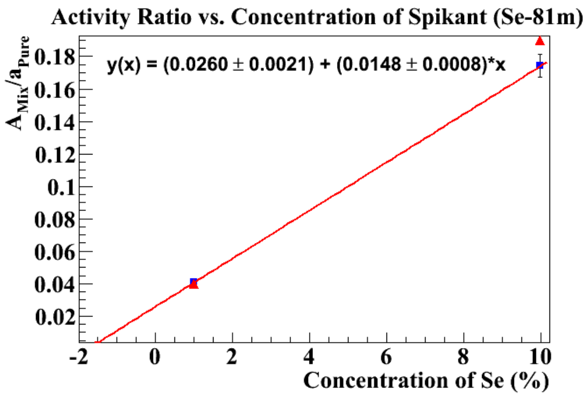

FIGURE 4.9: Uncorrected activity ratios (triangles) and corrected activity ratios (squares) for Se-81m. Only the blue points were fit.

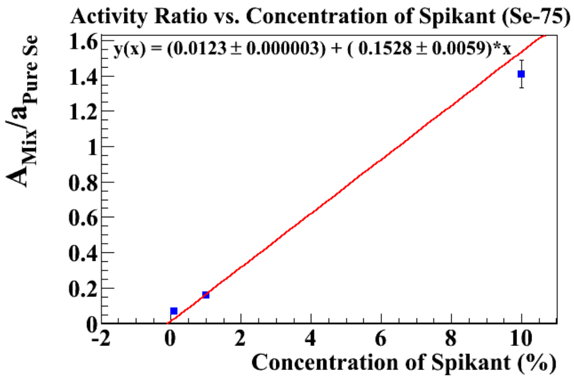

FIGURE 4.10: Activity ratio for Se-75 (fit restrictions).

sample. A linear fit was done to determine a y-intercept. The uncertainty in the fit's y-intercept was used to define a detection limit. The y-intercept in Figures 4.12 and 4.13 was increased by two standard deviations, defined by the uncertainty in the y-intercept of Figures 4.12 and 4.13, and the corresponding concentration on the x-axis was found via

$$x = \frac{2\sigma}{m} \tag{4.21}$$

The detection limit for Se-75 in soil was observed to be (0.005 ± 0.003)% and the detection limit for Se-81m in soil was observed to be (0.13 ± 0.06)%.

Two samples were not included for the analysis of the Se-81m 103 keV energy line (50%, 0.1%), while one sample was not included for the analysis of

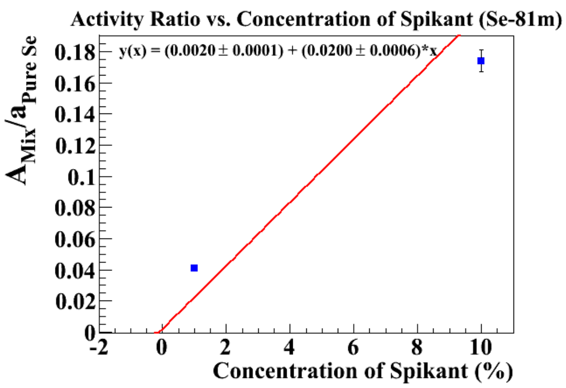

FIGURE 4.11: Activity ratio for Se-81m (fit restrictions).

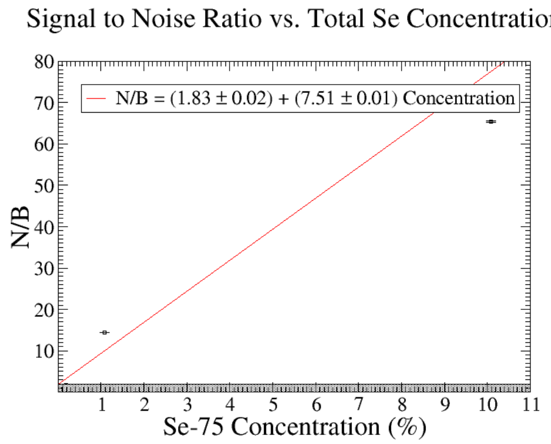

FIGURE 4.12: SNR vs. total concentration of Se-75. The shaded region represents the two standard deviation increase from the y-intercept. It intercepts with the linear fit at a concentration of (0.005 ± 0.0003)%, p-value < 0.05.

the Se-75 265 keV energy line (0.1%). The 50% sample was not included in either analysis because the results were not physical. The signal to noise ratio for both isotopes' characteristic gamma decay lines was lower than the signal to noise ratio of the 10% sample. Due to the fact that the sample was very small compared to the volume of the aluminium cylinder it was contained in, the lab technician may have placed the middle of the cylinder at the center of the beamline instead of the bottom. This would result in the sample receiving a decreased amount of photon flux when compared to the sample being placed correctly on the beamline axis. The 0.1% was not analyzed for the Se-81m sample because the 103 keV line was not visible as a result of waiting roughly two hours (two Se-81m half lives) for the matrix to cool down enough to reach a dead time below 20%.

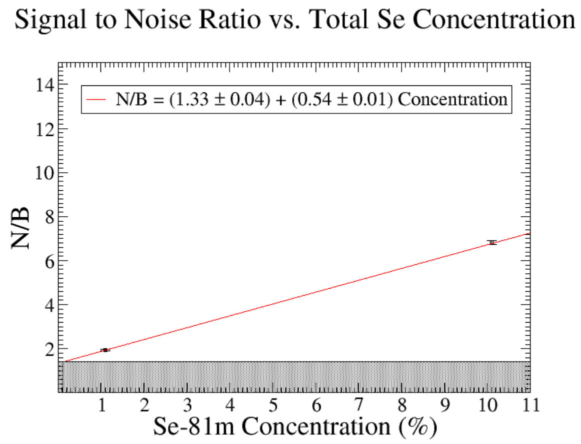

FIGURE 4.13: SNR vs. total concentration of Se-81m. The shaded region represents the two standard deviation increase from the y-intercept. It intersects with the linear fit at a concentration of $(0.13 \pm 0.06)\%$.

4.4 Discussion of Errors

There were two sets of errors and a notable ambiguity within this experiment. The first set was produced by errors from irradiation which include beam energy, beam divergence, attenuation, and the relative position of the pure outer selenium to the selenium embedded within the soil matrix. The second set of errors were produced during the measurements using the HpGe detector. One error that could arise from the counting process is the presence of an energy line produced by the irradiated soil within less than one channel of the selenium's characteristic decay lines of interest. Another form of error could be produced by other radioactive materials within the counting room which would result in more noise within the detector. The ambiguity arose by not being able to accurately identify the mechanism in which Se-81m was produced.

For the first set, the simplest error was that Segebade used a beam energy of 30 MeV [4], while this experiment used 32 MeV. This resulted in a change in expected energy of the bremsstrahlung photons, which in turn changed the portion of the cross section included. While this did not directly affect the results presented, it did complicate the comparison to Segebade's work. The next source of error can be attributed to the divergence and attenuation of the beam. Since a pure selenium sample was irradiated within the same target as the mixture, assuming the flux was the same, a ratio of the net production can be written as

$$\frac{N_{Se}^{Mix}}{N_{Se}^{Pure}} = \frac{n_T^{SeMix} V_T^{SeMix}}{n_T^{SePure} V_T^{SePure}}. \tag{4.22}$$

One would believe that ratio of the specific activities of the pure sample and the mixture would be unity if the flux through the target was the same. Unfortunately this was not the case, which would imply that the flux through the samples was not the same. Another instance of this error was found when comparing the ratios of the specific activities of Se-81m and Se-75 to Ni-57 performed by Segebade. The ratios calculated for this experiment did not match Segebade's work, which implies the flux seen by the nickel foil and the selenium pellets were different from each other. An increase in the divergence and attenuation of the beam could also be attributed to the presence of other targets in front of mine. Another source of error was produced by the relative position of the pure outer selenium and the selenium within the soil matrix. Since the level of soil varied, it is highly possible that the selenium within the mixture was higher or lower (relative to the beam axis) than the pure selenium. This would impact the flux seen by both sets of selenium.

During the HpGe measurement, one source of error could be the presence of lines produced from the soil matrix within 1 channel of the selenium's energy lines of interest competing with the characteristic energy lines from selenium. As a result the measurement would be higher than expected which would impact the number of counts seen within the chosen window width. Another source of error is simply the noise from within the counting room. Many sources and samples were brought into and out of the counting room which produced more noise to muddle the measurement.

Finally, the purpose of PAA is to identify the parent nuclei within a sample by studying the radioactive daughter nuclei post-irradiation. Unfortunately there are two ways to obtain Se-81m, which are Se-80(n,γ)Se-81m and Se-82(γ,n)Se-81m. Even though photon activation dominates in the angular region the sample was placed in with respect to the beamline, neutrons were still present within the irradiation hall. This means that some of the Se-81m produced may have come from neutron capture in Se-80. This experiment was performed to determine the minimum detectable concentration of selenium in soil, so the reaction producing the radioisotope was less important. If one wishes to identify the parent nucleus, this ambiguity must be considered.

Chapter 5

Conclusion

The purpose of this experiment was to determine the minimum detectable concentration of selenium in soil. Photon activation analysis was used to measure this concentration by creating the unstable isotopes of Se-81m and Se-75. The observed minimum detectable concentration for Se-81m was (0.13 ± 0.06)% $\left(1300 \pm 600 \frac{\mu g}{g}\right)$, which is consistent with the inability to observe the Se-81m energy lines in the 0.1% Se/Soil sample. The minimum detectable concentration for Se-75, as measured 56 days after irradiation, was a (0.005 ± 0.003)% (50 ± 30 $\frac{\mu g}{g}$). Note that some of the Se-81m produced may have come from neutron capture on Se-80. The Se-75 signal was still visible as of May of 2018.

Bibliography

[1] J.W. Motz H.W. Koch. Bremsstrahlung cross-section formulas and related data. *Rev. Mod. Phys*, 31:920, 1959.

[2] Zalesnyy G. N. Goryachev, A. M. The studying of the photoneutron reactions cross sections in the region of the giant dipole resonance in zinc, germanium, selenium, and strontium isotopes, . URL http://www-nds.indcentre.org.in/exfor/servlet/X4sSearch5?EntryID=220070.

[3] Ishkhanov B. S. Kapitonov I. M. Piskarev I. M. Piskarev V. G. Piskarev O. P. Goryachev, B. I. Giant dipole resonance on ni isotopes, . URL http://www-nds.indcentre.org.in/exfor/servlet/X4sGetSubent?reqx=119235&subID=220597006&plus=1.

[4] Hans-Peter Weise Christian Segebade and George J. Lutz. *Photon Activation Analysis*. Walter de Gruyter Co., Berlin, Germany, 1988.

[5] Varshni YP. Temperature depence of the energy gap in semiconductors. *Physica*, 34:149–154, 1967.

Appendix A

Detector Specifications

A.1 Energy Calibrations

The data acquisition system converts the analog signal from the HpGe detector's post amp into a channel number, but it is left to the experimenter to find out how to find which channel number corresponds to which energy. By using several calibrated sources with several characteristic energy lines spanning from 80-2000 keV, calibration constants can be found. Obviously, the more energy lines used will result with better fit parameters. Once the calibrated source has been measured by the HpGe detector, the energy lines of interest were fitted with a Gaussian function and the mean and its error were recorded. Plot the expected energy vs. the channel number with its error and fit the plot with a line. The equation of the line can be applied when plotting histograms to convert from channel number to energy via

$$E = b + m(Channel)$$

where m and b are the linear fit parameters.

It is worth noting that there could be some problems with binning when applying the energy calibrations, which is referred to as "picket fencing". This was due to the histogram bins being smaller than the hardware resolution.

This can be overcome by simply fitting the energy peak of interest to a Gaussian function, then applying the calibration to the mean of the fit.

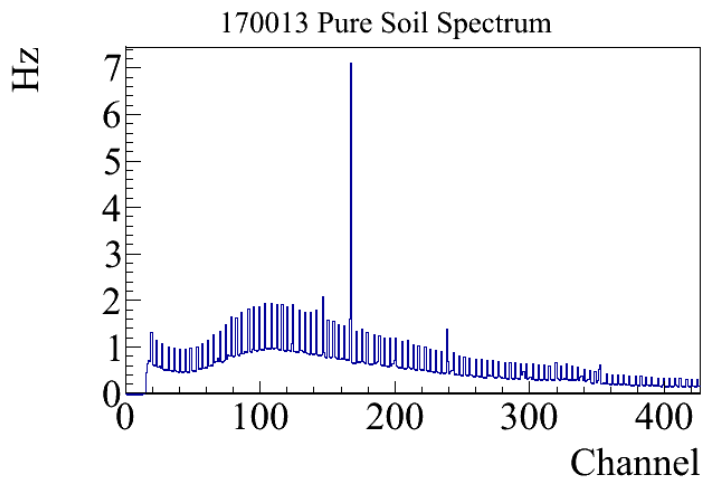

FIGURE A.1: Picket fencing due to binning incompatibility.

A.2 Efficiency

There are two types of efficiency for the HpGe detector: geometric and energy. Geometric efficiency deals with the detector's acceptance of radiation from a source as defined by the solid angle subtended by the detector. Energy efficiency deals with the detector's ability to accurately count photons of varying energies. To find the efficiency of the HpGe detector, the radiation was measured from calibrated sources with known activity and characteristic energy lines near the sample's characteristic energy lines (to account for the energy portion of the efficiency). The HpGe detectors have a track system set up near them. Samples can be placed on the track and the distance from the face of the detector to the sample can be varied up to one meter. Using this, make measurements at points of interest defined by where the irradiated samples were measured to account for the geometric efficiency. After the measurements, the experimenter can use the activation dates of the calibrated sources to find the activity of the source on the day of the efficiency measurement and take the ratio of the activity of the source seen by the HpGe detector and the actual activity of the calibrated source. A sample calculation is described below. Consider a Ba-133 source with an activity of $10.54 \pm 3\%$ μCi on its date of activation, which was July 1, 2008. The first step is to correct the activity to the date the efficiency measurement was taken, which in this case was May 27, 2017. To correct the activity to the day of the efficiency measurement, use equations

$$A_{TC} = Ae^{-\lambda t} \tag{A.1}$$

$$\sigma_{A_{TC}} = \sqrt{\sigma_A^2 e^{-2\lambda t} + A^2 t^2 e^{-2\lambda t} \sigma_\lambda^2} \tag{A.2}$$

. The correction yielded an activity of 5.87 ± 0.96 μCi. Once the activity has been found, the theoretical value of the number of counts of an energy line given off by the source was calculated via

$$A_{TC} \times \%I \times (3.7 \times 10^{10} \frac{Hz}{Ci}) \tag{A.3}$$

Where A_{TC} is the time corrected activity and $\%I$ is the intensity of the decay. Next, the activity of a line of interest in a 10 channel window was measured and take the ratio between the theoretical and the actual activities to find the efficiency, or

$$\epsilon = \frac{A_E}{A_T} \tag{A.4}$$

Where A_E is the experimental activity measured by the HpGe detector and A_T is the theoretical activity of the source. The error may be quantified by

$$\sigma_\epsilon = A_\epsilon \sqrt{(\frac{\sigma_{A_E}}{A_E})^2 + (\frac{\sigma_{A_T}^2}{A_T^2})} \tag{A.5}$$

The table below shows the information of the sources used. The parentheses in the energy column represent the intensity for the decay.

Source	Inventory Number	Activity (μCi)	Irradiation Date	Energy (keV)
Ba-133	129791	10.54 ± 3%	07/01/08	81.00 (32.9%)
Co-60	129790	10.42 ± 3%	07/01/08	1332.49 (99.98%)
Co-60	129739	1.082 ± 3%	07/01/08	1332.49 (99.98%)

Table A.1: Efficiency sources.

A.3 Detector A Specifications

Below are tables showing the intrinsic properties of Detector A along with the calculated values for the efficiency of the detector.

Serial No.	TP43076A
Relative ϵ @ 1.33MeV	44
FWHM @ 1.33MeV	1.93
Ratio FW.1M FWHM	2.0
Ratio FW.02M FWHM	2.9
Peak to Peak Compton	60
FWHM@122keV	700
Crystal Diameter (mm)	66.7
Crystal Length (mm)	49.2

TABLE A.2: Detector A specifications.

Serial	Date Measured	Corrected Activity (μCi)	Position (cm)	A_T (Hz)	A_E (Hz)	% ϵ
129791	05/27/17	5.87 ± 0.18	90	71455.51 ±2143.66	13.81 ± 0.26	0.02 ± 3.60 %
129791	05/27/17	5.87 ± 0.18	70	71455.51 ± 2143.66	23.18 ± 0.29	0.03 ± 3.25 %
129791	05/27/17	5.87 ± 0.18	50	71455.51 ± 2143.66	42.14 ± 0.49	0.06 ± 3.22 %
129791	05/27/17	5.87 ± 0.18	44	71455.51 ± 2143.66	56.14 ± 0.67	0.08 ± 3.23 %
129791	05/27/17	5.87 ± 0.18	30	71455.51 ± 2143.66	112.86 ± 1.41	0.16 ± 3.21 %
129791	05/27/17	5.87 ± 0.18	20	71455.51 ± 2143.66	230.39 ± 1.53	0.32 ± 3.07%
129791	09/06/17	5.75 ± 0.17	10	69994.75 ± 2069.41	642.33 ± 5.15	0.92 ± 3.10%
129790	09/14/17	2.72 ± 0.15	70	100622.49 ± 5782.52	8.95 ± 0.18	0.0089 ± 6 %
129790	09/14/17	2.72 ± 0.15	50	100622.49 ± 5782.52	17.18 ± 0.20	0.0170 ± 6%
129790	09/14/17	2.72 ± 0.15	30	100622.49 ± 5782.52	42.45 ± 0.47	0.0422 ± 6%
129790	09/14/17	2.72 ± 0.15	20	100622.49 ± 5782.52	85.20 ± 0.71	0.0847 ± 6%
129739	09/15/17	0.283 ± 0.016	10	10469.187 ± 314.08	32.76 ± 0.338	0.31 ± 3%

TABLE A.3: Table of efficiencies.

Appendix B

Data Tables and Graphs

B.1 Analysis Tables

	0<t<500	1050<t<1577 s	2240<t<2740 s	3431<t<3931 s	4600<t<5100 s
I $\pm\sqrt{I}$	2.093 $\times 10^5 \pm$ 0.22%	1.969 $\times 10^5 \pm$ 0.22%	1.486 $\times 10^4 \pm$ 0.26%	1.157 $\times 10^5 \pm$ 0.29%	9.031 $\times 10^4 \pm$ 0.33%
$B \pm \sigma_B$	5.800 $\times 10^4 \pm$ 0.38%	5.229 $\times 10^4 \pm$ 0.39%	3.954 $\times 10^4 \pm$ 0.44 %	3.291 $\times 10^4 \pm$ 0.49%	2.289 $\times 10^4 \pm$ 0.58%
N $\pm \sigma_N$	1.513 $\times 10^5 \pm$ 0.33 %	1.446 $\times 10^5 \pm$ 0.34%	1.091 $\times 10^5 \pm$ 0.39%	8.279 $\times 10^4 \pm$ 0.45%	6.742 $\times 10^4 \pm$ 0.49%
Runtime (S)	500	527	500	500	500
$A_{Measured} \pm \sigma_{A_{Measured}}$	302.6 $\pm$ 1.0	274.4 $\pm$ 0.9	218.1 $\pm$ 0.9	165.6 $\pm$ 0.8	134.8 $\pm$ 0.7
$A_{True} \pm \sigma_{A_{True}}$ (Hz)	318.1 $\pm$ 1.2	289.2 $\pm$ 1.0	229.3 $\pm$ 0.9	174.1 $\pm$ 0.8	141.8 $\pm$ 0.7
% Dead	5.06 $\pm$ 0.39	3.95 $\pm$ 0.42	3.06 $\pm$ 0.30	2.53 $\pm$ 0.31	1.65 $\pm$ 0.34
$A_{DTC} \pm \sigma_{A_{DTC}}$	340 $\pm$ 2	300 $\pm$ 2	240 $\pm$ 1	180 $\pm$ 1	140 $\pm$ 0.9
% Efficiency	0.34% $\pm$ 3.0%	0.34% $\pm$ 3.0%	0.34% $\pm$ 3.0%	0.34% $\pm$ 3.0%	0.34% $\pm$ 3.0%
$A_\epsilon \pm \sigma_{A_\epsilon}$	9.9 $\times 10^4 \pm$ 3.0%	8.9 $\times 10^4 \pm$ 3.1%	7.0 $\times 10^4 \pm$ 3.0%	5.3 $\times 10^4 \pm$ 3.1%	4.3 $\times 10^4 \pm$ 3.1%

TABLE B.1: 50% Se/soil data, 10 channel (Se-81m).

	0<t<500	1050<t<1577 s	2240<t<2740 s	3431<t<3931 s	4600<t<5100 s
I $\pm\sqrt{I}$	1.665 $\times 10^5 \pm$ 0.24%	1.586 $\times 10^5 \pm$ 0.25%	1.196 $\times 10^5 \pm$ 0.29%	9.186 $\times 10^4 \pm$ 0.33 %	7.362 $\times 10^4 \pm$ 0.37%
$B \pm \sigma_B$	1.740 $\times 10^4 \pm$ 0.37%	1.569 $\times 10^4 \pm$ 0.39%	1.186 $\times 10^4 \pm$ 0.44%	9.874 $\times 10^3 \pm$ 0.49%	6.867 $\times 10^3 \pm$ 0.58%
N $\pm\sigma_N$	1.491 $\times 10^5 \pm$ 0.28%	1.429 $\times 10^5 \pm$ 0.28%	1.077 $\times 10^5 \pm$ 0.32%	8.199 $\times 10^4 \pm$ 0.37%	6.675 $\times 10^4 \pm$ 0.41%
Runtime (S)	500	527	500	500	500
$A_{Measured} \pm \sigma_{A_{Measured}}$	298.2 $\pm$ 0.8	271.2 $\pm$ 0.8	215.5 $\pm$ 0.7	164.0 $\pm$ 0.6	133.5 $\pm$ 0.6
$A_{True} \pm \sigma_{A_{True}}$ (Hz)	313.5 $\pm$ 0.9	285.9 $\pm$ 0.8	226.5 $\pm$ 0.7	172.4 $\pm$ 0.6	140.3 $\pm$ 0.6
% Dead	5.06 $\pm$ 0.39	3.95 $\pm$ 0.42	3.06 $\pm$ 0.30	2.53 $\pm$ 0.31	1.65 $\pm$ 0.34
$A_{DTC} \pm \sigma_{A_{DTC}}$	330 $\pm$ 2	300 $\pm$ 2	230 $\pm$ 1	180 $\pm$ 0.9	140 $\pm$ 0.8
% Efficiency	0.34% $\pm$ 3.0%	0.34% $\pm$ 3.0%	0.34% $\pm$ 3.0%	0.34% $\pm$ 3.0%	0.34% $\pm$ 3.0%
$A_\epsilon \pm \sigma_{A_\epsilon}$	9.7 $\times 10^4 \pm$ 3.0%	8.8 $\times 10^4 \pm$ 3.0%	6.9 $\times 10^4 \pm$ 3.0%	5.2 $\times 10^4 \pm$ 3.0%	4.2 $\times 10^4 \pm$ 3.0%

TABLE B.2: 50% Se/soil data, 3 channel (Se-81m).

	0<t<500	1050<t<1577 s	2240<t<2740 s	3431<t<3931 s	4600<t<5100 s
I $\pm\sqrt{I}$	1.081 $\times 10^5 \pm$ 0.30%	1.040 $\times 10^5 \pm$ 0.31%	8.039 $\times 10^4 \pm$ 0.35%	6.163 $\times 10^4 \pm$ 0.40%	5.083 $\times 10^4 \pm$ 0.44%
$B \pm \sigma_B$	5.800 $\times 10^3 \pm$ 0.37%	5.229 $\times 10^3 \pm$ 0.39%	3.954 $\times 10^3 \pm$ 0.44%	3.291 $\times 10^3 \pm$ 0.49%	2.289 $\times 10^3 \pm$ 0.58%
N $\pm \sigma_N$	1.023 $\times 10^5 \pm$ 0.30 %	9.877 $\times 10^4 \pm$ 0.33%	7.644 $\times 10^4 \pm$ 0.37%	5.834 $\times 10^4 \pm$ 0.43%	4.854 $\times 10^4 \pm$ 0.47%
Runtime (S)	500	527	500	500	500
$A_{Measured} \pm \sigma_{A_{Measured}}$	204.6 $\pm$ 0.7	187.4 $\pm$ 0.6	152.9 $\pm$ 0.6	116.7 $\pm$ 0.5	97.1 $\pm$ 0.5
$A_{True} \pm \sigma_{A_{True}}$ (Hz)	215.1 $\pm$ 0.7	197.6 $\pm$ 0.6	160.7 $\pm$ 0.6	122.7 $\pm$ 0.5	102.1 $\pm$ 0.5
% Dead	5.06 $\pm$ 0.39	3.95 $\pm$ 0.42	3.06 $\pm$ 0.30	2.53 $\pm$ 0.31	1.65 $\pm$ 0.34
$A_{DTC} \pm \sigma_{A_{DTC}}$	230 $\pm$ 1	210 $\pm$ 1	170 $\pm$ 1	130 $\pm$ 1	100 $\pm$ 1
% Efficiency	0.34% $\pm$ 3.0%	0.34% $\pm$ 3.0%	0.34% $\pm$ 3.0%	0.34% $\pm$ 3.0%	0.34% $\pm$ 3.0%
$A_\epsilon \pm \sigma_{A_\epsilon}$	6.7 $\times 10^4 \pm$ 3.0%	6.1 $\times 10^4 \pm$ 3.0%	4.9 $\times 10^4 \pm$ 3.0%	3.7 $\times 10^4 \pm$ 3.0%	3.1 $\times 10^4 \pm$ 3.1%

TABLE B.3: 50% Se/soil 1 channel data (Se-81m).

	602 < t < 1000	1710<t<2090	2940<t<3240	4020<t<4520
I $\pm\sqrt{I}$	2.515 $\times 10^5 \pm$ 0.20%	2.345 $\times 10^5 \pm$ 0.21%	1.646 $\times 10^5 \pm$ 0.25%	2.115 $\times 10^5 \pm$ 0.22%
$B \pm \sigma_B$	1.569 $\times 10^5 \pm$ 0.22%	1.525 $\times 10^5 \pm$ 0.22%	1.205 $\times 10^5 \pm$ 0.24%	1.450 $\times 10^5 \pm$ 0.24%
N $\pm\sigma_N$	9.460 $\times 10^4 \pm$ 0.65%	8.198 $\times 10^4 \pm$ 0.72%	4.408 $\times 10^4 \pm$ 1.1%	6.649 $\times 10^4 \pm$ 0.87%
Runtime (S)	398	380	300	500
$A_{Measured} \pm \sigma_{A_{Measured}}$ (Hz)	237.7 $\pm$ 1.5	215.7 $\pm$ 1.6	146.9 $\pm$ 1.7	133.00 $\pm$ 1.2
$A_{True} \pm \sigma_{A_{True}}$ (Hz)	247.4 $\pm$ 1.6	224.1 $\pm$ 1.6	153.5 $\pm$ 1.8	139.8 $\pm$ 1.2
% Dead	1.34 $\pm$ 0.18	1.34 $\pm$ 0.18	1.34 $\pm$ 0.18	0.84 $\pm$ 0.16
$A_{DTC} \pm \sigma_{A_{DTC}}$	250 $\pm$ 2	230 $\pm$ 2	150 $\pm$ 2	140 $\pm$ 1
% Efficiency	0.34% $\pm$ 3.0%	0.34% $\pm$ 3.0%	0.34% $\pm$ 3.0%	0.34% $\pm$ 3.0%
$A_\epsilon \pm \sigma_{A_\epsilon}$	7.4 $\times 10^4 \pm$ 3.1%	6.7 $\times 10^4 \pm$ 3.1%	4.5 $\times 10^4 \pm$ 3.2%	4.1 $\times 10^4 \pm$ 3.1%

Table B.4: 50% sample pure selenium 10 channel data (Se-81m).

	602 < t < 1000	1710<t<2090	2940<t<3240	4020<t<4520
I $\pm\sqrt{I}$	1.338 $\times 10^5 \pm$ 0.27%	1.251 $\times 10^5 \pm$ 0.28%	8.339 $\times 10^4 \pm$ 0.35%	1.076 $\times 10^5 \pm$ 0.30%
$B \pm \sigma_B$	4.707 $\times 10^4 \pm$ 0.22 %	4.576 $\times 10^4 \pm$ 0.22%	3.616 $10^4 \pm$ 0.24%	4.350 $\times 10^4 \pm$ 0.24 %
N $\pm$ σ_N	8.673 $\times 10^4 \pm$ 0.44%	7.934 $\times 10^4 \pm$ 0.46%	4.723 $\times 10^4 \pm$ 0.64%	6.410 $\times 10^4 \pm$ 0.54%
Runtime (S)	398	380	300	500
$A_{Measured} \pm \sigma_{A_{Measured}}$ (Hz)	217.9 $\pm$ 1.0	208.8 $\pm$ 1.0	157.5 $\pm$ 1.0	128.2 $\pm$ 0.7
$A_{True} \pm \sigma_{A_{True}}$ (Hz)	226.8 $\pm$ 1.0	216.9 $\pm$ 1.0	162.3 $\pm$ 1.0	134.8 $\pm$ 0.7
% Dead	1.34 $\pm$ 0.18	1.34 $\pm$ 0.18	1.34 $\pm$ 0.18	0.84 $\pm$ 0.16
$A_{DTC} \pm \sigma_{A_{DTC}}$	230 $\pm$ 1	220 $\pm$ 1	164 $\pm$ 1	136 $\pm$ 1
% Efficiency	0.34% $\pm$ 3.0%	0.34% $\pm$ 3.0%	0.34% $\pm$ 3.0%	0.34% $\pm$ 3.0%
$A_\epsilon \pm \sigma_{A_\epsilon}$	6.8 $\times 10^4 \pm$ 3.0%	6.5 $\times 10^4 \pm$ 3.0%	4.9 $\times 10^4 \pm$ 3.1%	4.0 $\times 10^4 \pm$ 3.1%

TABLE B.5: 50% sample pure selenium 3 channel data (Se-81m).

	602 < t < 1000	1710<t<2090	2940<t<3240	4020<t<4520
I $\pm\sqrt{I}$	8.266 $\times 10^4 \pm$ 0.35%	7.226 $\times 10^4 \pm$ 0.37%	4.742 $\times 10^4 \pm$ 0.46%	6.119 $\times 10^4 \pm$ 0.40%
$B \pm \sigma_B$	1.569 $\times 10^4 \pm$ 0.22%	1.525 $\times 10^4 \pm$ 0.22 %	1.205 $\times 10^4 \pm$ 0.24%	1.450 $\times 10^4 \pm$ 0.24
N $\pm$ σ_N	6.697 $\times 10^4 \pm$ 0.43 %	5.701 $\times 10^4 \pm$ 0.48%	3.537 $\times 10^4 \pm$ 0.62%	4.669 $\times 10^4 \pm$ 0.54%
Runtime (S)	398	380	300	500
$A_{Measured} \pm \sigma_{A_{Measured}}$ (Hz)	168.3 $\pm$ 0.7	150.0 $\pm$ 0.5	117.9 $\pm$ 0.7	93.4 $\pm$ 0.50
$A_{True} \pm \sigma_{A_{True}}$ (Hz)	175.1 $\pm$ 0.8	155.8 $\pm$ 0.6	121.5 $\pm$ 0.8	98.2 $\pm$ 0.5
% Dead	1.34 $\pm$ 0.18	1.34 $\pm$ 0.18	1.34 $\pm$ 0.18	0.84 $\pm$ 0.16
$A_{DTC} \pm \sigma_{A_{DTC}}$	180 $\pm$ 1	160 $\pm$ 1	120 $\pm$ 1	99 $\pm$ 1
% Efficiency	0.34% $\pm$ 3.0%	0.34% $\pm$ 3.0%	0.34% $\pm$ 3.0%	0.34% $\pm$ 3.0%
$A_\epsilon \pm \sigma_{A_\epsilon}$	5.2 $\times 10^4 \pm$ 3.0%	4.7 $\times 10^4 \pm$ 3.0%	3.6 $\times 10^4 \pm$ 3.1%	2.9 $\times 10^4 \pm$ 3.1%

TABLE B.6: 50% sample pure selenium 1 channel data (Se-81m).

	09/07/17	10/11/17	11/28/17	05/18/18
I $\pm\sqrt{I}$	6.453 $\times 10^5 \pm$ 0.12%	7.692 $\times 10^5 \pm$ 0.11%	6.905 $\times 10^5 \pm$ 0.12%	2.419 $\times 10^4 \pm$ 0.64%
$B \pm \sigma_B$	7.394 $\times 10^4 \pm$ 0.44%	8.440 $\times 10^4 \pm$ 0.41%	9.521 $\times 10^4 \pm$ 0.39%	6.370 $\times 10^3 \pm$ 1.48%
N $\pm$ σ_N	5.714 $\times 10^5 \pm$ 0.15%	6.848 $\times 10^5 \pm$ 0.14%	5.953 $\times 10^5 \pm$ 0.15%	1.782 $\times 10^4 \pm$ 1.02%
Runtime (S)	5.0827 $\times 10^4$	7.3755 $\times 10^4$	9.7212 $\times 10^4$	6.400 $\times 10^3$
$A_{Measured} \pm \sigma_{A_{Measured}}$ (Hz)	11.24 $\pm$ 0.02	9.28 $\pm$ 0.01	6.12 $\pm$ 0.01	2.78 $\pm$ 0.03
% Efficiency	0.93 $\pm$ 3.1%	0.93 $\pm$ 3.1%	0.93 $\pm$ 3.1%	0.93 $\pm$ 3.1%
$A_\epsilon \pm \sigma_{A_\epsilon}$	1.3 $\times 10^3 \pm$ 3.1%	1.1 $\times 10^3 \pm$ 3.1%	7.1 $\times 10^2 \pm$ 3.1%	3.2 $\times 10^2 \pm$ 3.3%

TABLE B.7: 50% Se/soil sample 10 channel data (Se-75).

	09/07/17	10/11/17	11/28/17	05/18/18
I $\pm\sqrt{I}$	5.798 $\times 10^5 \pm$ 0.13%	6.888 $\times 10^5 \pm$ 0.12%	6.033 $\times 10^5 \pm$ 0.13%	1.877 $\times 10^4 \pm$ 0.73%
$B \pm \sigma_B$	1.397 $\times 10^4 \pm$ 0.42%	1.607 $\times 10^4 \pm$ 0.39%	1.801 $\times 10^4 \pm$ 0.37%	1.197 $\times 10^3 \pm$ 1.42%
N $\pm \sigma_N$	5.658 $\times 10^5 \pm$ 0.13%	6.727 $\times 10^5 \pm$ 0.12%	5.853 $\times 10^5 \pm$ 0.13%	1.757 $\times 10^4 \pm$ 0.79%
Runtime (S)	5.0827 $\times 10^4$	7.3755 $\times 10^4$	9.7212 $\times 10^4$	6.400 $\times 10^3$
$A_{Measured} \pm \sigma_{A_{Measured}}$ (Hz)	11.13 $\pm$ 0.02	9.12 $\pm$ 0.01	6.02 $\pm$ 0.01	2.75 $\pm$ 0.02
% Efficiency	0.93 $\pm$ 3.1%	0.93 $\pm$ 3.1%	0.93 $\pm$ 3.1%	0.93 $\pm$ 3.1%
$A_\epsilon \pm \sigma_{A_\epsilon}$	1.2 $\times 10^3 \pm$ 3.1%	9.8 $\times 10^2 \pm$ 3.1%	6.5 $\times 10^2 \pm$ 3.1%	3.0 $\times 10^2 \pm$ 3.2%

Table B.8: 50% Se/soil sample 3 channel data (Se-75).

	09/07/17	10/11/17	11/28/17	05/18/18
I $\pm\sqrt{I}$	3.795 $\times 10^5 \pm$ 0.16%	4.135 $\times 10^5 \pm$ 0.16%	3.624 $\times 10^5 \pm$ 0.17%	1.176 $\times 10^4 \pm$ 0.92%
$B \pm \sigma_B$	4.655 $\times 10^3 \pm$ 0.41%	5.355 $\times 10^3 \pm$ 0.39%	6.002 $\times 10^3 \pm$ 0.37%	3.990 $\times 10^3 \pm$ 1.42%
N $\pm$ σ_N	3.748 $\times 10^5 \pm$ 0.16%	4.081 $\times 10^5 \pm$ 0.16%	3.564 $\times 10^5 \pm$ 0.16%	1.136 $\times 10^4 \pm$ 0.96%
Runtime (S)	5.0827 $\times 10^4$	7.3755 $\times 10^4$	9.7212 $\times 10^4$	6.400 $\times 10^3$
$A_{Measured} \pm \sigma_{A_{Measured}}$ (Hz)	7.37 $\pm$ 0.01	5.53 $\pm$ 0.01	3.67 $\pm$ 0.01	1.76 $\pm$ 0.02
% Efficiency	0.93 $\pm$ 3.1%	0.93 $\pm$ 3.1%	0.93 $\pm$ 3.1%	0.93 $\pm$ 3.1%
$A_\epsilon \pm \sigma_{A_\epsilon}$	7.9 $\times 10^2 \pm$ 3.1%	5.9 $\times 10^2 \pm$ 3.1%	3.9 $\times 10^2 \pm$ 3.1%	1.9 $\times 10^2 \pm$ 3.3%

TABLE B.9: 50% Se/soil sample 1 channel data (Se-75).

	08/29/17	10/30/17	1/20/18
I $\pm\sqrt{I}$	7.462 $\times10^6\pm$ 0.04%	1.691 $\times10^6\pm$ 0.08%	4.655 $\times10^6\pm$ 0.05%
$B \pm \sigma_B$	2.562 $\times10^6\pm$ 0.07%	7.316 $\times10^5\pm$ 0.14%	3.356 $\times10^6\pm$ 0.07%
N $\pm$ σ_N	4.900 $\times10^6\pm$ 0.07%	9.593 $\times10^5\pm$ 0.14%	1.299 $\times10^6\pm$ 0.24%
Runtime (S)	2.42049 $\times10^5$	7.91226 $\times10^4$	1.70289 $\times10^5$
$A_{Measured} \pm \sigma_{A_{Measured}}$ (Hz)	20.24 $\pm$ 0.01	12.12 $\pm$ 0.02	7.63 $\pm$ 0.02
% Efficiency	0.93 $\pm$ 3.1%	0.93 $\pm$ 3.1%	0.93 $\pm$ 3.1%
$A_\epsilon \pm \sigma_{A_\epsilon}$	2.4 $\times10^3\pm$ 3.1%	1.4 $\times10^2\pm$ 3.1%	8.9 $\times10^2\pm$ 3.1%

TABLE B.10: 50% pure witness Se sample 10 channel data (Se-75).

	08/29/17	10/30/17	1/20/18
I $\pm\sqrt{I}$	5.516 $\times10^6\pm$ 0.04%	1.079 $\times10^6\pm$ 0.10%	1.858 $\times10^6\pm$ 0.07%
$B \pm \sigma_B$	4.831 $\times10^5\pm$ 0.07%	1.379 $\times10^5\pm$ 0.13%	6.338 $\times10^5\pm$ 0.06%
N $\pm$ σ_N	5.033 $\times10^6\pm$ 0.05%	9.411 $\times10^5\pm$ 0.11%	1.224 $\times10^6\pm$ 0.11%
Runtime (S)	2.42049 $\times10^5$	7.91226 $\times10^4$	1.70289 $\times10^5$
$A_{Measured} \pm \sigma_{A_{Measured}}$ (Hz)	20.79 $\pm$ 0.01	11.89 $\pm$ 0.01	7.19 $\pm$ 0.01
% Efficiency	0.93 $\pm$ 3.1%	0.93 $\pm$ 3.1%	0.93 $\pm$ 3.1%
$A_\epsilon \pm \sigma_{A_\epsilon}$	2.2 $\times10^3\pm$ 3.1%	1.3 $\times10^3\pm$ 3.1%	7.3 $\times10^2\pm$ 3.1%

TABLE B.11: 50% pure witness Se sample 3 channel data (Se-75).

	08/29/17	10/30/17	1/20/18
I $\pm\sqrt{I}$	3.551 $\times10^6\pm$ 0.05%	6.114 $\times10^5\pm$ 0.13%	8.291 $\times10^5\pm$ 0.11%
$B \pm \sigma_B$	1.610 $\times10^5\pm$ 0.07%	4.597 $\times10^4\pm$ 0.13%	2.113 $\times10^5\pm$ 0.06%
N $\pm$ σ_N	3.390 $\times10^6\pm$ 0.06%	5.654 $\times10^5\pm$ 0.14%	6.178 $\times10^5\pm$ 0.15%
Runtime (S)	2.42049 $\times10^5$	7.91226 $\times10^4$	1.70289 $\times10^5$
$A_{Measured} \pm \sigma_{A_{Measured}}$ (Hz)	14.01 $\pm$ 0.01	7.15 $\pm$ 0.01	3.63 $\pm$ 0.01
% Efficiency	0.93 $\pm$ 3.1%	0.93 $\pm$ 3.1%	0.93 $\pm$ 3.1%
$A_\epsilon \pm \sigma_{A_\epsilon}$	1.5 $\times10^3\pm$ 3.1%	7.7 $\times10^2\pm$ 3.1%	3.9 $\times10^2\pm$ 3.1%

Table B.12: 50% pure witness Se sample 1 channel data (Se-75).

	5/24/17	5/26/17	5/29/17	5/30/17
I $\pm\sqrt{I}$	6014 $\pm$ 77.55	6471 $\pm$ 80.44	9911 $\pm$ 99.56	6987 $\pm$ 83.59
$B \pm \sigma_B$	194.454 $\pm$ 17.238	184.678 $\pm$ 16.718	427.96 $\pm$ 25.22	308.88 $\pm$ 21.58
N $\pm$ σ_N	5819.55 $\pm$ 79.44	6286.322 $\pm$ 82.16	9483.04 $\pm$ 102.70	6678.12 $\pm$ 86.33
Runtime (S)	300.657	300.307	300.581	340.742
$A_{Measured} \pm \sigma_{A_{Measured}}$ (Hz)	19.36 $\pm$ 0.26	20.93 $\pm$ 0.27	31.55 $\pm$ 0.34	19.60 $\pm$ 0.25
$A_{True} \pm \sigma_{A_{True}}$ (Hz)	19.37 $\pm$ 0.26	20.95 $\pm$ 0.27	31.56 $\pm$ 0.34	19.62 $\pm$ 0.25
% Dead	1.33 $\pm$ 0.23	1.33 $\pm$ 0.23	2.26 $\pm$ 0.33	1.65 $\pm$ 0.34
$A_{DTC} \pm \sigma_{A_{DTC}}$	20 $\pm$ 0.3	21 $\pm$ 0.3	32 $\pm$ 0.4	20 $\pm$ 0.3
% Efficiency	0.017 $\pm$ 6%	0.042 $\pm$ 6%	0.31 $\pm$ 3%	0.31 $\pm$ 3%
$A_\epsilon \pm \sigma_{A_\epsilon}$	1.2 $\times 10^5 \pm$ 6.0%	5.0 $\times 10^4 \pm$ 6.2%	1.0 $\times 10^4 \pm$ 333.36	6.4 $\times 10^3 \pm$ 3.3%

Table B.13: 170047 front outer foil data.

	5/23/17	5/25/17	5/27/17	5/29/17	5/30/17
I $\pm\sqrt{I}$	4263 $\pm$ 65.29	7979 $\pm$ 89.33	6400 $\pm$ 80	7270 $\pm$ 85.26	4887 $\pm$ 69.91
$B \pm \sigma_B$	129.844 $\pm$ 13.858	276.64 $\pm$ 20.54	383.24 $\pm$ 23.66	301.08 $\pm$ 21.06	204.88 $\pm$ 17.42
N $\pm$ σ_N	4133.16 $\pm$ 66.74	7702.36 $\pm$ 91.66	6016.76 $\pm$ 83.42	6968.92 $\pm$ 87.82	4682.12 $\pm$ 72.05
Runtime (S)	339.18	300.763	301.113	300.989	300.332
$A_{Measured} \pm \sigma_{A_{Measured}}$ (Hz)	12.19 $\pm$ 0.20	25.61 $\pm$ 0.30	19.98 $\pm$ 0.28	23.15 $\pm$ 0.29	15.59 $\pm$ 0.24
$A_{True} \pm \sigma_{A_{True}}$ (Hz)	12.20 $\pm$ 0.20	25.63 $\pm$ 0.30	20.00 $\pm$ 0.28	23.17 $\pm$ 0.29	15.60 $\pm$ 0.24
% Dead	0.84 $\pm$ 0.16	1.65 $\pm$ 0.34	1.55 $\pm$ 0.18	1.65 $\pm$ 0.34	1.33 $\pm$ 0.23
$A_{DTC} \pm \sigma_{A_{DTC}}$	12 $\pm$ 0.2	26 $\pm$ 0.3	20 $\pm$ 0.3	23 $\pm$ 0.3	16 $\pm$ 0.3
% Efficiency	0.009 $\pm$ 6%	0.042 $\pm$ 6%	0.085 $\pm$ 6%	0.31 $\pm$ 3%	0.31 $\pm$ 3%
$A_\epsilon \pm \sigma_{A_\epsilon}$	1.4 $\times 10^5 \pm$ 6%	6.2 $\times 10^4 \pm$ 6%	2.4 $\times 10^4 \pm$ 6%	7.6 $\times 10^3 \pm$ 3%	5.1 $\times 10^3 \pm$ 3%

TABLE B.14: 170047 rear outer foil data.

	5/23/17	5/24/17	5/29/17	5/30/17
I $\pm\sqrt{I}$	5.827 $\times 10^3 \pm$ 1.3%	7.245 $\times 10^3 \pm$ 1.2%	1.176 $\times 10^4 \pm$ 1.0%	7.262 $\times 10^3 \pm$ 1.2%
$B \pm \sigma_B$	190.56 $\pm$ 16.79	172.39 $\pm$ 16.51	411.59 $\pm$ 24.35	250.59 $\pm$ 18.87
N $\pm$ σ_N	5.636 $\times 10^3 \pm$ 1.4%	7.072 $\times 10^3 \pm$ 1.2%	1.135 $\times 10^3 \pm$ 1.0%	7.011 $\times 10^3 \pm$ 1.2%
Runtime (S)	300.173	301.536	301.126	300.611
$A_{Measured} \pm \sigma_{A_{Measured}}$ (Hz)	18.78 $\pm$ 0.26	23.46 $\pm$ 0.29	37.69 $\pm$ 0.37	23.32 $\pm$ 0.29
% Efficiency	8.9 $\times 10^{-3} \pm$ 6%	1.7 $\times 10^{-2} \pm$ 6%	3.1 $\times 10^{-1} \pm$ 3%	3.1 $\times 10^{-1} \pm$ 3%
$A_\epsilon \pm \sigma_{A_\epsilon}$	2.1 $\times 10^5 \pm$ 6.2%	1.4 $\times 10^5 \pm$ 6.1%	1.2 $\times 10^4 \pm$ 3.2%	7.5 $\times 10^3 \pm$ 3.0%

TABLE B.15: 170047 front inner foil data.

	5/23/17	5/24/17	5/27/17	5/29/17	5/30/17
I $\pm\sqrt{I}$	5.295 $\times 10^3 \pm$ 1.4%	7.026 $\times 10^3 \pm$ 1.2%	9.708 $\times 10^3 \pm$ 1.0%	1.127 $\times 10^4 \pm$ 0.94%	7.289 $\times 10^3 \pm$ 1.2%
$B \pm \sigma_B$	218.01 $\pm$ 17.90	251.90 $\pm$ 19.09	461.77 $\pm$ 25.39	362.18 $\pm$ 22.91	185.49 $\pm$ 16.52
N $\pm\ \sigma_N$	5.077 $\times 10^3 \pm$ 1.5%	6.774 $\times 10^3 \pm$ 1.3%	9.246 $\times 10^3 \pm$ 1.1%	1.091 $\times 10^4 \pm$ 1.0%	7.103 $\times 10^3 \pm$ 1.2%
Runtime (S)	300.835	301.199	301.325	300.538	300.747
$A_{Measured} \pm \sigma_{A_{Measured}}$ (Hz)	16.88 $\pm$ 0.25	22.49 $\pm$ 0.29	30.69 $\pm$ 0.34	36.29 $\pm$ 0.36	23.62 $\pm$ 0.34
% Efficiency	8.9 $\times 10^{-3} \pm$ 6%	1.7 $\times 10^{-2} \pm$ 6%	8.5 $\times 10^{-2} \pm$ 6%	3.1 $\times 10^{-1} \pm$ 3%	3.1 $\times 10^{-1} \pm$ 3%
$A_\epsilon \pm \sigma_{A_\epsilon}$	1.9 $\times 10^5 \pm$ 6.2%	1.3 $\times 10^5 \pm$ 6.1%	3.6 $\times 10^4 \pm$ 6.1%	1.2 $\times 10^4 \pm$ 3.2%	7.6 $\times 10^3 \pm$ 3.2%

Table B.16: 170047 rear inner foil data.

	0 <t< 500 s	1210<t<1750 s	2430<t<2930 s	3616 <t< 3831 s
I $\pm\sqrt{I}$	1.644 $\times 10^5 \pm$ 0.25%	1.284 $\times 10^5 \pm$ 0.28%	9.142 $\times 10^4 \pm$ 0.33%	3.049 $\times 10^4 \pm$ 0.57%
$B \pm \sigma_B$	7.471 $\times 10^4 \pm$ 0.59%	4.722 $\times 10^4 \pm$ 0.56%	2.950 $\times 10^4 \pm$ 0.72%	9.768 $\times 10^3 \pm$ 1.2%
N $\pm$ σ_N	8.969 $\times 10^4 \pm$ 0.59%	8.118 $\times 10^4 \pm$ 0.55%	6.192 $\times 10^4 \pm$ 0.60%	2.072 $\times 10^4 \pm$ 1.0%
Runtime (S)	500	540	500	215
$A_{Measured} \pm \sigma_{A_{Measured}}$ (Hz)	179.4 $\pm$ 1.1	150.3 $\pm$ 0.8	123.8 $\pm$ 0.7	96.4 $\pm$ 1.0
$A_{True} \pm \sigma_{A_{True}}$ (Hz)	188.6 $\pm$ 1.1	158.7 $\pm$ 0.9	130.2 $\pm$ 0.8	98.5 $\pm$ 1.0
% Dead	6.59 $\pm$ 0.43	3.95 $\pm$ 0.42	2.26 $\pm$ 0.33	1.65 $\pm$ 0.34
$A_{DTC} \pm \sigma_{A_{DTC}}$	200 $\pm$ 2	170 $\pm$ 1	130 $\pm$ 1	100 $\pm$ 1
% Efficiency	0.08 $\pm$ 3.23 %	0.08 $\pm$ 3.23	0.08 $\pm$ 3.23	0.08 $\pm$ 3.23
$A_\epsilon \pm \sigma_{A_\epsilon}$	2.5 $\times 10^5 \pm$ 3%	2.1 $\times 10^5 \pm$ 3%	1.7 $\times 10^5 \pm$ 3%	1.3 $\times 10^5 \pm$ 3%

Table B.17: 10 % Se/soil mixture 10 channel data (Se-81m).

	0 <t< 500 s	1210<t<1750 s	2430<t<2930 s	3616 <t< 3831 s
I $\pm\sqrt{I}$	1.078 $\times 10^5 \pm$ 0.30%	9.266 $\times 10^4 \pm$ 0.33%	6.871 $\times 10^4 \pm$ 0.38%	2.293 $\times 10^4 \pm$ 0.66%
$B \pm \sigma_B$	2.241 $\times 10^4 \pm$ 0.45%	1.417 $\times 10^4 \pm$ 0.56%	8.850 $\times 10^3 \pm$ 0.72%	2.930 $\times 10^3 \pm$ 1.24%
N $\pm \sigma_N$	8.539 $\times 10^4 \pm$ 0.4%	7.849 $\times 10^4 \pm$ 0.40%	5.986 $\times 10^4 \pm$ 0.45 %	2.000 $\times 10^4 \pm$ 0.78 %
Runtime (S)	500	540	500	215
$A_{Measured} \pm \sigma_{A_{Measured}}$ (Hz)	170.8 $\pm$ 0.7	145.4 $\pm$ 0.6	119.7 $\pm$ 0.5	93.0 $\pm$ 0.7
$A_{True} \pm \sigma_{A_{True}}$ (Hz)	179.5 $\pm$ 0.7	153.4 $\pm$ 0.6	125.9 $\pm$ 0.6	95.1 $\pm$ 0.7
% Dead	6.59 $\pm$ 0.43	3.95 $\pm$ 0.42	2.26 $\pm$ 0.33	1.65 $\pm$ 0.34
$A_{DTC} \pm \sigma_{A_{DTC}}$	190 $\pm$ 1	160 $\pm$ 1	130 $\pm$ 1	97 $\pm$ 1
% Efficiency	0.08 $\pm$ 3.23 %	0.08 $\pm$ 3.23	0.08 $\pm$ 3.23	0.08 $\pm$ 3.23
$A_\epsilon \pm \sigma_{A_\epsilon}$	2.4 $\times 10^5 \pm$ 3.3%	2.0 $\times 10^5 \pm$ 3.3%	1.6 $\times 10^5 \pm$ 3.3%	1.2 $\times 10^5 \pm$ 3.3%

TABLE B.18: 10 % Se/soil mixture 3 channel data (Se-81m).

	0 <t< 500 s	1210<t<1750 s	2430<t<2930 s	3616 <t< 3831 s
I $\pm\sqrt{I}$	6.004 $\times10^4\pm$ 0.41%	5.592 $\times10^4\pm$ 0.42%	4.164 $\times10^4\pm$ 0.49%	1.404 $\times10^4\pm$ 0.84
$B \pm \sigma_B$	7.471 $10^3\pm$ 0.45%	4.722 $\times10^3\pm$ 0.56%	2.950 $\times10^3\pm$ 0.72	9.768 $\times10^2\pm$ 1.2%
N $\pm$ σ_N	5.257 $\times10^4\pm$ 0.47%	5.120 $\times10^4\pm$ 0.46%	3.869 $\times10^4\pm$ 0.53%	1.306 $\times10^4\pm$ 0.91
Runtime (S)	500	540	500	215
$A_{Measured} \pm \sigma_{A_{Measured}}$ (Hz)	105.1 $\pm$ 0.5	94.8 $\pm$ 0.4	77.4 $\pm$ 0.4	60.8 $\pm$ 0.6
$A_{True} \pm \sigma_{A_{True}}$ (Hz)	110.5 $\pm$ 0.5	100.1 $\pm$ 0.5	81.4 $\pm$ 0.4	62.1 $\pm$ 0.6
% Dead	6.59 $\pm$ 0.43	3.95 $\pm$ 0.42	2.26 $\pm$ 0.33	1.65 $\pm$ 0.34
$A_{DTC} \pm \sigma_{A_{DTC}}$	120 $\pm$ 1	100 $\pm$ 1	83 $\pm$ 1	63 $\pm$ 1
% Efficiency	0.08 $\pm$ 3.23 %	0.08 $\pm$ 3.23	0.08 $\pm$ 3.23	0.08 $\pm$ 3.23
$A_\epsilon \pm \sigma_{A_\epsilon}$	1.5 $\times10^5\pm$ 3.3%	1.3 $\times10^5\pm$ 3.3%	1.0 $\times10^5\pm$ 3.3%	7.9 $\times10^4\pm$ 3.4%

TABLE B.19: 10 % Se/soil mixture 1 channel data (Se-81m).

	615<t<1115	1850<t<2350	3015<t<3515
I $\pm\sqrt{I}$	2.632 $\times10^5\pm$ 0.19%	2.015 $\times10^5\pm$ 0.23%	1.573 $\times10^5\pm$ 0.25%
$B \pm \sigma_B$	4.788 $\times10^4\pm$ 0.66%	4.251 $\times10^4\pm$ 0.60%	3.621 $\times10^4\pm$ 0.65%
N $\pm$ σ_N	2.153 $\times10^5\pm$ 0.27%	1.590 $\times10^5\pm$ 0.32%	1.211 $\times10^5\pm$ 0.38%
Runtime (S)	500	500	500
$A_{Measured} \pm \sigma_{A_{Measured}}$ (Hz)	430.64 $\pm$ 1.2	318.0 $\pm$ 1.0	242.2 $\pm$ 0.9
$A_{True} \pm \sigma_{A_{True}}$ (Hz)	452.7 $\pm$ 1.2	334.3 $\pm$ 1.1	254.6 $\pm$ 1.0
% Dead	0.84 $\pm$ 0.16	0.65 $\pm$ 0.15	0.53 $\pm$ 0.14
$A_{DTC} \pm \sigma_{A_{DTC}}$	460 $\pm$ 1	340 $\pm$ 1	260 $\pm$ 1
% Efficiency	0.29 $\pm$ 3%	0.29 $\pm$ 3%	0.29 $\pm$ 3%
$A_\epsilon \pm \sigma_{A_\epsilon}$	5.7 $\times10^5\pm$ 3.2%	4.2 $\times10^5\pm$ 3.2%	3.2 $\times10^5\pm$ 3.3%

Table B.20: 10% sample pure selenium 10 channel data (Se-81m).

	615<t<1115	1850<t<2350	3015<t<3515
I $\pm\sqrt{I}$	2.239 $\times 10^5 \pm$ 0.21%	1.757 $\times 10^5 \pm$ 0.24%	1.280 $\times 10^5 \pm$ 0.28%
$B \pm \sigma_B$	1.436 $\times 10^4 \pm$ 0.56%	1.275 $\times 10^4 \pm$ 0.59%	1.086 $\times 10^4 \pm$ 0.65%
N $\pm$ σ_N	2.095 $\times 10^5 \pm$ 0.23 %	1.629 $\times 10^5 \pm$ 0.26 %	1.171 $\times 10^5 \pm$ 0.31 %
Runtime (S)	500	500	500
$A_{Measured} \pm \sigma_{A_{Measured}}$ (Hz)	419.1 $\pm$ 1.0	325.9 $\pm$ 0.9	234.3 $\pm$ 0.7
$A_{True} \pm \sigma_{A_{True}}$ (Hz)	440.6 $\pm$ 1.0	342.6 $\pm$ 0.9	246.3 $\pm$ 0.8
% Dead	0.84 $\pm$ 0.16	0.65 $\pm$ 0.15	0.53 $\pm$ 0.14
$A_{DTC} \pm \sigma_{A_{DTC}}$	440 $\pm$ 1	340 $\pm$ 1	250 $\pm$ 1
% Efficiency	0.29 $\pm$ 3%	0.29 $\pm$ 3%	0.29 $\pm$ 3%
$A_\epsilon \pm \sigma_{A_\epsilon}$	5.6 $\times 10^5 \pm$ 3.2%	4.3 $\times 10^5 \pm$ 3.2%	3.1 $\times 10^5 \pm$ 3.2%

Table B.21: 10% sample pure selenium 3 channel data (Se-81m).

	615<t<1115	1850<t<2350	3015<t<3515
I $\pm\sqrt{I}$	1.509 $\times 10^5 \pm$ 0.28%	1.147 $\times 10^5 \pm$ 0.30%	7.860 $\times 10^4 \pm$ 0.36%
$B \pm \sigma_B$	4.788 $\times 10^3 \pm$ 0.56 %	4.251 $\times 10^3 \pm$ 0.59%	3.621 $\times 10^3 \pm$ 0.65%
N $\pm \sigma_N$	1.461 $\times 10^5 \pm$ 0.27 %	1.104 $\times 10^5 \pm$ 0.30%	7.498 $\times 10^4 \pm$ 0.38%
Runtime (S)	500	500	500
$A_{Measured} \pm \sigma_{A_{Measured}}$ (Hz)	292.2 $\pm$ 0.8	220.9 $\pm$ 0.7	150.0 $\pm$ 0.6
$A_{True} \pm \sigma_{A_{True}}$ (Hz)	307.2 $\pm$ 0.8	232.2 $\pm$ 0.7	157.7 $\pm$ 0.6
% Dead	0.84 $\pm$ 0.16	0.65 $\pm$ 0.15	0.53 $\pm$ 0.14
$A_{DTC} \pm \sigma_{A_{DTC}}$	310 $\pm$ 1	230 $\pm$ 1	160 $\pm$ 1
% Efficiency	0.29 $\pm$ 3%	0.29 $\pm$ 3%	0.29 $\pm$ 3%
$A_\epsilon \pm \sigma_{A_\epsilon}$	3.9 $\times 10^5 \pm$ 3.2%	2.9 $\times 10^5 \pm$ 3.2%	2.0 $\times 10^5 \pm$ 3.3%

Table B.22: 10% sample pure selenium 1 channel data (Se-81m).

	07/18/17	10/17/17	1/22/18	5/17/18
I $\pm\sqrt{I}$	2.722 $\times 10^6 \pm$ 0.06%	3.301 $\times 10^6 \pm$ 0.06%	5.954 $\times 10^5 \pm$ 0.13%	4.249 $\times 10^3 \pm$ 1.53%
$B \pm \sigma_B$	2.013 $\times 10^5 \pm$ 0.27%	3.341 $\times 10^5 \pm$ 0.21%	8.216 $\times 10^4 \pm$ 0.42%	8.350 $\times 10^2 \pm$ 4.04%
N $\pm \sigma_N$	2.521 $\times 10^6 \pm$ 0.07%	2.967 $\times 10^6 \pm$ 0.05%	5.132 $\times 10^5 \pm$ 0.16%	3.414 $\times 10^3 \pm$ 2.15%
Runtime (S)	8.645 $\times 10^4$	2.340 $\times 10^5$	7.221 $\times 10^4 \pm$	9.058 $\times 10^2$
$A_{Measured} \pm \sigma_{A_{Measured}}$ (Hz)	29.16 $\pm$ 0.02	12.68 $\pm$ 0.01	7.11 $\pm$ 0.01	3.77 $\pm$ 0.08
% Efficiency	0.93 $\pm$ 3.1%	0.93 $\pm$ 3.1%	0.93 $\pm$ 3.1%	0.93 $\pm$ 3.1%
$A_\epsilon \pm \sigma_{A_\epsilon}$	3.4 $\times 10^3 \pm$ 3.1%	1.5 $\times 10^3 \pm$ 3.1%	8.3 $\times 10^2 \pm$ 3.1%	4.4 $\times 10^2 \pm$ 3.8%

Table B.23: 10% Se/soil mix 10 channel data (Se-75).

	07/18/17	10/17/17	1/22/18	5/17/18
I $\pm\sqrt{I}$	2.538 $\times 10^6 \pm$ 0.06%	2.997 $\times 10^6 \pm$ 0.06%	5.127 $\times 10^5 \pm$ 0.14%	3.537 $\times 10^3 \pm$ 1.68%
$B \pm \sigma_B$	3.825 $\times 10^4 \pm$ 0.26%	6.330 $\times 10^4 \pm$ 0.20%	1.557 $\times 10^4 \pm$ 0.40%	1.575 $\times 10^2 \pm$ 3.87%
N $\pm$ σ_N	2.500 $\times 10^6 \pm$ 0.06%	2.934 $\times 10^6 \pm$ 0.06%	4.971 $\times 10^5 \pm$ 0.14%	3.379 $\times 10^3 \pm$ 1.77%
Runtime (S)	8.645 $\times 10^4$	2.340 $\times 10^5$	7.221 $\times 10^4 \pm$	9.058 $\times 10^2$
$A_{Measured} \pm \sigma_{A_{Measured}}$ (Hz)	28.92 $\pm$ 0.02	12.54 $\pm$ 0.01	6.88 $\pm$ 0.01	3.73 $\pm$ 0.07
% Efficiency	0.93 $\pm$ 3.1%	0.93 $\pm$ 3.1%	0.93 $\pm$ 3.1%	0.93 $\pm$ 3.1%
$A_\epsilon \pm \sigma_{A_\epsilon}$	3.1 $\times 10^3 \pm$ 3.1%	1.3 $\times 10^3 \pm$ 3.1%	7.4 $\times 10^2 \pm$ 3.1%	4.0 $\times 10^2 \pm$ 3.6%

TABLE B.24: 10% Se/soil mix 3 channel data (Se-75).

	07/18/17	10/17/17	1/22/18	5/17/18
I $\pm\sqrt{I}$	1.667 $\times 10^6 \pm$ 0.08%	1.948 $\times 10^6 \pm$ 0.07%	2.594 $\times 10^5 \pm$ 0.20%	2.433 $\times 10^3 \pm$ 2.02%
$B \pm \sigma_B$	1.275 $\times 10^4 \pm$ 0.26%	2.110 $\times 10^4 \pm$ 0.20%	5.189 $\times 10^3 \pm$ 0.40%	52.49 $\pm$ 2.03
N $\pm$ σ_N	1.654 $\times 10^6 \pm$ 0.08%	1.927 $\times 10^6 \pm$ 0.07%	2.542 $\times 10^5 \pm$ 0.20%	2.381 $\times 10^3 \pm$ 2.07%
Runtime (S)	8.645 $\times 10^4$	2.340 $\times 10^5$	7.221 $\times 10^4 \pm$	9.058 $\times 10^2$
$A_{Measured} \pm \sigma_{A_{Measured}}$ (Hz)	19.14 $\pm$ 0.01	8.24 $\pm$ 0.01	3.52 $\pm$ 0.01	2.63 $\pm$ 0.05
% Efficiency	0.93 $\pm$ 3.1%	0.93 $\pm$ 3.1%	0.93 $\pm$ 3.1%	0.93 $\pm$ 3.1%
$A_\epsilon \pm \sigma_{A_\epsilon}$	2.1 $\times 10^3 \pm$ 3.1%	8.9 $\times 10^2 \pm$ 3.1%	3.8 $\times 10^2 \pm$ 3.1%	2.8 $\times 10^2 \pm$ 3.6%

Table B.25: 10% Se/soil mix 1 channel data (Se-75).

	08/01/17	11/06/17	01/18/18	5/21/18
I $\pm\sqrt{I}$	4.520 $\times 10^6 \pm$ 0.05%	1.832 $\times 10^6 \pm$ 0.07%	1.354 $\times 10^6 \pm$ 0.09%	7.554 $\times 10^5 \pm$ 0.12%
$B \pm \sigma_B$	1.626 $\times 10^6 \pm$ 0.09%	2.742 $\times 10^5 \pm$ 0.23%	2.701 $\times 10^5 \pm$ 0.23%	2.394 $\times 10^5 \pm$ 0.24%
N $\pm$ σ_N	2.894 $\times 10^6 \pm$ 0.09%	1.558 $\times 10^6 \pm$ 0.10%	1.084 $\times 10^6 \pm$ 0.12%	5.160 $\times 10^5 \pm$ 0.20%
Runtime (S)	7.4054 $\times 10^4$	7.2135 $\times 10^4$	7.3888 $\times 10^4$	7.0177 $\times 10^4$
$A_{Measured} \pm \sigma_{A_{Measured}}$ (Hz)	39.08 $\pm$ 0.04	21.60 $\pm$ 0.02	14.67 $\pm$ 0.02	7.35 $\pm$ 0.01
% Efficiency	0.93 $\pm$ 3.1%	0.93 $\pm$ 3.1%	0.93 $\pm$ 3.1%	0.93 $\pm$ 3.1%
$A_\epsilon \pm \sigma_{A_\epsilon}$	4.5 $\times 10^3 \pm$ 3.1%	2.5 $\times 10^3 \pm$ 3.1%	1.7 $\times 10^3 \pm$ 3.1%	8.5 $\times 10^2 \pm$ 3.1%

Table B.26: 10% pure witness Se 10 channel data (Se-75).

	08/01/17	11/06/17	01/18/18	5/21/18
I $\pm\sqrt{I}$	3.172 $\times 10^6 \pm$ 0.06%	1.572 $\times 10^6 \pm$ 0.08%	1.110 $\times 10^6 \pm$ 0.09%	5.561 $\times 10^5 \pm$ 0.13%
$B \pm \sigma_B$	3.060 $\times 10^5 \pm$ 0.09%	5.187 $\times 10^4 \pm$ 0.22%	5.091 $\times 10^4 \pm$ 0.22%	4.530 $\times 10^4 \pm$ 0.23%
N $\pm \sigma_N$	2.866 $\times 10^6 \pm$ 0.06%	1.520 $\times 10^6 \pm$ 0.08%	1.059 $\times 10^6 \pm$ 0.10%	5.108 $\times 10^5 \pm$ 0.15%
Runtime (S)	7.4054 $\times 10^4$	7.2135 $\times 10^4$	7.3888 $\times 10^4$	7.0177 $\times 10^4$
$A_{Measured} \pm \sigma_{A_{Measured}}$ (Hz)	38.70 $\pm$ 0.02	21.07 $\pm$ 0.02	14.33 $\pm$ 0.01	7.28 $\pm$ 0.01
% Efficiency	0.93 $\pm$ 3.1%	0.93 $\pm$ 3.1%	0.93 $\pm$ 3.1%	0.93 $\pm$ 3.1%
$A_\epsilon \pm \sigma_{A_\epsilon}$	4.2 $\times 10^3 \pm$ 3.1%	2.3 $\times 10^3 \pm$ 3.1%	1.5 $\times 10^3 \pm$ 3.1%	7.8 $\times 10^2 \pm$ 3.1%

TABLE B.27: 10% pure witness Se 3 channel data (Se-75).

	08/01/17	11/06/17	01/18/18	5/21/18
I $\pm\sqrt{I}$	2.011 $\times 10^6 \pm$ 0.07%	8.627 $\times 10^5 \pm$ 0.11%	6.004 $\times 10^5 \pm$ 0.13%	3.660 $\times 10^5 \pm$ 0.17%
$B \pm \sigma_B$	1.020 $\times 10^5 \pm$ 0.09%	1.729 $\times 10^4 \pm$ 0.22%	1.697 $\times 10^4 \pm$ 0.22%	1.510 $\times 10^4 \pm$ 0.23%
N $\pm$ σ_N	1.909 $\times 10^6 \pm$ 0.07%	8.454 $\times 10^5 \pm$ 0.11%	5.834 $\times 10^5 \pm$ 0.13%	3.509 $\times 10^5 \pm$ 0.17%
Runtime (S)	7.4054 $\times 10^4$	7.2135 $\times 10^4$	7.3888 $\times 10^4$	7.0177 $\times 10^4$
$A_{Measured} \pm \sigma_{A_{Measured}}$ (Hz)	25.78 $\pm$ 0.02	11.72 $\pm$ 0.01	7.90 $\pm$ 0.01	5.00 $\pm$ 0.01
% Efficiency	0.93 $\pm$ 3.1%	0.93 $\pm$ 3.1%	0.93 $\pm$ 3.1%	0.93 $\pm$ 3.1%
$A_\epsilon \pm \sigma_{A_\epsilon}$	2.8 $\times 10^3 \pm$ 3.1%	1.3 $\times 10^3 \pm$ 3.1%	8.5 $\times 10^2 \pm$ 3.1%	5.4 $\times 10^2 \pm$ 3.1%

TABLE B.28: 10% pure witness Se 1 channel data (Se-75).

	5/23/17	5/26/17	5/29/17	5/30/17
I $\pm\sqrt{I}$	13120 $\pm$ 114.54	17770 $\pm$ 133.30	24790 $\pm$ 157.45	16900 $\pm$ 130
$B \pm \sigma_B$	388.8 $\pm$ 63.2	297.2 $\pm$ 72.8	1145.6 $\pm$ 115.2	1024 $\pm$ 92
N $\pm$ σ_N	12731.2 $\pm$ 130.82	17472.8 $\pm$ 151.88	23644.4 $\pm$ 195.09	15876 $\pm$ 159.26
Runtime (s)	301.049	300.562	301.366	301.313
$A_{Measured} \pm \sigma_{A_{Measured}}$ (Hz)	42.29 $\pm$ 0.43	58.13 $\pm$ 0.51	78.46 $\pm$ 0.65	52.69 $\pm$ 0.53
$A_{True} \pm \sigma_{A_{True}}$ (Hz)	42.32 $\pm$ 0.43	58.18 $\pm$ 0.51	78.52 $\pm$ 0.65	52.73 $\pm$ 0.53
% Dead	2.26 $\pm$ 0.33	3.06 $\pm$ 0.30	5.06 $\pm$ 0.39	3.95 $\pm$ 0.42
$A_{DTC} \pm \sigma_{A_{DTC}}$	43.30 $\pm$ 0.46	60.02 $\pm$ 0.56	82.70 $\pm$ 0.76	54.90 $\pm$ 0.60
% Efficiency	0.0089 $\pm$ 6%	0.0422 $\pm$ 6%	0.31 $\pm$ 3%	0.31 $\pm$ 3%
$A_\epsilon \pm \sigma_{A_\epsilon}$	4.9 $\times 10^5 \pm$ 6%	1.4 $\times 10^5 \pm$ 6%	2.7 $\times 10^4 \pm$ 3%	1.8 $\times 10^4 \pm$ 3%

TABLE B.29: 170048 front outer foil data.

	5/23/17	5/26/17	5/29/17	5/30/17
I $\pm\sqrt{I}$	10360 $\pm$ 101.78	13690 $\pm$ 117.00	22570 $\pm$ 150.23	12570 $\pm$ 112.12
$B \pm \sigma_B$	344.16 $\pm$ 53.44	273.2 $\pm$ 60.16	1164.8 $\pm$ 105.6	718.32 $\pm$ 72
N $\pm$ σ_N	10015.84 $\pm$ 114.96	13416.8 $\pm$ 131.56	21405.2 $\pm$ 183.63	11851.68 $\pm$ 133.25
Runtime (s)	300.826	300.455	336.806	300.414
$A_{Measured} \pm \sigma_{A_{Measured}}$ (Hz)	33.29 $\pm$ 0.38	44.65 $\pm$ 0.44	63.55 $\pm$ 0.55	39.45 $\pm$ 0.44
$A_{True} \pm \sigma_{A_{True}}$ (Hz)	33.32 $\pm$ 0.38	44.69 $\pm$ 0.44	63.61 $\pm$ 0.55	39.48 $\pm$ 0.44
% Dead	1.65 $\pm$ 0.34	2.26 $\pm$ 0.33	3.95 $\pm$ 0.42	2.53 $\pm$ 0.31
$A_{DTC} \pm \sigma_{A_{DTC}}$	33.88 $\pm$ 0.40	45.72 $\pm$ 0.48	66.22 $\pm$ 0.64	40.50 $\pm$ 0.47
% Efficiency	0.0089 $\pm$ 6%	0.0422 $\pm$ 6%	0.31 $\pm$ 3%	0.31 $\pm$ 3%
$A_\epsilon \pm \sigma_{A_\epsilon}$	3.8 $\times 10^5 \pm$ 6%	1.1 $\times 10^5 \pm$ 6%	2.1 $\times 10^4 \pm$ 3%	1.3 $\times 10^4 \pm$ 3%

TABLE B.30: 170048 rear outer foil data.

	5/23/17	5/27/17	5/29/17
I $\pm\sqrt{I}$	1.065 $\times 10^4 \pm$ 0.97%	1.818 $\times 10^4 \pm$ 0.74%	2.081 $\times 10^4 \pm$ 0.69%
$B \pm \sigma_B$	299.25 $\pm$ 20.75	590.50 $\pm$ 29.25	676.25 $\pm$ 31.25
N $\pm\ \sigma_N$	1.035 $\times 10^4 \pm$ 1.0%	1.759 $\times 10^4 \pm$ 0.78%	2.013 $\times 10^4 \pm$ 0.73%
Runtime (s)	301.329	300.45	300.626
$A_{Measured} \pm \sigma_{A_{Measured}}$ (Hz)	34.35 $\pm$ 0.35	58.54 $\pm$ 0.46	66.97 $\pm$ 0.49
% Efficiency	(8.9 $\times 10^{-3} \pm$ 6)%	(8.5 $\times 10^{-2} \pm$ 6)%	(3.1 $\times 10^{-1} \pm$ 3)%
$A_\epsilon \pm \sigma_{A_\epsilon}$	3.9 $\times 10^5 \pm$ 6.1%	6.9 $\times 10^4 \pm$ 6.1%	2.2 $\times 10^4 \pm$ 3.1%

Table B.31: 170048 front inner foil data.

	5/23/17	5/24/17	5/27/17
I $\pm\sqrt{I}$	1.119 $\times10^4\pm$ 0.94%	1.398 $\times10^4\pm$ 0.85%	1.834 $\times10^4\pm$ 0.74%
$B \pm \sigma_B$	531.00 $\pm$ 27.50	430.25 $\pm$ 24.75	569.50 $\pm$ 29.25
N $\pm$ σ_N	1.066 $\times10^4\pm$ 1.03%	1.355 $\times10^4\pm$ 0.89%	1.778 $\times10^4\pm$ 0.78%
Runtime (s)	300.988	300.974	301.500
$A_{Measured} \pm \sigma_{A_{Measured}}$ (Hz)	35.41 $\pm$ 0.36	45.02 $\pm$ 0.40	58.94 $\pm$ 0.46
% Efficiency	8.9 $\times10^{-3}\pm$ 6%	1.7 $\times10^{-2}\pm$ 6%	8.0 $\times10^{-2}\pm$ 6%
$A_\epsilon \pm \sigma_{A_\epsilon}$	3.979 $\times10^5\pm$ 6.1%	2.648 $\times10^5\pm$ 6.1%	6.959 $\times10^4\pm$ 6.1%

Table B.32: 170048 rear inner foil data.

	0<t<300	750<t<1050	1508<t<1808	2260<5<2560
I $\pm\sqrt{I}$	2.441 $\times 10^5 \pm$ 0.20%	1.607 $\times 10^5 \pm$ 0.25%	1.126 $\times 10^5 \pm$ 0.30%	8.337 $\times 10^4 \pm$ 0.35%
$B \pm \sigma_B$	2.210 $\times 10^5 \pm$ 0.24%	1.374 $\times 10^5 \pm$ 0.30%	9.130 $\times 10^4 \pm$ 0.37%	6.233 $\times 10^4 \pm$ 0.46%
N $\pm \sigma_N$	2.310 $\times 10^5 \pm$ 3.1%	2.330 $\times 10^5 \pm$ 2.5%	2.130 $\times 10^4 \pm$ 2.2%	2.104 $\times 10^4 \pm$ 1.9%
Runtime (S)	300	300	300	300
$A_{Measured} \pm \sigma_{A_{Measured}}$ (Hz)	77.0 $\pm$ 2.4	77.7 $\pm$ 1.9	71.0 $\pm$ 1.6	70.1 $\pm$ 1.4
$A_{True} \pm \sigma_{A_{True}}$ (Hz)	79.4 $\pm$ 2.5	80.0 $\pm$ 2.0	73.2 $\pm$ 1.6	72.3 $\pm$ 1.4
% Dead	6.59 $\pm$ 0.43	5.95 $\pm$ 0.42	2.53 $\pm$ 0.31	1.92 $\pm$ 0.26
$A_{DTC} \pm \sigma_{A_{DTC}}$	85 $\pm$ 3	85 $\pm$ 2	75 $\pm$ 2	74 $\pm$ 1
% Efficiency	0.03 $\pm$ 3.25%	0.03 $\pm$ 3.25%	0.03 $\pm$ 3.25%	0.03 $\pm$ 3.25%
$A_\epsilon \pm \sigma_{A_\epsilon}$	2.8 $\times 10^5 \pm$ 5%	2.8 $\times 10^5 \pm$ 4%	2.5 $\times 10^5 \pm$ 4%	2.4 $\times 10^5 \pm$ 4%

Table B.33: 1% Se/soil mix 10 channel data part 1 (Se-81m).

	3030<5<3330	3829<t<4120	4580<t<4880	5325<t<5625
I $\pm\sqrt{I}$	6.522 $\times 10^4 \pm$ 0.39%	4.862 $\times 10^4 \pm$ 0.45%	4.037 $\times 10^4 \pm$ 0.50%	3.441 $\times 10^4 \pm$ 0.54%
$B \pm \sigma_B$	4.716 $\times 10^4 \pm$ 0.53%	3.327 $\times 10^4 \pm$ 0.64%	2.671 $\times 10^4 \pm$ 0.72 %	2.219 $\times 10^4 \pm$ 0.83%
N $\pm$ σ_N	1.806 $\times 10^4 \pm$ 2.0%	1.535 $\times 10^4 \pm$ 2.0%	1.366 $\times 10^4 \pm$ 2.0%	1.222 $\times 10^4 \pm$ 2.1%
Runtime (S)	300	300	300	300
$A_{Measured} \pm \sigma_{A_{Measured}}$ (Hz)	60.2 $\pm$ 1.2	51.2 $\pm$ 1.0	45.5 $\pm$ 0.9	40.7 $\pm$ 0.9
$A_{True} \pm \sigma_{A_{True}}$ (Hz)	72.3 $\pm$ 1.4	62.0 $\pm$ 1.2	52.7 $\pm$ 1.1	46.9 $\pm$ 1.0
% Dead	1.33 $\pm$ 0.23	0.84 $\pm$ 0.16	0.65 $\pm$ 0.15	0.65 $\pm$ 0.15
$A_{DTC} \pm \sigma_{A_{DTC}}$	63 $\pm$ 1	53 $\pm$ 1	47 $\pm$ 1	42 $\pm$ 1
% Efficiency	0.03 $\pm$ 3.25%	0.03 $\pm$ 3.25%	0.03 $\pm$ 3.25%	0.03 $\pm$ 3.25%
$A_\epsilon \pm \sigma_{A_\epsilon}$	2.1 $\times 10^5 \pm$ 4%	1.8 $\times 10^5 \pm$ 4%	1.6 $\times 10^5 \pm$ 4%	1.4 $\times 10^5 \pm$ 4%

TABLE B.34: 1% Se/soil mix 10 channel data part 2 (Se-81m).

	6085<t<6385	6835<t<7135	7585<t<7930
I $\pm\sqrt{I}$	2.866 $\times 10^4 \pm$ 0.59%	2.463 $\times 10^4 \pm$ 0.64%	2.839 $\times 10^4 \pm$ 0.59%
$B \pm \sigma_B$	1.795 $\times 10^4 \pm$ 0.90%	1.533 $\times 10^4 \pm$ 0.96%	1.948 $\times 10^4 \pm$ 0.85%
N $\pm \sigma_N$	1.071 $\times 10^4 \pm$ 2.2%	9.300 $\times 10^3 \pm$ 2.3%	8.910 $\times 10^3 \pm$ 2.6%
Runtime (S)	300	300	300
$A_{Measured} \pm \sigma_{A_{Measured}}$ (Hz)	35.7 $\pm$ 0.8	31.0 $\pm$ 0.7	25.8 $\pm$ 0.7
$A_{True} \pm \sigma_{A_{True}}$ (Hz)	36.8 $\pm$ 0.8	32.0 $\pm$ 0.7	26.7 $\pm$ 0.7
% Dead	0.51 $\pm$ 0.18	0.51 $\pm$ 0.18	0.51 $\pm$ 0.18
$A_{DTC} \pm \sigma_{A_{DTC}}$	37 $\pm$ 1	32 $\pm$ 1	27 $\pm$ 1
% Efficiency	0.03 $\pm$ 3.25%	0.03 $\pm$ 3.25%	0.03 $\pm$ 3.25%
$A_\epsilon \pm \sigma_{A_\epsilon}$	1.2 $\times 10^5 \pm$ 4%	1.1 $\times 10^5 \pm$ 4%	9.0 $\times 10^4 \pm$ 4%

TABLE B.35: 1% Se/soil mix 10 channel data part 3 (Se-81m).

	0<t<300	750<t<1050	1508<t<1808	2260<5<2560
I $\pm\sqrt{I}$	9.202 $\times 10^4 \pm$ 0.33%	6.656 $\times 10^4 \pm$ 0.39 %	4.981 $\times 10^4 \pm$ 0.45 %	3.943 $\times 10^4 \pm$ 0.50%
$B \pm \sigma_B$	6.630 $\times 10^4 \pm$ 0.24 %	4.122 $\times 10^4 \pm$ 0.30%	2.758 $\times 10^4 \pm$ 0.37%	1.870 $\times 10^4 \pm$ 0.46%
N $\pm\ \sigma_N$	2.572 $\times 10^4 \pm$ 1.3 %	2.534 $\times 10^4 \pm$ 1.1%	2.223 $\times 10^4 \pm$ 1.1%	2.073 $\times 10^4 \pm$ 1.0%
Runtime (S)	300	300	300	300
$A_{Measured} \pm \sigma_{A_{Measured}}$ (Hz)	85.73 $\pm$ 1.14	84.47 $\pm$ 0.96	74.10 $\pm$ 0.82	69.10 $\pm$ 0.72
$A_{True} \pm \sigma_{A_{True}}$ (Hz)	88.4 $\pm$ 1.2	87.1 $\pm$ 1.0	76.4 $\pm$ 0.9	71.2 $\pm$ 0.7
% Dead	6.59 $\pm$ 0.43	5.95 $\pm$ 0.42	2.53 $\pm$ 0.31	1.92 $\pm$ 0.26
$A_{DTC} \pm \sigma_{A_{DTC}}$	95 $\pm$ 1	93 $\pm$ 1	78 $\pm$ 1	73 $\pm$ 1
% Efficiency	0.03 $\pm$ 3.25%	0.03 $\pm$ 3.25%	0.03 $\pm$ 3.25%	0.03 $\pm$ 3.25%
$A_\epsilon \pm \sigma_{A_\epsilon}$	3.2 $\times 10^5 \pm$ 3.5%	3.1 $\times 10^5 \pm$ 3.5%	2.6 $\times 10^5 \pm$ 3.5%	2.4 $\times 10^5 \pm$ 3.4%

TABLE B.36: 1% Se/soil mix 3 channel data part 1 (Se-81m).

	3030<5<3330	3829<t<4120	4580<t<4880	5325<t<5625
I $\pm\sqrt{I}$	3.259 $\times10^4\pm$ 0.55%	2.578 $\times10^4\pm$ 0.62 %	2.167 $\times10^4\pm$ 0.68 %	1.863 $\times10^4\pm$ 0.73 %
$B \pm \sigma_B$	1.415 $\times10^4\pm$ 0.53 %	9.981 $\times10^3\pm$ 0.64 %	8.013 $\times10^3\pm$ 0.72 %	6.657 $\times10^3\pm$ 0.82 %
N $\pm$ σ_N	1.844 $\times10^4\pm$ 1.1%	1.580 $\times10^4\pm$ 1.1%	1.366 $\times10^4\pm$ 1.2 %	1.197 $\times10^4\pm$ 1.2%
Runtime (S)	300	300	300	300
$A_{Measured} \pm \sigma_{A_{Measured}}$ (Hz)	61.47 $\pm$ 0.65	52.66 $\pm$ 0.58	45.52 $\pm$ 0.53	39.91 $\pm$ 0.49
$A_{True} \pm \sigma_{A_{True}}$ (Hz)	63.4 $\pm$ 0.7	54.3 $\pm$ 0.6	46.9 $\pm$ 0.6	41.1 $\pm$ 0.5
% Dead	1.33 $\pm$ 0.23	0.84 $\pm$ 0.16	0.65 $\pm$ 0.15	0.65 $\pm$ 0.15
$A_{DTC} \pm \sigma_{A_{DTC}}$	64 $\pm$ 1	55 $\pm$ 1	47 $\pm$ 1	41 $\pm$ 1
% Efficiency	0.03 $\pm$ 3.25%	0.03 $\pm$ 3.25%	0.03 $\pm$ 3.25%	0.03 $\pm$ 3.25%
$A_\epsilon \pm \sigma_{A_\epsilon}$	2.1 $\times10^5\pm$ 3.4%	1.8 $\times10^5\pm$ 3.4%	1.6 $\times10^5\pm$ 3.4%	1.4 $\times10^5\pm$ 3.5%

TABLE B.37: 1% Se/soil mix 3 channel data part 2 (Se-81m).

	6085<t<6385	6835<t<7135	7585<t<7930
I $\pm\sqrt{I}$	1.577 $\times 10^4 \pm$ 0.80 %	1.331 $\times 10^4 \pm$ 0.87 %	1.481 $\times 10^4 \pm$ 0.82 %
$B \pm \sigma_B$	5.385 $\times 10^3 \pm$ 0.90 %	4.599 $\times 10^3 \pm$ 0.96 %	5.844 $\times 10^3 \pm$ 0.85 %
N $\pm \sigma_N$	1.039 $\times 10^4 \pm$ 1.3 %	8.711 $\times 10^3 \pm$ 1.4%	8.966 $\times 10^3 \pm$ 1.5%
Runtime (S)	300	300	300
$A_{Measured} \pm \sigma_{A_{Measured}}$ (Hz)	34.62 $\pm$ 0.45	29.04 $\pm$ 0.41	25.99 $\pm$ 0.38
$A_{True} \pm \sigma_{A_{True}}$ (Hz)	35.7 $\pm$ 0.5	29.9 $\pm$ 0.4	26.8 $\pm$ 0.4
% Dead	0.51 $\pm$ 0.18	0.51 $\pm$ 0.18	0.51 $\pm$ 0.18
$A_{DTC} \pm \sigma_{A_{DTC}}$	36 $\pm$ 1	30 $\pm$ 1	27 $\pm$ 1
% Efficiency	0.03 $\pm$ 3.25%	0.03 $\pm$ 3.25%	0.03 $\pm$ 3.25%
$A_\epsilon \pm \sigma_{A_\epsilon}$	1.2 $\times 10^5 \pm$ 3.5%	1.0 $\times 10^5 \pm$ 3.5%	9.0 $\times 10^4 \pm$ 3.6%

Table B.38: 1% Se/soil mix 3 channel data part 3 (Se-81m).

	0<t<300	750<t<1050	1508<t<1808	2260<5<2560
I $\pm\sqrt{I}$	3.686 $\times 10^4 \pm$ 0.52%	3.014 $\times 10^4 \pm$ 0.58%	2.396 $\times 10^4 \pm$ 0.65%	2.024 $\times 10^4 \pm$ 0.70 %
$B \pm \sigma_B$	2.210 $\times 10^4 \pm$ 0.24%	1.374 $\times 10^4 \pm$ 0.30%	9.193 $\times 10^3 \pm$ 0.37%	6.233 $\times 10^3 \pm$ 0.46%
N $\pm$ σ_N	1.476 $\times 10^4 \pm$ 1.3%	1.640 $\times 10^4 \pm$ 1.1%	1.477 $\times 10^4 \pm$ 1.1%	1.400 $\times 10^4 \pm$ 1.0%
Runtime (S)	300	300	300	300
$A_{Measured} \pm \sigma_{A_{Measured}}$ (Hz)	49.2 $\pm$ 0.7	54.7 $\pm$ 0.6	49.2 $\pm$ 0.5	46.7 $\pm$ 0.5
$A_{True} \pm \sigma_{A_{True}}$ (Hz)	50.7 $\pm$ 0.7	56.3 $\pm$ 0.6	50.7 $\pm$ 0.6	48.1 $\pm$ 0.5
% Dead	6.59 $\pm$ 0.43	5.95 $\pm$ 0.42	2.53 $\pm$ 0.31	1.92 $\pm$ 0.26
$A_{DTC} \pm \sigma_{A_{DTC}}$	54 $\pm$ 1	60 $\pm$ 1	52 $\pm$ 1	49 $\pm$ 1
% Efficiency	0.03 $\pm$ 3.25%	0.03 $\pm$ 3.25%	0.03 $\pm$ 3.25%	0.03 $\pm$ 3.25%
$A_\epsilon \pm \sigma_{A_\epsilon}$	1.8 $\times 10^5 \pm$ 3.5%	2.0 $\times 10^5 \pm$ 3.5%	1.7 $\times 10^5 \pm$ 3.4%	1.6 $\times 10^5 \pm$ 3.4%

TABLE B.39: 1% Se/soil mix 1 channel data part 1 (Se-81m).

	3030<5<3330	3829<t<4120	4580<t<4880	5325<t<5625
I $\pm\sqrt{I}$	1.711 $\times 10^4 \pm$ 0.76%	1.385 $\times 10^4 \pm$ 0.85 %	1.179 $\times 10^4 \pm$ 0.92%	9.988 $\times 10^3 \pm$ 1.0%
$B \pm \sigma_B$	4.716 $\times 10^3 \pm$ 0.53%	3.327 $\times 10^3 \pm$ 0.64%	2.671 $\times 10^3 \pm$ 0.72%	2.219 $\times 10^3 \pm$ 0.82 %
N $\pm$ σ_N	1.239 $\times 10^4 \pm$ 1.1%	1.052 $\times 10^4 \pm$ 1.1%	9.119 $\times 10^3 \pm$ 1.2%	7.769 $\times 10^3 \pm$ 1.3%
Runtime (S)	300	300	300	300
$A_{Measured} \pm \sigma_{A_{Measured}}$ (Hz)	41.3 $\pm$ 0.4	35.1 $\pm$ 0.4	30.4 $\pm$ 0.4	25.9 $\pm$ 0.3
$A_{True} \pm \sigma_{A_{True}}$ (Hz)	42.6 $\pm$ 0.5	36.2 $\pm$ 0.4	31.3 $\pm$ 0.4	26.7 $\pm$ 0.4
% Dead	1.33 $\pm$ 0.23	0.84 $\pm$ 0.16	0.65 $\pm$ 0.15	0.65 $\pm$ 0.15
$A_{DTC} \pm \sigma_{A_{DTC}}$	43 $\pm$ 1	36 $\pm$ 1	31 $\pm$ 1	27 $\pm$ 1
% Efficiency	0.03 $\pm$ 3.25%	0.03 $\pm$ 3.25%	0.03 $\pm$ 3.25%	0.03 $\pm$ 3.25%
$A_\epsilon \pm \sigma_{A_\epsilon}$	1.4 $\times 10^5 \pm$ 3.4%	1.2 $\times 10^5 \pm$ 3.4%	1.1 $\times 10^5 \pm$ 3.5%	9.0 $\times 10^4 \pm$ 3.5%

Table B.40: 1% Se/soil mix 1 channel data part 2 (Se-81m).

	6085<t<6385	6835<t<7135	7585<t<7930
I $\pm\sqrt{I}$	8.615 $\times 10^3 \pm$ 1.1%	7.053 $\times 10^3 \pm$ 1.2%	7.724 $\times 10^3 \pm$ 1.1%
$B \pm \sigma_B$	1.795 $\times 10^3 \pm$ 0.90%	1.533 $\times 10^3 \pm$ 0.96%	1.948 $\times 10^3 \pm$ 0.85%
N $\pm \sigma_N$	6.820 $\times 10^3 \pm$ 1.4%	5.520 $\times 10^3 \pm$ 1.5%	5.776 $\times 10^3 \pm$ 1.5%
Runtime (S)	300	300	300
$A_{Measured} \pm \sigma_{A_{Measured}}$ (Hz)	22.7 $\pm$ 0.3	18.4 $\pm$ 0.3	16.7 $\pm$ 0.3
$A_{True} \pm \sigma_{A_{True}}$ (Hz)	23.4 $\pm$ 0.3	19.0 $\pm$ 0.3	17.3 $\pm$ 0.3
% Dead	0.51 $\pm$ 0.18	0.51 $\pm$ 0.18	0.51 $\pm$ 0.18
$A_{DTC} \pm \sigma_{A_{DTC}}$	23 $\pm$ 1	19 $\pm$ 1	17 $\pm$ 1
% Efficiency	0.03 $\pm$ 3.25%	0.03 $\pm$ 3.25%	0.03 $\pm$ 3.25%
$A_\epsilon \pm \sigma_{A_\epsilon}$	7.8 $\times 10^4 \pm$ 3.5%	6.4 $\times 10^4 \pm$ 3.6%	5.8 $\times 10^4 \pm$ 3.6%

Table B.41: 1% Se/soil mix 1 channel data part 3 (Se-81m).

	367<t<667	1126<t<1426	1886 <t<2186	2640<t<2940
I $\pm\sqrt{I}$	8.423 $\times10^4\pm$ 0.34%	7.285 $\times10^4\pm$ 0.37%	6.282 $\times10^4\pm$ 0.40%	5.343 $\times10^4\pm$ 0.43%
$B \pm \sigma_B$	2.171 $\times10^4\pm$ 0.83%	1.867 $\times10^4\pm$ 0.89%	1.432 $\times10^4\pm$ 1.0%	1.284 $\times10^4\pm$ 1.1%
N $\pm$ σ_N	6.252 $\times10^4\pm$ 0.55%	5.418 $\times10^4\pm$ 0.58%	4.850 $\times10^4\pm$ 0.60%	4.059 $\times10^4\pm$ 0.66%
Runtime (S)	300	300	300	300
$A_{Measured} \pm \sigma_{A_{Measured}}$ (Hz)	208.4 $\pm$ 1.1	180.6 $\pm$ 1.1	161.7 $\pm$ 1.0	135.3 $\pm$ 0.9
$A_{True} \pm \sigma_{A_{True}}$ (Hz)	214.8 $\pm$ 1.2	186.1 $\pm$ 1.1	166.6 $\pm$ 1.0	139.4 $\pm$ 0.9
% Dead	0.41 $\pm$ 0.11	0.29 $\pm$ 0.11	0.29 $\pm$ 0.11	0.24 $\pm$ 0.10
$A_{DTC} \pm \sigma_{A_{DTC}}$	220 $\pm$ 1	190 $\pm$ 1	170 $\pm$ 1	140 $\pm$ 1
% Efficiency	0.03 $\pm$ 3.25%	0.03 $\pm$ 3.25%	0.03 $\pm$ 3.25%	0.03 $\pm$ 3.25%
$A_\epsilon \pm \sigma_{A_\epsilon}$	7.2 $\times10^5\pm$ 3.3%	6.2 $\times10^5\pm$ 3.3%	5.6 $\times10^5\pm$ 3.3%	4.7 $\times10^5\pm$ 3.3%

TABLE B.42: 1% pure selenium 10 channel data (Se-81m) part 1.

	3440<t<3740	4200<t<4500	4950<t<5250	5710<t<6010
I $\pm\sqrt{I}$	4.726 $\times 10^4 \pm$ 0.46%	4.030 $\times 10^4 \pm$ 0.50%	3.714 $\times 10^4 \pm$ 0.52%	3.187 $\times 10^4 \pm$ 0.56%
$B \pm \sigma_B$	1.193 $\times 10^4 \pm$ 1.1%	1.084 $\times 10^4 \pm$ 1.2%	1.032 $\times 10^4 \pm$ 1.2%	9.377 $\times 10^3 \pm$ 1.3%
N $\pm$ σ_N	3.533 $\times 10^4 \pm$ 0.72%	2.946 $\times 10^4 \pm$ 0.81%	2.682 $\times 10^4 \pm$ 0.85%	2.249 $\times 10^4 \pm$ 0.95%
Runtime (S)	300	300	300	300
$A_{Measured} \pm \sigma_{A_{Measured}}$ (Hz)	117.8 $\pm$ 0.9	98.2 $\pm$ 0.8	89.4 $\pm$ 0.8	75.0 $\pm$ 0.7
$A_{True} \pm \sigma_{A_{True}}$ (Hz)	121.4 $\pm$ 0.9	101.2 $\pm$ 0.8	92.1 $\pm$ 0.8	77.3 $\pm$ 0.7
% Dead	0.24 $\pm$ 0.10	0.24 $\pm$ 0.10	0.24 $\pm$ 0.10	0.24 $\pm$ 0.10
$A_{DTC} \pm \sigma_{A_{DTC}}$	120 $\pm$ 1	100 $\pm$ 1	92 $\pm$ 1	77 $\pm$ 1
% Efficiency	0.03 $\pm$ 3.25%	0.03 $\pm$ 3.25%	0.03 $\pm$ 3.25%	0.03 $\pm$ 3.25%
$A_\epsilon \pm \sigma_{A_\epsilon}$	4.1 $\times 10^5 \pm$ 3.3%	3.4 $\times 10^5 \pm$ 3.3%	3.1 $\times 10^5 \pm$ 3.4%	2.6 $\times 10^4 \pm$ 3.4%

TABLE B.43: 1% pure selenium 10 channel data (Se-81m) part 2.

	6460 <t<6760	7210<t<7510	8010 <t<8310
I $\pm\sqrt{I}$	2.887 $\times 10^4 \pm$ 0.59%	2.492 $\times 10^4 \pm$ 0.63%	2.291 $\times 10^4 \pm$ 0.66%
$B \pm \sigma_B$	1.031 $\times 10^4 \pm$ 1.2%	9.055 $\times 10^3 \pm$ 1.3%	8.741 $\times 10^3 \pm$ 1.3%
N $\pm$ σ_N	1.856 $\times 10^4 \pm$ 1.1 %	1.587 $\times 10^4 \pm$ 1.2%	1.417 $\times 10^4 \pm$ 1.3%
Runtime (S)	300	300	300
$A_{Measured} \pm \sigma_{A_{Measured}}$ (Hz)	61.9 $\pm$ 0.7	52.9 $\pm$ 0.7	47.2 $\pm$ 0.6
$A_{True} \pm \sigma_{A_{True}}$ (Hz)	63.8 $\pm$ 0.7	54.5 $\pm$ 0.7	48.7 $\pm$ 0.7
% Dead	0.24 $\pm$ 0.10	0.24 $\pm$ 0.10	0.24 $\pm$ 0.10
$A_{DTC} \pm \sigma_{A_{DTC}}$	64 $\pm$ 1	55 $\pm$ 1	49 $\pm$ 1
% Efficiency	0.03 $\pm$ 3.25%	0.03 $\pm$ 3.25%	0.03 $\pm$ 3.25%
$A_\epsilon \pm \sigma_{A_\epsilon}$	2.1 $\times 10^5 \pm$ 3.4%	1.8 $\times 10^5 \pm$ 3.5%	1.6 $\times 10^5 \pm$ 3.5%

Table B.44: 1% pure selenium 10 channel data (Se-81m) part 3.

	367<t<667	1126<t<1426	1886 <t<2186	2640<t<2940
I $\pm\sqrt{I}$	6.687 $\times 10^4 \pm$ 0.39 %	5.807 $\times 10^4 \pm$ 0.41 %	5.182 $\times 10^4 \pm$ 0.44 %	4.300 $\times 10^4 \pm$ 0.48%
$B \pm \sigma_B$	6.513 $\times 10^3 \pm$ 0.83%	5.601 $\times 10^3 \pm$ 0.89%	4.296 $\times 10^3 \pm$ 1.0%	3.852 $\times 10^3 \pm$ 1.1%
N $\pm\ \sigma_N$	6.036 $\times 10^4 \pm$ 0.44%	5.247 $\times 10^4 \pm$ 0.47%	4.752 $\times 10^4 \pm$ 0.49%	3.915 $\times 10^4 \pm$ 0.54 %
Runtime (S)	300	300	300	300
$A_{Measured} \pm \sigma_{A_{Measured}}$ (Hz)	201.2 $\pm$ 0.9	174.9 $\pm$ 0.8	158.4 $\pm$ 0.8	130.5 $\pm$ 0.7
$A_{True} \pm \sigma_{A_{True}}$ (Hz)	207.3 $\pm$ 0.9	180.2 $\pm$ 0.9	163.7 $\pm$ 0.8	134.5 $\pm$ 0.7
% Dead	0.41 $\pm$ 0.11	0.29 $\pm$ 0.11	0.29 $\pm$ 0.11	0.24 $\pm$ 0.10
$A_{DTC} \pm \sigma_{A_{DTC}}$	210 $\pm$ 1	180 $\pm$ 1	160 $\pm$ 1	130 $\pm$ 1
% Efficiency	0.03 $\pm$ 3.25%	0.03 $\pm$ 3.25%	0.03 $\pm$ 3.25%	0.03 $\pm$ 3.25%
$A_\epsilon \pm \sigma_{A_\epsilon}$	6.9 $\times 10^5 \pm$ 3.3%	6.0 $\times 10^5 \pm$ 3.3%	5.5 $\times 10^5 \pm$ 3.3%	4.5 $\times 10^5 \pm$ 3.3%

TABLE B.45: 1% pure selenium 3 channel data (Se-81m) part 1.

	3440<t<3740	4200<t<4500	4950<t<5250	5710<t<6010
I $\pm\sqrt{I}$	3.797 $\times10^4\pm$ 0.51 %	3.167 $\times10^4\pm$ 0.56 %	2.913 $\times10^4\pm$ 0.59%	2.454 $\times10^4\pm$ 0.64 %
$B \pm \sigma_B$	3.579 $\times10^3\pm$ 1.1%	3.252 $\times10^3\pm$ 1.2%	3.096 $\times10^3\pm$ 1.2%	2.813 $\times10^3\pm$ 1.3%
N $\pm$ σ_N	3.439 $\times10^4\pm$ 0.58%	2.842 $\times10^4\pm$ 0.64%	2.603 $\times10^4\pm$ 0.67%	2.173 $\times10^4\pm$ 0.74%
Runtime (S)	300	300	300	300
$A_{Measured} \pm \sigma_{A_{Measured}}$ (Hz)	114.6 $\pm$ 0.7	94.7 $\pm$ 0.6	86.8 $\pm$ 0.6	72.4 $\pm$ 0.5
$A_{True} \pm \sigma_{A_{True}}$ (Hz)	118.1 $\pm$ 0.7	97.6 $\pm$ 0.6	89.4 $\pm$ 0.6	74.6 $\pm$ 0.6
% Dead	0.24 $\pm$ 0.10	0.24 $\pm$ 0.10	0.24 $\pm$ 0.10	0.24 $\pm$ 0.10
$A_{DTC} \pm \sigma_{A_{DTC}}$	120 $\pm$ 1	98 $\pm$ 1	90 $\pm$ 1	75 $\pm$ 1
% Efficiency	0.03 $\pm$ 3.25%	0.03 $\pm$ 3.25%	0.03 $\pm$ 3.25%	0.03 $\pm$ 3.25%
$A_\epsilon \pm \sigma_{A_\epsilon}$	3.9 $\times10^5\pm$ 3.3%	3.3 $\times10^5\pm$ 3.3%	3.0 $\times10^5\pm$ 3.3%	2.5 $\times10^5\pm$ 3.3%

TABLE B.46: 1% pure selenium 3 channel data (Se-81m) part 2.

	6460 <t<6760	7210<t<7510	8010 <t<8310
I $\pm\sqrt{I}$	2.096 $\times 10^4 \pm$ 0.69%	1.840 $\times 10^4 \pm$ 0.74%	1.642 $\times 10^4 \pm$ 0.78%
$B \pm \sigma_B$	3.093 $\times 10^3 \pm$ 1.2%	2.716 $\times 10^3 \pm$ 1.3%	2.622 $\times 10^3 \pm$ 1.3%
N $\pm$ σ_N	1.787 $\times 10^4 \pm$ 0.84%	1.569 $\times 10^4 \pm$ 0.89%	1.380 $\times 10^4 \pm$ 0.96 %
Runtime (S)	300	300	300
$A_{Measured} \pm \sigma_{A_{Measured}}$ (Hz)	59.6 $\pm$ 0.5	52.3 $\pm$ 0.5	46.0 $\pm$ 0.4
$A_{True} \pm \sigma_{A_{True}}$ (Hz)	61.4 $\pm$ 0.5	53.9 $\pm$ 0.5	47.4 $\pm$ 0.5
% Dead	0.24 $\pm$ 0.10	0.24 $\pm$ 0.10	0.24 $\pm$ 0.10
$A_{DTC} \pm \sigma_{A_{DTC}}$	62 $\pm$ 1	54 $\pm$ 1	48 $\pm$ 1
% Efficiency	0.03 $\pm$ 3.25%	0.03 $\pm$ 3.25%	0.03 $\pm$ 3.25%
$A_\epsilon \pm \sigma_{A_\epsilon}$	2.1 $\times 10^5 \pm$ 3.3%	1.8 $\times 10^5 \pm$ 3.4%	1.6 $\times 10^5 \pm$ 3.4%

Table B.47: 1% pure selenium 3 channel data (Se-81m) part 3.

	367<t<667	1126<t<1426	1886 <t<2186	2640<t<2940
I $\pm\sqrt{I}$	4.239 $\times 10^4 \pm$ 0.49%	3.743 $\times 10^4 \pm$ 0.52%	3.292 $\times 10^4 \pm$ 0.55%	2.812 $\times 10^4 \pm$ 0.60%
$B \pm \sigma_B$	2.171 $\times 10^3 \pm$ 0.83 %	1.867 $\times 10^3 \pm$ 0.89%	1.432 $\times 10^3 \pm$ 1.0%	1.284 $\times 10^3 \pm$ 1.1%
N $\pm$ σ_N	4.022 $\times 10^4 \pm$ 0.51 %	3.556 $\times 10^4 \pm$ 0.55%	3.149 $\times 10^4 \pm$ 0.58%	2.684 $\times 10^4 \pm$ 0.63%
Runtime (S)	300	300	300	300
$A_{Measured} \pm \sigma_{A_{Measured}}$ (Hz)	134.1 $\pm$ 0.7	118.5 $\pm$ 0.7	105.0 $\pm$ 0.6	89.5 $\pm$ 0.6
$A_{True} \pm \sigma_{A_{True}}$ (Hz)	138.2 $\pm$ 0.7	122.2 $\pm$ 0.7	108.2 $\pm$ 0.6	92.2 $\pm$ 0.6
% Dead	0.41 $\pm$ 0.11	0.29 $\pm$ 0.11	0.29 $\pm$ 0.11	0.24 $\pm$ 0.10
$A_{DTC} \pm \sigma_{A_{DTC}}$	140 $\pm$ 1	120 $\pm$ 1	110 $\pm$ 1	92 $\pm$ 1
% Efficiency	0.03 $\pm$ 3.25%	0.03 $\pm$ 3.25%	0.03 $\pm$ 3.25%	0.03 $\pm$ 3.25%
$A_\epsilon \pm \sigma_{A_\epsilon}$	4.6 $\times 10^5 \pm$ 3.3%	4.1 $\times 10^5 \pm$ 3.3%	3.6 $\times 10^5 \pm$ 3.3%	3.1 $\times 10^5 \pm$ 3.3%

Table B.48: 1% pure selenium 1 channel data (Se-81m) part 1.

	3440<t<3740	4200<t<4500	4950<t<5250	5710<t<6010
I $\pm\sqrt{I}$	2.456 $\times 10^4 \pm$ 0.64%	2.016 $\times 10^4 \pm$ 0.70%	1.829 $\times 10^4 \pm$ 0.74%	1.539 $\times 10^4 \pm$ 0.81 %
$B \pm \sigma_B$	1.193 $\times 10^3 \pm$ 1.1%	1.084 $\times 10^3 \pm$ 1.2 %	1.032 $\times 10^3 \pm$ 1.2%	9.377 $\times 10^2 \pm$ 1.3%
N $\pm$ σ_N	2.337 $\times 10^4 \pm$ 0.67%	1.908 $\times 10^4 \pm$ 0.75%	1.726 $\times 10^4 \pm$ 0.79%	1.445 $\times 10^4 \pm$ 0.86 %
Runtime (S)	300	300	300	300
$A_{Measured} \pm \sigma_{A_{Measured}}$ (Hz)	77.9 $\pm$ 0.5	63.6 $\pm$ 0.5	57.5 $\pm$ 0.5	48.2 $\pm$ 0.4
$A_{True} \pm \sigma_{A_{True}}$ (Hz)	80.3 $\pm$ 0.5	65.5 $\pm$ 0.5	59.3 $\pm$ 0.5	49.6 $\pm$ 0.4
% Dead	0.24 $\pm$ 0.10	0.24 $\pm$ 0.10	0.24 $\pm$ 0.10	0.24 $\pm$ 0.10
$A_{DTC} \pm \sigma_{A_{DTC}}$	80 $\pm$ 1	66 $\pm$ 1	59 $\pm$ 1	50 $\pm$ 1
% Efficiency	0.03 $\pm$ 3.25%	0.03 $\pm$ 3.25%	0.03 $\pm$ 3.25%	0.03 $\pm$ 3.25%
$A_\epsilon \pm \sigma_{A_\epsilon}$	2.7 $\times 10^5 \pm$ 3.3%	2.2 $\times 10^5 \pm$ 3.3%	2.0 $\times 10^5 \pm$ 3.3%	1.7 $\times 10^5 \pm$ 3.3%

TABLE B.49: 1% pure selenium 1 channel data (Se-81m) part 2.

	6460 <t<6760	7210<t<7510	8010 <t<8310
I $\pm\sqrt{I}$	2.096 $\times10^4\pm$ 0.69%	1.840 $\times10^4\pm$ 0.74%	1.642 $\times10^4\pm$ 0.78%
$B \pm \sigma_B$	3.093 $\times10^3\pm$ 1.2%	2.716 $\times10^3\pm$ 1.3%	2.622 $\times10^3\pm$ 1.3%
N $\pm$ σ_N	1.787 $\times10^4\pm$ 0.84%	1.569 $\times10^4\pm$ 0.89%	1.380 $\times10^4\pm$ 0.96 %
Runtime (S)	300	300	300
$A_{Measured} \pm \sigma_{A_{Measured}}$ (Hz)	59.6 $\pm$ 0.5	52.3 $\pm$ 0.5	46.0 $\pm$ 0.4
$A_{True} \pm \sigma_{A_{True}}$ (Hz)	61.4 $\pm$ 0.5	53.9 $\pm$ 0.5	47.4 $\pm$ 0.5
% Dead	0.24 $\pm$ 0.10	0.24 $\pm$ 0.10	0.24 $\pm$ 0.10
$A_{DTC} \pm \sigma_{A_{DTC}}$	62 $\pm$ 1	54 $\pm$ 1	48 $\pm$ 1
% Efficiency	0.03 $\pm$ 3.25%	0.03 $\pm$ 3.25%	0.03 $\pm$ 3.25%
$A_\epsilon \pm \sigma_{A_\epsilon}$	2.1 $\times10^5\pm$ 3.3%	1.8 $\times10^5\pm$ 3.4%	1.6 $\times10^5\pm$ 3.4%

Table B.50: 1% pure selenium 1 channel data (Se-81m) part 3.

	6/23/17	10/26/17	11/29/17	05/16/18
I $\pm\sqrt{I}$	1.712 $\times 10^6 \pm$ 0.08%	1.366 $\times 10^6 \pm$ 0.09%	1.887n $\times 10^6 \pm$ 0.07%	5.810 $\times 10^5 \pm$ 0.10%
$B \pm \sigma_B$	3.178 $\times 10^5 \pm$ 0.12%	5.778 $\times 10^5 \pm$ 0.16%	8.032 $\times 10^5 \pm$ 0.13%	3.517 $\times 10^5 \pm$ 0.20%
N $\pm$ σ_N	1.394 $\times 10^6 \pm$ 0.10%	7.882 $\times 10^5 \pm$ 0.19%	1.084 $\times 10^6 \pm$ 0.16%	2.293 $\times 10^5 \pm$ 0.45%
Runtime (S)	6.6683 $\times 10^4$	7.906 $\times 10^4$	1.44371 $\times 10^5$	6.4418 $\times 10^4$
$A_{Measured} \pm \sigma_{A_{Measured}}$ (Hz)	20.91 $\pm$ 0.02	9.97 $\pm$ 0.02	7.51 $\pm$ 0.01	3.56 $\pm$ 0.02
% Efficiency	0.93 $\pm$ 3.1%	0.93 $\pm$ 3.1%	0.93 $\pm$ 3.1%	0.93 $\pm$ 3.1%
$A_\epsilon \pm \sigma_{A_\epsilon}$	2.3 $\times 10^3 \pm$ 3.1%	1.2 $\times 10^3 \pm$ 3.1%	8.7 $\times 10^2 \pm$ 3.1%	4.1 $\times 10^2 \pm$ 6.5%

Table B.51: 1% Se/soil mix 10 channel data (Se-75).

	6/23/17	10/26/17	11/29/17	05/16/18
I $\pm\sqrt{I}$	1.481 $\times 10^6 \pm$ 0.08%	8.494 $\times 10^5 \pm$ 0.11%	1.162 $\times 10^6 \pm$ 0.09%	2.776 $\times 10^5 \pm$ 0.19%
$B \pm \sigma_B$	9.594 $\times 10^5 \pm$ 0.16%	1.040 $\times 10^5 \pm$ 0.15%	1.451 $\times 10^4 \pm$ 0.13%	6.354 $\times 10^4 \pm$ 0.19%
N $\pm$ σ_N	1.385 $\times 10^6 \pm$ 0.09%	7.454 $\times 10^5 \pm$ 0.13%	1.098 $\times 10^6 \pm$ 0.09%	2.141 $\times 10^5 \pm$ 0.25%
Runtime (S)	6.6683 $\times 10^4$	7.906 $\times 10^4$	1.44371 $\times 10^5$	6.4418 $\times 10^4$
$A_{Measured} \pm \sigma_{A_{Measured}}$ (Hz)	20.77 $\pm$ 0.02	9.43 $\pm$ 0.01	7.61 $\pm$ 0.01	3.32 $\pm$ 0.01
% Efficiency	0.93 $\pm$ 3.1%	0.93 $\pm$ 3.1%	0.93 $\pm$ 3.1%	0.93 $\pm$ 3.1%
$A_\epsilon \pm \sigma_{A_\epsilon}$	2.2 $\times 10^3 \pm$ 3.1$	1.0 $\times 10^3 \pm$ 3.1%	8.3 $\times 10^2 \pm$ 3.1%	3.6 $\times 10^2 \pm$ 3.1%

TABLE B.52: 1% Se/soil mix 3 channel data (Se-75).

	6/23/17	10/26/17	11/29/17	05/16/18
I $\pm\sqrt{I}$	1.481 $\times 10^6 \pm$ 0.08%	8.494 $\times 10^5 \pm$ 0.11%	1.162 $\times 10^6 \pm$ 0.09%	2.776 $\times 10^5 \pm$ 0.19%
$B \pm \sigma_B$	9.594 $\times 10^5 \pm$ 0.16%	1.040 $\times 10^5 \pm$ 0.15%	1.451 $\times 10^4 \pm$ 0.13%	6.354 $\times 10^4 \pm$ 0.19%
N $\pm$ σ_N	1.385 $\times 10^6 \pm$ 0.09%	7.454 $\times 10^5 \pm$ 0.13%	1.098 $\times 10^6 \pm$ 0.09%	2.141 $\times 10^5 \pm$ 0.25%
Runtime (S)	6.6683 $\times 10^4$	7.906 $\times 10^4$	1.44371 $\times 10^5$	6.4418 $\times 10^4$
$A_{Measured} \pm \sigma_{A_{Measured}}$ (Hz)	20.77 $\pm$ 0.02	9.43 $\pm$ 0.01	7.61 $\pm$ 0.01	3.32 $\pm$ 0.01
% Efficiency	0.93 $\pm$ 3.1%	0.93 $\pm$ 3.1%	0.93 $\pm$ 3.1%	0.93 $\pm$ 3.1%
$A_\epsilon \pm \sigma_{A_\epsilon}$	2.2 $\times 10^3 \pm$ 3.1%	1.0 $\times 10^3 \pm$ 3.1%	8.3 $\times 10^2 \pm$ 3.1%	3.6 $\times 10^2 \pm$ 3.1%

TABLE B.53: 1% Se/soil mix 1 channel data (Se-75).

	07/20/17	10/09/17	12/05/17
I $\pm\sqrt{I}$	3.594 $\times 10^6 \pm$ 0.05%	1.288 $\times 10^6 \pm$ 0.09%	1.769 $\times 10^6 \pm$ 0.08%
$B \pm \sigma_B$	5.810 $\times 10^5 \pm$ 0.16%	2.739 $\times 10^5 \pm$ 0.23%	4.192 $\times 10^5 \pm$ 0.19%
N $\pm\ \sigma_N$	3.013 $\times 10^6 \pm$ 0.07%	1.014 $\times 10^6 \pm$ 0.13%	1.350 $\times 10^6 \pm$ 0.11%
Runtime (S)	8.3683 $\times 10^4$	5.3016 $\times 10^4$	9.0643 $\times 10^4$
$A_{Measured} \pm \sigma_{A_{Measured}}$ (Hz)	36.01 $\pm$ 0.03	19.13 $\pm$ 0.02	14.89 $\pm$ 0.02
% Efficiency	0.93 $\pm$ 3.1%	0.93 $\pm$ 3.1%	0.93 $\pm$ 3.1%
$A_\epsilon \pm \sigma_{A_\epsilon}$	4.2 $\times 10^3 \pm$ 3.1%	2.2 $\times 10^3 \pm$ 3.1%	1.7 $\times 10^3 \pm$ 3.1%

Table B.54: 1% pure witness Se 10 channel data (Se-75).

	07/20/17	10/09/17	12/05/17
I $\pm\sqrt{I}$	3.099 $\times 10^6 \pm$ 0.06%	1.048 $\times 10^6 \pm$ 0.10%	1.368 $\times 10^6 \pm$ 0.09%
$B \pm \sigma_B$	1.097 $\times 10^5 \pm$ 0.15%	5.157 $\times 10^4 \pm$ 0.22%	7.923 $\times 10^4 \pm$ 0.18%
N $\pm\ \sigma_N$	2.989 $\times 10^6 \pm$ 0.06%	9.964 $\times 10^5 \pm$ 0.10%	1.289 $\times 10^6 \pm$ 0.09%
Runtime (S)	8.3683 $\times 10^4$	5.3016 $\times 10^4$	9.0643 $\times 10^4$
$A_{Measured} \pm \sigma_{A_{Measured}}$ (Hz)	35.72 $\pm$ 0.02	18.79 $\pm$ 0.02	14.22 $\pm$ 0.01
% Efficiency	0.93 $\pm$ 3.1%	0.93 $\pm$ 3.1%	0.93 $\pm$ 3.1%
$A_\epsilon \pm \sigma_{A_\epsilon}$	3.8 $\times 10^3 \pm$ 3.1%	2.0 $\times 10^3 \pm$ 3.1%	1.5 $\times 10^3 \pm$ 3.1%

TABLE B.55: 1% pure witness Se 3 channel data (Se-75).

	07/20/17	10/09/17	12/05/17
I $\pm\sqrt{I}$	$2.022 \times 10^{6} \pm 0.07\%$	$6.010 \times 10^{5} \pm 0.13\%$	$6.947 \times 10^{5} \pm 0.12\%$
$B \pm \sigma_B$	$3.655 \times 10^{4} \pm 0.15\%$	$1.719 \times 10^{4} \pm 0.22\%$	$2.641 \times 10^{4} \pm 0.18\%$
N $\pm \sigma_N$	$1.985 \times 10^{6} \pm 0.07\%$	$5.838 \times 10^{5} \pm 0.13\%$	$6.683 \times 10^{5} \pm 0.12\%$
Runtime (S)	8.3683×10^{4}	5.3016×10^{4}	9.0643×10^{4}
$A_{Measured} \pm \sigma_{A_{Measured}}$ (Hz)	23.73 ± 0.02	11.01 ± 0.01	7.37 ± 0.01
% Efficiency	$0.93 \pm 3.1\%$	$0.93 \pm 3.1\%$	$0.93 \pm 3.1\%$
$A_{\epsilon} \pm \sigma_{A_{\epsilon}}$	$2.6 \times 10^{3} \pm 3.1\%$	$1.2 \times 10^{3} \pm 3.1\%$	$7.9 \times 10^{2} \pm 3.1\%$

TABLE B.56: 1% pure witness Se 1 channel data (Se-75).

	5/23/17	5/26/17	5/27/17	5/29/17	5/30/17
I $\pm\sqrt{I}$	5593 $\pm$ 77.03	8045 $\pm$ 89.69	9845 $\pm$ 99.22	11620 $\pm$ 107.80	7532 $\pm$ 86.79
$B \pm \sigma_B$	365.28 $\pm$ 28.16	291.36 $\pm$ 24.96	428.48 $\pm$ 30.4	688 $\pm$ 38.4	365.38 $\pm$ 28.16
N $\pm$ σ_N	5227.72 $\pm$ 2.02	7753.64 $\pm$ 93.10	9416.52 $\pm$ 103.77	10932 $\pm$ 114.44	7166.72 $\pm$ 91.24
Runtime (S)	300.587	300.511	300.622	302.195	301.247
$A_{Measured} \pm \sigma_{A_{Measured}}$ (Hz)	17.39 $\pm$ 0.27	25.80 $\pm$ 0.31	31.32 $\pm$ 0.35	36.18 $\pm$ 0.38	23.79 $\pm$ 0.30
$A_{True} \pm \sigma_{A_{True}}$ (Hz)	17.40 $\pm$ 0.27	25.82 $\pm$ 0.31	31.35 $\pm$ 0.35	36.21 $\pm$ 0.38	23.81 $\pm$ 0.30
% Dead	2.53 $\pm$ 0.31	3.95 $\pm$ 0.42	5.06 $\pm$ 0.39	5.87 $\pm$ 0.54	5.06 $\pm$ 0.39
$A_{DTC} \pm \sigma_{A_{DTC}}$	17.85 $\pm$ 0.28	26.88 $\pm$ 0.34	33.02 $\pm$ 0.39	38.47 $\pm$ 0.46	25.08 $\pm$ 0.33
% Efficiency	0.0089 $\pm$ 6%	0.0422 $\pm$ 6%	0.0847 $\pm$ 6%	0.31 $\pm$ 3%	0.31 $\pm$ 3%
$A_\epsilon \pm \sigma_{A_\epsilon}$	2.0 $\times 10^5 \pm$ 6%	6.4 $\times 10^4 \pm$ 6%	3.9 $\times 10^4 \pm$ 6%	1.2 $\times 10^4 \pm$ 3%	8.1 $\times 10^3 \pm$ 3%

TABLE B.57: 170049 front outer foil data.

	5/23/17	5/29/17	5/30/17
I $\pm\sqrt{I}$	4337 $\pm$ 65.86	8243 $\pm$ 90.79	5573 $\pm$ 74.65
$B \pm \sigma_B$	122.90 $\pm$ 16	388.96 $\pm$ 28.96	250.88 $\pm$ 23.36
N $\pm$ σ_N	4214.1 $\pm$ 67.78	7854.04 $\pm$ 95.30	5322.12 $\pm$ 78.22
Runtime (S)	301.51	300.197	300.631
$A_{Measured} \pm \sigma_{A_{Measured}}$ (Hz)	13.98 $\pm$ 0.22	26.16 $\pm$ 0.32	17.70 $\pm$ 0.26
$A_{True} \pm \sigma_{A_{True}}$ (Hz)	13.99 $\pm$ 0.22	26.18 $\pm$ 0.32	17.71 $\pm$ 0.26
% Dead	1.92 $\pm$ 0.26	3.95 $\pm$ 0.42	3.06 $\pm$ 0.30
$A_{DTC} \pm \sigma_{A_{DTC}}$	14.26 $\pm$ 0.23	27.26 $\pm$ 0.35	18.27 $\pm$ 0.27
% Efficiency	0.0089 $\pm$ 6%	0.31 $\pm$ 3%	0.31 $\pm$ 3%
$A_\epsilon \pm \sigma_{A_\epsilon}$	1.6 $\times 10^5 \pm$ 6%	8.8 $\times 10^3 \pm$ 3%	5.9 $\times 10^3 \pm$ 3%

TABLE B.58: 170049 rear outer foil data.

	5/23/17	5/24/17	5/29/17	5/30/17
I $\pm\sqrt{I}$	7.491 $\times 10^3 \pm$ 1.2%	9.907 $\times 10^3 \pm$ 1.0%	1.69 $\times 10^4 \pm$ 0.77%	1.029 $\times 10^4 \pm$ 0.99%
$B \pm \sigma_B$	494.25 $\pm$ 26.50	364.50 $\pm$ 23.00	915.00 $\pm$ 37.5	527.75 $\pm$ 27.50
N $\pm$ σ_N	6.997 $\times 10^3 \pm$ 1.3%	9.542 $\times 10^3 \pm$ 1.1%	1.598 $\times 10^4 \pm$ 0.85%	9.762 $\times 10^3 \pm$ 1.1%
Runtime (S)	300.673	301.121	301.584	304.911
$A_{Measured} \pm \sigma_{A_{Measured}}$ (Hz)	23.27 $\pm$ 0.30	31.69 $\pm$ 0.34	53.00 $\pm$ 0.45	32.02 $\pm$ 0.34
% Efficiency	8.9 $\times 10^{-3} \pm$ 6%	1.7 $\times 10^{-2} \pm$ 6%	3.1 $\times 10^{-1} \pm$ 3%	3.1 $\times 10^{-1} \pm$ 3%
$A_\epsilon \pm \sigma_{A_\epsilon}$	2.6 $\times 10^5 \pm$ 6.1%	1.9 $\times 10^5 \pm$ 6.1%	1.7 $\times 10^4 \pm$ 3.1%	1.0 $\times 10^4 \pm$ 3.2%

Table B.59: 170049 front inner foil data.

	5/23/17	5/27/17	5/29/17	5/30/17
I $\pm\sqrt{I}$	8.572 $\times 10^3 \pm$ 1.08%	1.551 $\times 10^4 \pm$ 0.80%	1.794 $\times 10^4 \pm$ 0.75%	1.250 $\times 10^4 \pm$ 0.89%
$B \pm \sigma_B$	516.00 $\pm$ 27.25	749.50 $\pm$ 32.75	972.25 $\pm$ 37.25	624.00 $\pm$ 30.00
N $\pm$ σ_N	8.056 $\times 10^3 \pm$ 1.20%	1.476 $\times 10^4 \pm$ 0.87%	1.696 $\times 10^4 \pm$ 0.82%	1.188 $\times 10^4 \pm$ 0.97%
Runtime (S)	300.530	301.682	301.255	300.592
$A_{Measured} \pm \sigma_{A_{Measured}}$ (Hz)	26.81 $\pm$ 0.32	48.93 $\pm$ 0.43	56.32 $\pm$ 0.46	39.51 $\pm$ 0.39
% Efficiency	8.9 $\times 10^{-3} \pm$ 6%	8.0 $\times 10^{-2} \pm$ 6%	3.1 $\times 10^{-1} \pm$ 3%	3.1 $\times 10^{-1} \pm$ 3%
$A_\epsilon \pm \sigma_{A_\epsilon}$	3.0 $\times 10^5 \pm$ 6.1%	5.8 $\times 10^4 \pm$ 6.1%	1.8 $\times 10^4 \pm$ 3.1%	1.3 $\times 10^4 \pm$ 3.2%

TABLE B.60: 170049 rear inner foil data.

	06/19/17	10/25/17	12/18/17
I $\pm\sqrt{I}$	$4.674 \times 10^6 \pm$ 0.05%	$1.668 \times 10^6 \pm$ 0.08 %	$1.378 \times 10^6 \pm$ 0.09 %
$B \pm \sigma_B$	$3.469 \times 10^6 \pm$ 0.19%	$1.407 \times 10^6 \pm$ 0.09%	$1.185 \times 10^5 \pm$ 0.10%
N $\pm$ σ_N	$1.205 \times 10^6 \pm$ 0.25%	$2.611 \times 10^5 \pm$ 0.71%	$1.927 \times 10^5 \pm$ 0.88%
Runtime (S)	1.46360 $\times 10^5$	8.4386 $\times 10^4$	7.5321 $\times 10^4$
$A_{Measured} \pm \sigma_{A_{Measured}}$ (Hz)	8.23 $\pm$ 0.02	3.09 $\pm$ 0.02	2.56 $\pm$ 0.02
% Efficiency	0.92 $\pm$ 3.1%	0.92 $\pm$ 3.1%	0.92 $\pm$ 3.1%
$A_\epsilon \pm \sigma_{A_\epsilon}$	$9.6 \times 10^2 \pm$ 3.1%	$3.6 \times 10^2 \pm$ 3.1%	$3.0 \times 10^2 \pm$ 3.1%

TABLE B.61: 0.1% Se/soil mix Se-75 10 channel data.

	06/19/17	10/25/17	12/18/17
I $\pm\sqrt{I}$	1.809 $\times 10^6 \pm$ 0.07%	5.382 $\times 10^5 \pm$ 0.14%	4.137 $\times 10^5 \pm$ 0.16%
$B \pm \sigma_B$	6.534 $\times 10^5 \pm$ 0.06%	2.641 $\times 10^5 \pm$ 0.09%	2.226 $\times 10^5 \pm$ 0.01%
N $\pm$ σ_N	1.156 $\times 10^6 \pm$ 0.12%	2.741 $\times 10^5 \pm$ 0.28	1.911 $\times 10^5 \pm$ 0.34%
Runtime (S)	1.46360 $\times 10^5$	8.4386 $\times 10^4$	7.5321 $\times 10^4$
$A_{Measured} \pm \sigma_{A_{Measured}}$ (Hz)	7.90 $\pm$ 0.01	3.25 $\pm$ 0.01	2.54 $\pm$ 0.01
% Efficiency	0.92 $\pm$ 3.1%	0.92 $\pm$ 3.1%	0.92 $\pm$ 3.1%
$A_\epsilon \pm \sigma_{A_\epsilon}$	8.5 $\times 10^2 \pm$3.1%	3.5 $\times 10^2 \pm$ 3.1%	2.7 $\times 10^2 \pm$ 3.1%

Table B.62: 0.1% Se/soil mix Se-75 3 channel data.

	06/19/17	10/25/17	12/18/17
I $\pm\sqrt{I}$	9.854 $\times 10^5 \pm$ 0.10%	2.675 $\times 10^5 \pm$ 0.19%	1.751 $\times 10^5 \pm$ 0.24%
$B \pm \sigma_B$	2.178 $\times 10^5 \pm$ 0.06%	8.803 $\times 10^4 \pm$ 0.09%	0.10%
N $\pm \sigma_N$	7.676 $\times 10^5 \pm$ 1.3%	1.795 $\times 10^5 \pm$ 0.29%	1.009 $\times 10^5 \pm$ 0.42%
Runtime (S)	1.46360 $\times 10^5$	8.4386 $\times 10^4$	7.5321 $\times 10^4$
$A_{Measured} \pm \sigma_{A_{Measured}}$ (Hz)	5.24 $\pm$ 0.01	2.13 $\pm$ 0.01	1.34 $\pm$ 0.01
% Efficiency	0.92 $\pm$ 3.1%	0.92 $\pm$ 3.1%	0.92 $\pm$ 3.1%
$A_\epsilon \pm \sigma_{A_\epsilon}$	5.6 $\times 10^2 \pm$ 3.0%	2.3 $\times 10^2 \pm$ 3.0%	1.4 $\times 10^2 \pm$ 3.0%

TABLE B.63: 0.1% Se/soil mix Se-75 1 channel data.

	07/25/17	10/31/17	12/09/17
I $\pm\sqrt{I}$	3.161 $\times 10^6 \pm$ 0.05%	5.174 $\times 10^5 \pm$ 0.13%	1.697 $\times 10^6 \pm$ 0.08%
$B \pm \sigma_B$	1.215 $\times 10^6 \pm$ 0.11%	2.576 $\times 10^5 \pm$ 0.23%	9.698 $\times 10^5 \pm$ 0.13%
N $\pm \sigma_N$	1.946 $\times 10^6 \pm$ 0.11%	2.598 $\times 10^5 \pm$ 0.23%	7.272 $\times 10^5 \pm$ 0.25%
Runtime (S)	2.48251 $\times 10^5$	6.6348 $\times 10^4$	2.58001 $\times 10^5$
$A_{Measured} \pm \sigma_{A_{Measured}}$ (Hz)	7.84 $\pm$ 0.01	3.92 $\pm$ 0.01	2.82 $\pm$ 0.01
% Efficiency	0.92 $\pm$ 3.1%	0.92 $\pm$ 3.1%	0.92 $\pm$ 3.1%
$A_\epsilon \pm \sigma_{A_\epsilon}$	9.1 $\times 10^2 \pm$ 3.0%	4.6 $\times 10^2 \pm$ 3.1%	3.3 $\times 10^2 \pm$ 3.0%

TABLE B.64: 0.1% pure witness Se 10 channel data (Se-75).

	07/25/17	10/31/17	12/09/17
I $\pm\sqrt{I}$	2.115 $\times 10^6 \pm$ 0.07%	3.038 $\times 10^5 \pm$ 0.18%	8.143 $\times 10^5 \pm$ 0.11%
$B \pm \sigma_B$	2.287 $\times 10^5 \pm$ 0.10%	4.860 $\times 10^4 \pm$ 0.22%	1.828 $\times 10^5 \pm$ 0.12%
N $\pm \sigma_N$	1.926 $\times 10^6 \pm$ 0.07%	2.552 $\times 10^5 \pm$ 0.22%	6.315 $\times 10^5 \pm$ 0.15%
Runtime (S)	2.48251 $\times 10^5$	6.6348 $\times 10^4$	2.58001 $\times 10^5$
$A_{Measured} \pm \sigma_{A_{Measured}}$ (Hz)	7.76 $\pm$ 0.01	3.85 $\pm$ 0.01	2.45 $\pm$ 0.01
% Efficiency	0.92 $\pm$ 3.1%	0.92 $\pm$ 3.1%	0.92 $\pm$ 3.1%
$A_\epsilon \pm \sigma_{A_\epsilon}$	8.3 $\times 10^2 \pm$ 3.1%	4.1 $\times 10^2 \pm$ 3.1%	2.6 $\times 10^2$ 3.1%

TABLE B.65: 0.1% pure witness Se 3 channel data (Se-75).

	07/25/17	10/31/17	12/09/17
I $\pm\sqrt{I}$	$1.371 \times 10^6 \pm 0.09\%$	$1.757 \times 10^5 \pm 0.24\%$	$3.576 \times 10^5 \pm 0.17\%$
$B \pm \sigma_B$	$7.623 \times 10^4 \pm 0.10\%$	$1.620 \times 10^4 \pm 0.22\%$	$6.092 \times 10^4 \pm 0.12\%$
N $\pm \sigma_N$	$1.295 \times 10^6 \pm 0.09\%$	$1.595 \times 10^5 \pm 0.26\%$	$2.967 \times 10^5 \pm 0.20\%$
Runtime (S)	2.48251×10^5	6.6348×10^4	2.58001×10^5
$A_{Measured} \pm \sigma_{A_{Measured}}$ (Hz)	5.22 ± 0.01	2.40 ± 0.01	1.15 ± 0.01
% Efficiency	$0.92 \pm 3.1\%$	$0.92 \pm 3.1\%$	$0.92 \pm 3.1\%$
$A_\epsilon \pm \sigma_{A_\epsilon}$	$5.6 \times 10^2 \pm 3.1\%$	$2.6 \times 10^2 \pm 3.1\%$	$1.2 \times 10^2 \pm 3.2\%$

TABLE B.66: 0.1% pure witness Se 1 channel data (Se-75).

	5/26/17	5/27/17	5/29/17	5/30/17	5/31/17
I $\pm\sqrt{I}$	9442 $\pm$ 97.17	11890 $\pm$ 109.04	13400 $\pm$ 115.76	8865 $\pm$ 94.15	5702 $\pm$ 75.51
$B \pm \sigma_B$	333.58 $\pm$ 22.36	628.68 $\pm$ 30.42	562.9 $\pm$ 29.12	360.36 $\pm$ 23.4	214.47 $\pm$ 18.04
N $\pm$ σ_N	9108.42 $\pm$ 99.71	11261.32 $\pm$ 113.20	12837.1 $\pm$ 119.37	8504.64 $\pm$ 97.01	5487.53 $\pm$ 77.64
Runtime (S)	301.043	300.467	300.803	300.857	300.639
$A_{Measured} \pm \sigma_{A_{Measured}}$ (Hz)	30.26 $\pm$ 0.33	37.48 $\pm$ 0.38	42.68 $\pm$ 0.40	28.27 $\pm$ 0.32	18.25 $\pm$ 0.26
$A_{True} \pm \sigma_{A_{True}}$ (Hz)	30.28 $\pm$ 0.33	37.51 $\pm$ 0.38	42.71 $\pm$ 0.40	28.29 $\pm$ 0.32	18.26 $\pm$ 0.26
% Dead	1.65 $\pm$ 0.34	2.26 $\pm$ 0.33	2.53 $\pm$ 0.31	1.92 $\pm$ 0.26	1.55 $\pm$ 0.18
$A_{DTC} \pm \sigma_{A_{DTC}}$	30.79 $\pm$ 0.35	38.38 $\pm$ 0.41	43.82 $\pm$ 0.43	28.84 $\pm$ 0.34	18.55 $\pm$ 0.27
% Efficiency	0.0422 $\pm$ 6%	0.0847 $\pm$ 6%	0.31 $\pm$ 3%	0.31 $\pm$ 3%	0.31 $\pm$ 3%
$A_\epsilon \pm \sigma_{A_\epsilon}$	7.3 $\times 10^4 \pm$ 6%	4.5 $\times 10^4 \pm$ 6%	1.4 $\times 10^4 \pm$ 3%	9.3 $\times 10^3 \pm$ 3%	6.0 $\times 10^3 \pm$ 3%

TABLE B.67: 170050 front outer foil data.

	5/26/17	5/27/17	5/29/17	5/30/17	5/31/17
I $\pm\sqrt{I}$	14690 $\pm$ 121.20	8972 $\pm$ 94.72	11260 $\pm$ 106.11	6955 $\pm$ 83.40	4511 $\pm$ 67.16
$B \pm \sigma_B$	547.56 $\pm$ 28.6	300.82 $\pm$ 21.32	505.44 $\pm$ 27.3	285.22 $\pm$ 20.8	161.49 $\pm$ 15.65
N $\pm$ σ_N	14142.22 $\pm$ 124.53	8671.18 $\pm$ 97.09	10754.56 $\pm$ 109.57	6669.78 $\pm$ 85.95	4349.51 $\pm$ 68.96
Runtime (S)	301.170	301.342	314.769	301.470	300.967
$A_{Measured} \pm \sigma_{A_{Measured}}$ (Hz)	46.96 $\pm$ 0.41	28.77 $\pm$ 0.32	34.17 $\pm$ 0.35	22.12 $\pm$ 0.29	14.45 $\pm$ 0.23
$A_{True} \pm \sigma_{A_{True}}$ (Hz)	47.00 $\pm$ 0.41	28.79 $\pm$ 0.32	34.20 $\pm$ 0.35	22.14 $\pm$ 0.29	14.46 $\pm$ 0.23
% Dead	1.65 $\pm$ 0.34	2.26 $\pm$ 0.33	2.53 $\pm$ 0.31	1.92 $\pm$ 0.26	1.55 $\pm$ 0.18
$A_{DTC} \pm \sigma_{A_{DTC}}$	47.79 $\pm$ 0.45	29.46 $\pm$ 0.34	35.09 $\pm$ 0.38	22.57 $\pm$ 0.30	14.69 $\pm$ 0.24
% Efficiency	0.0422 $\pm$ 6%	0.0847 $\pm$ 6%	0.31 $\pm$ 3%	0.31 $\pm$ 3%	0.31 $\pm$ 3%
$A_\epsilon \pm \sigma_{A_\epsilon}$	1.1 $\times 10^5 \pm$ 6%	3.5 $\times 10^4 \pm$ 6%	1.1 $\times 10^4 \pm$ 3%	7.3 $\times 10^3 \pm$ 3%	4.7 $\times 10^3 \pm$ 3%

TABLE B.68: 170050 rear outer foil data.

	5/24/17	5/29/17	5/30/17	5/31/17
I $\pm\sqrt{I}$	6.217 $\times 10^3 \pm$ 1.3%	9.541 $\times 10^3 \pm$ 1.0%	7.233 $\times 10^3 \pm$ 1.2%	4.088 $\times 10^3 \pm$ 1.6%
$B \pm \sigma_B$	153.78 $\pm$ 15.33	253.75 $\pm$ 19.00	214.60 $\pm$ 17.60	169.55 $\pm$ 16.13
N $\pm$ σ_N	6.063 $\times 10^3 \pm$ 1.3%	9.287 $\times 10^3 \pm$ 1.1%	7.018 $\times 10^3 \pm$ 1.2%	3.918 $\times 10^3 \pm$ 1.7%
Runtime (S)	301.239	301.223	300.720	300.662
$A_{Measured} \pm \sigma_{A_{Measured}}$ (Hz)	20.13 $\pm$ 0.27	30.83 $\pm$ 0.33	23.34 $\pm$ 0.29	13.03 $\pm$ 0.22
% Efficiency	1.7 $\times 10^{-2} \pm$ 6%	3.1 $\times 10^{-1} \pm$ 6%	3.1 $\times 10^{-1} \pm$ 3%	3.1 $\times 10^{-1} \pm$ 3%
$A_\epsilon \pm \sigma_{A_\epsilon}$	1.2 $\times 10^5 \pm$ 6.1%	9.9 $\times 10^3 \pm$ 3.2%	7.5 $\times 10^3 \pm$ 3.2%	4.2 $\times 10^3 \pm$ 3.4%

TABLE B.69: 170050 front inner foil data.

	5/27/17	5/29/17	5/30/17	5/31/17
I $\pm\sqrt{I}$	8.399 $\times 10^3 \pm$ 1.09%	1.042 $\times 10^4 \pm$ 0.98%	6.821 $\times 10^3 \pm$ 1.21%	3.913 $\times 10^3 \pm$ 1.60%
$B \pm \sigma_B$	148.78 $\pm$ 17.90	230.85 $\pm$ 18.98	203.80 $\pm$ 18.30	156.65 $\pm$ 16.33
N $\pm$ σ_N	8.250 $\times 10^3 \pm$ 1.14%	1.019 $\times 10^4 \pm$ 1.02%	6.617 $\times 10^3 \pm$ 1.28%	3.756 $\times 10^3 \pm$ 1.72 %
Runtime (S)	300.458	301.542	296.142	301.393
$A_{Measured} \pm \sigma_{A_{Measured}}$ (Hz)	27.46 $\pm$ 0.31	33.79 $\pm$ 0.34	22.34 $\pm$ 0.29	12.46 $\pm$ 0.21
% Efficiency	8.0 $\times 10^{-2} \pm$ 6%	3.1 $\times 10^{-1} \pm$ 6%	3.1 $\times 10^{-1} \pm$ 3%	3.1 $\times 10^{-1} \pm$ 3%
$A_\epsilon \pm \sigma_{A_\epsilon}$	3.2 $\times 10^4 \pm$ 6.1%	1.1 $\times 10^4 \pm$ 3.2%	7.2 $\times 10^3 \pm$ 3.3%	4.0 $\times 10^3 \pm$ 3.4%

Table B.70: 170050 rear inner foil data.

B.2 Half Life Plots

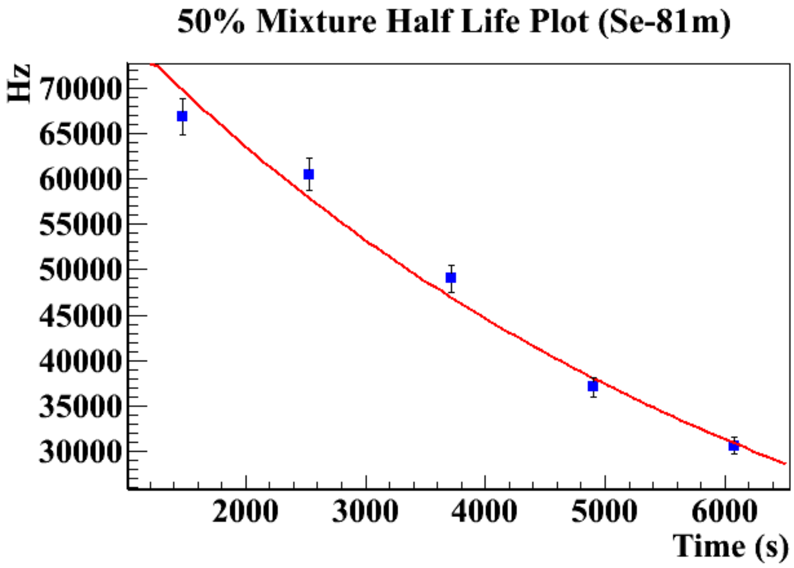

FIGURE B.1: 50% Se/soil mix half life plot Se-81m.

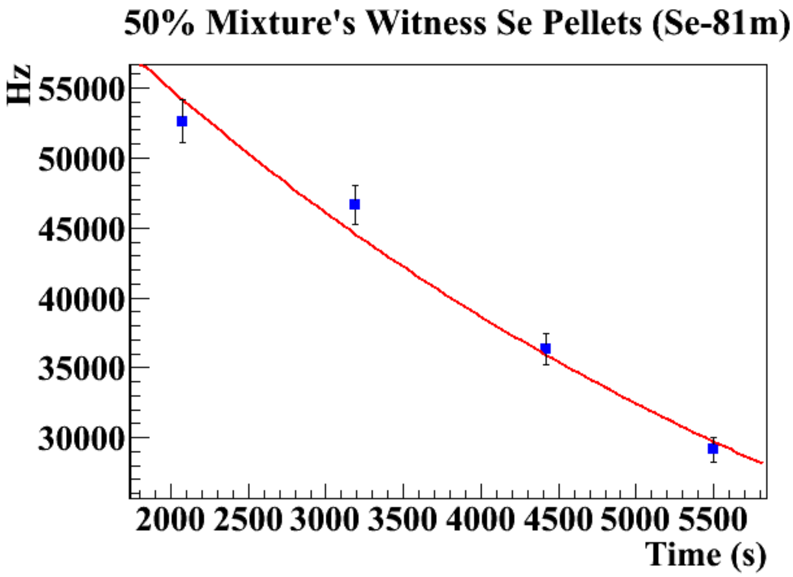

FIGURE B.2: 50% mixture pure witness selenium half life plot Se-81m.

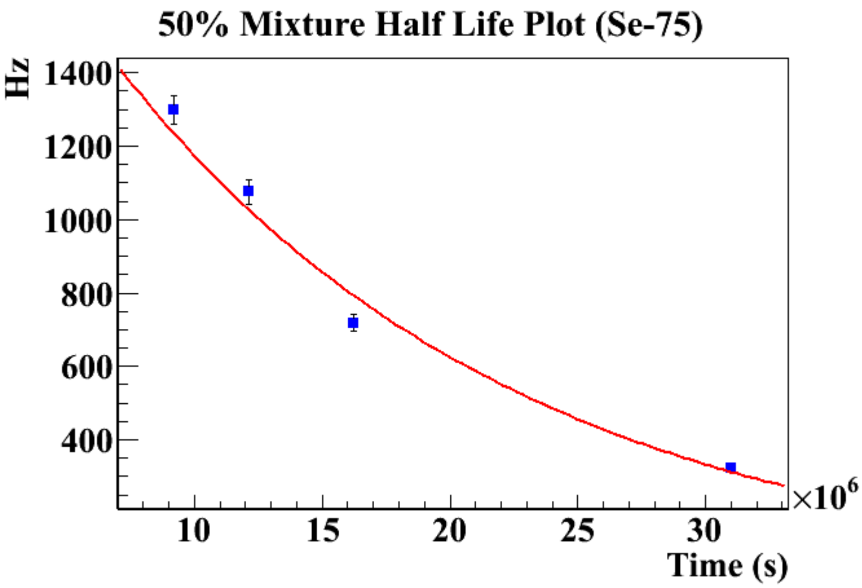

FIGURE B.3: 50 % Se/soil mix half life plot Se-75.

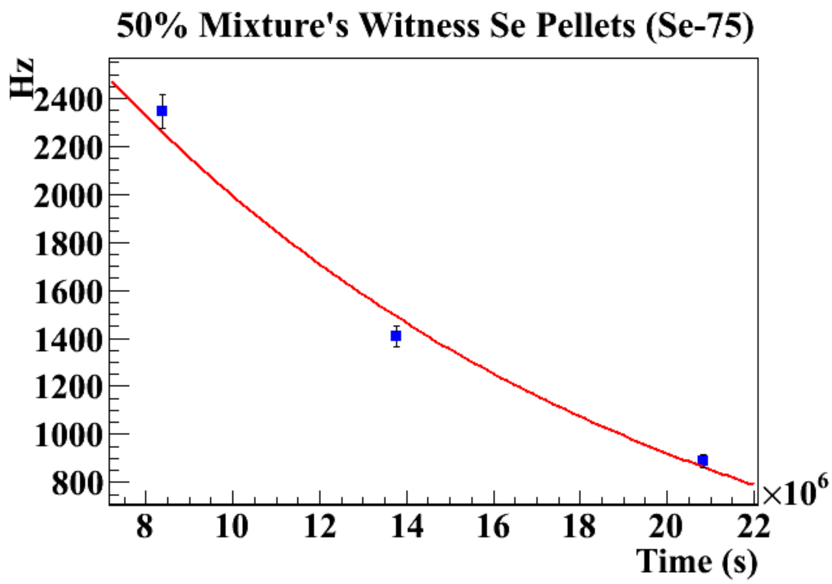

FIGURE B.4: 50% mixture pure selenium half life plot Se-75.

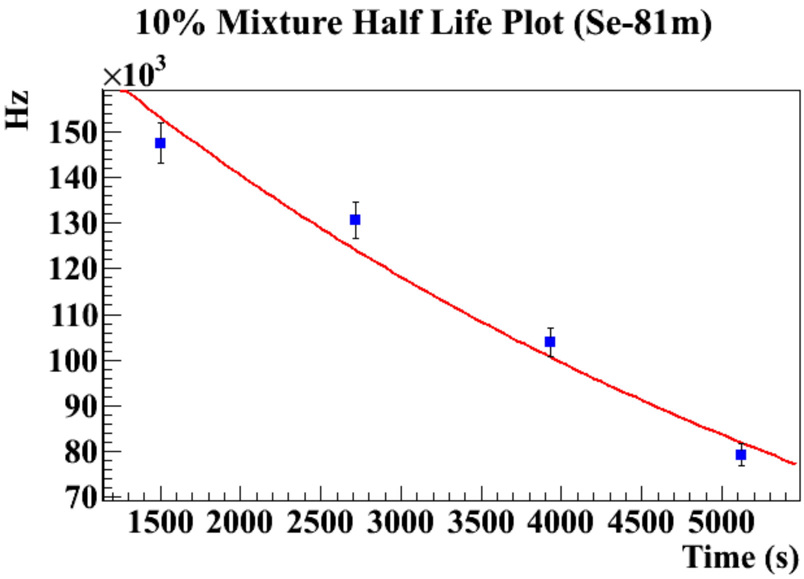

FIGURE B.5: 10 % Se/soil mix half life plot Se-81m.

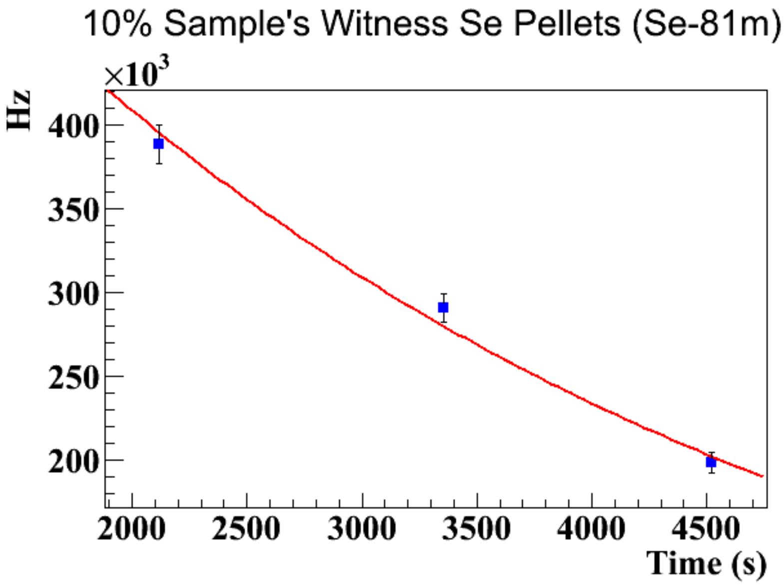

FIGURE B.6: 10% Se/soil pure selenium half life plot Se-81m.

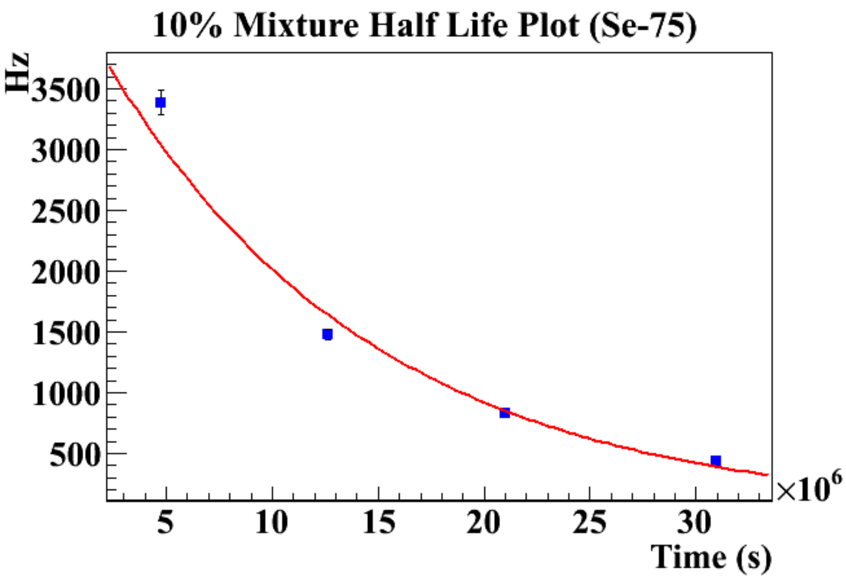

FIGURE B.7: 10 % Se/soil mix half life plot Se-75.

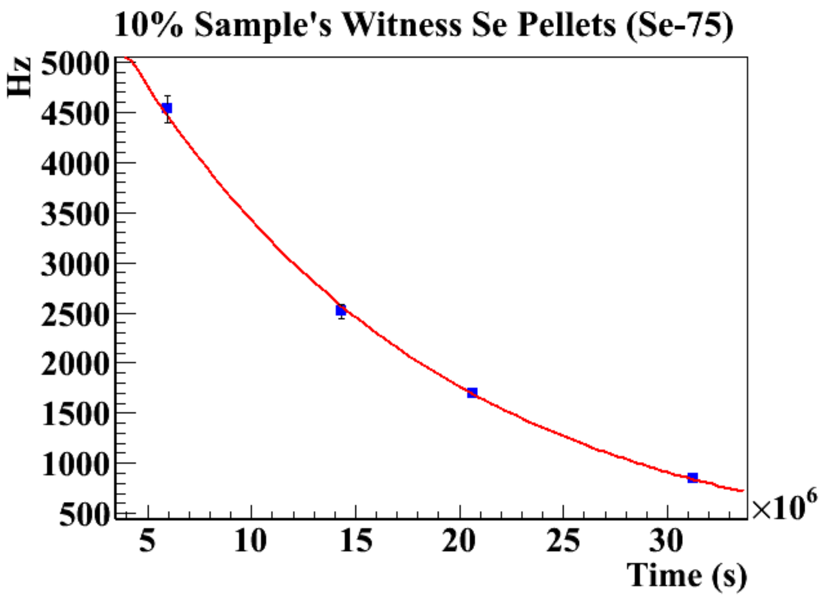

FIGURE B.8: 10% mixture pure selenium half life plot Se-75.

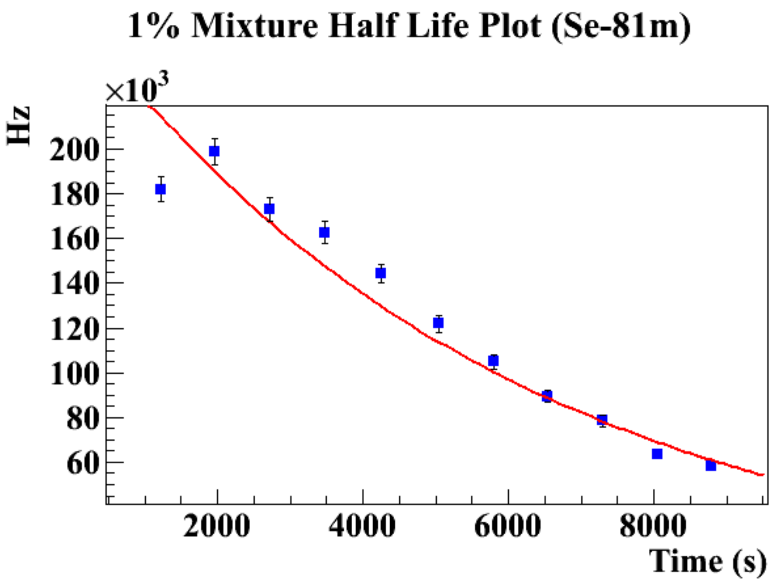

FIGURE B.9: 1 % Se/soil mix half life plot Se-81m.

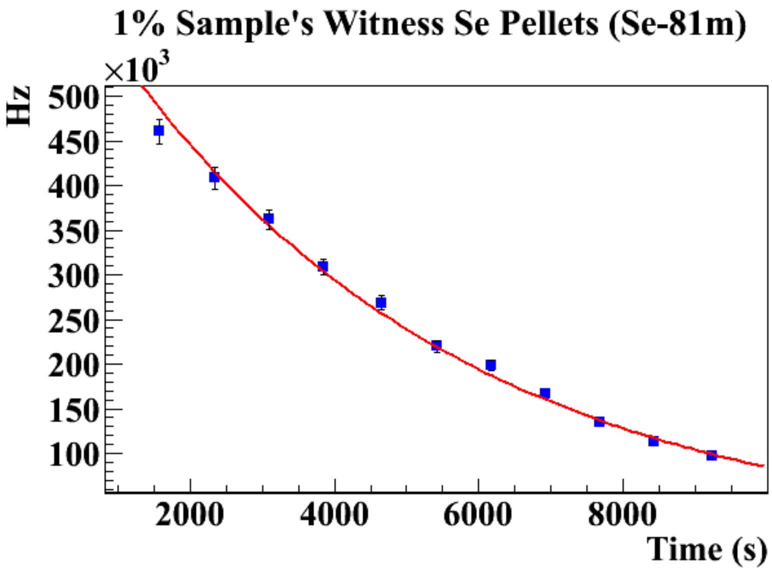

FIGURE B.10: 1% mixture pure selenium half life plot Se-81m.

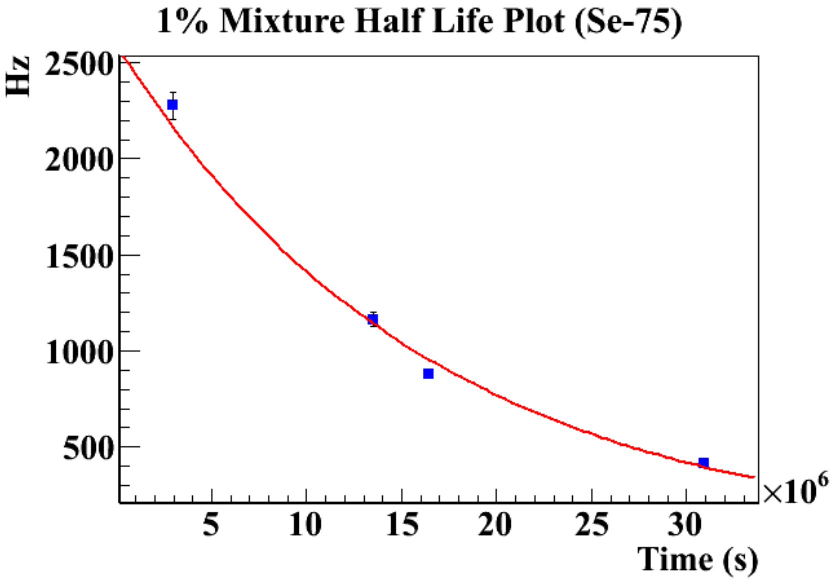

FIGURE B.11: 1 % Se/soil mix half life plot Se-75.

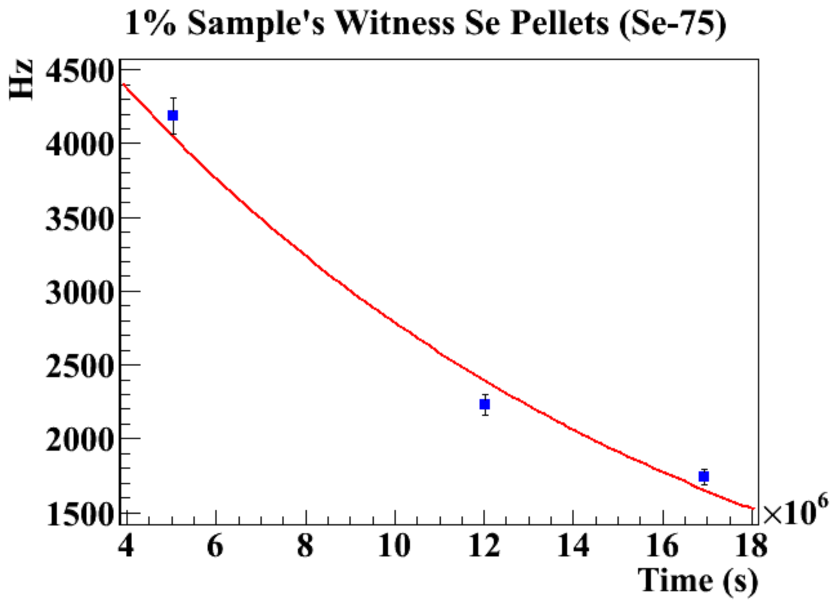

FIGURE B.12: 1% mixture pure selenium half life plot Se-75.

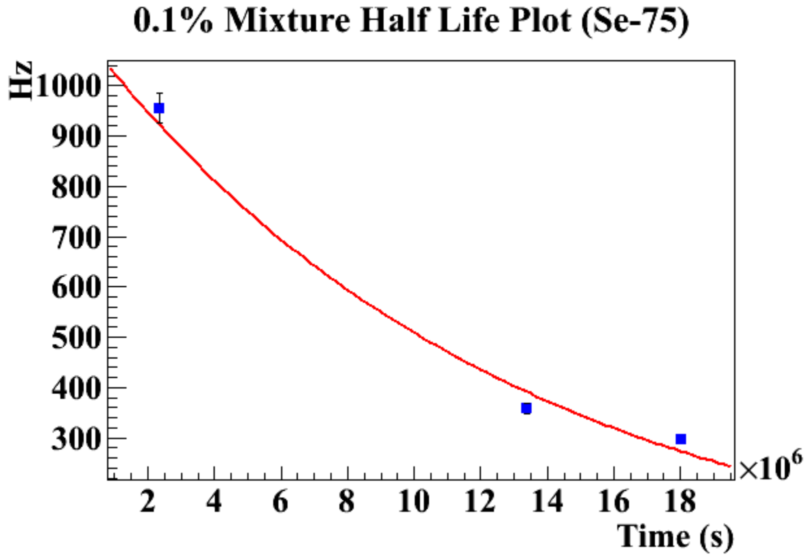

FIGURE B.13: 0.1 % Se/soil mix half life plot Se-75.

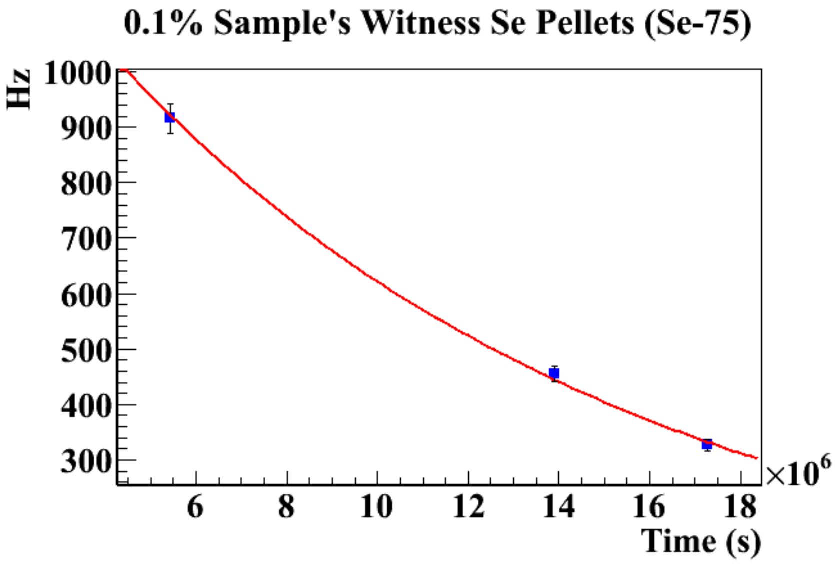

FIGURE B.14: 0.1% mixture pure selenium half life plot Se-75.

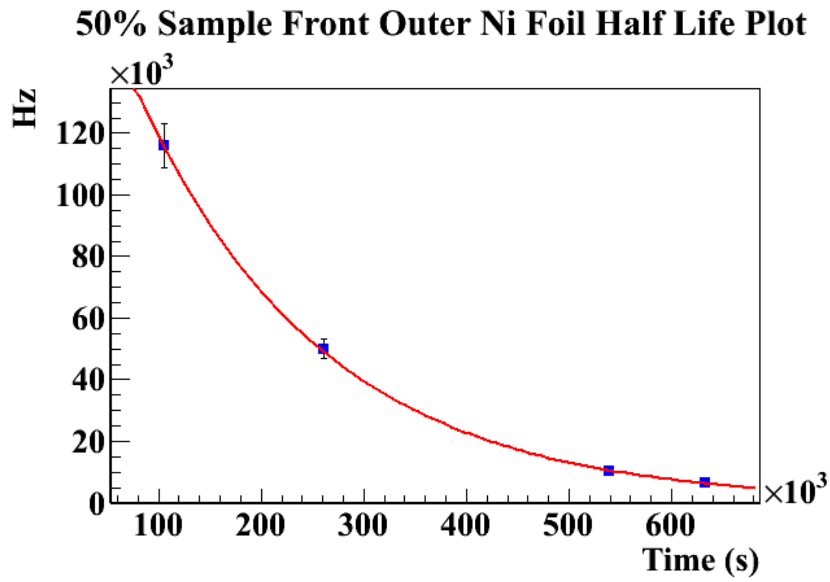

FIGURE B.15: 50% mixture front outer nickel foil half life plot.

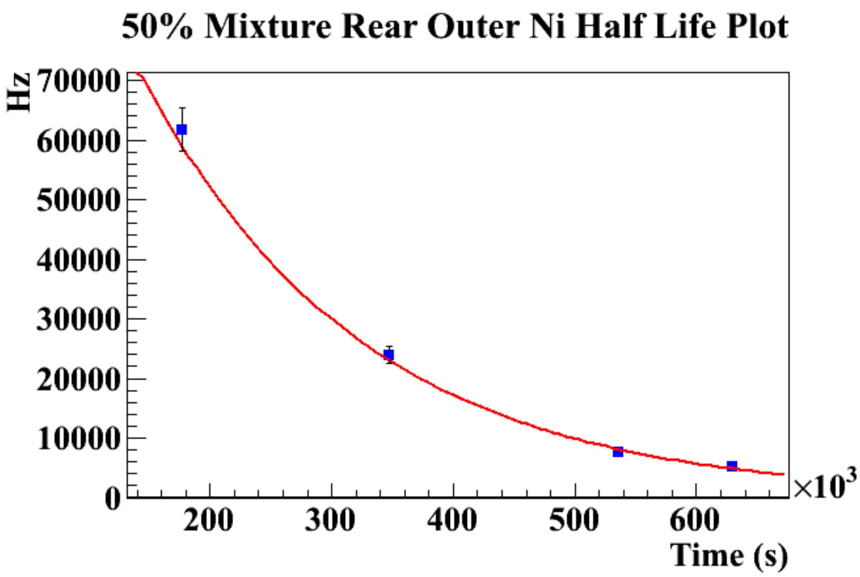

FIGURE B.16: 50% mixture rear outer nickel foil half life plot.

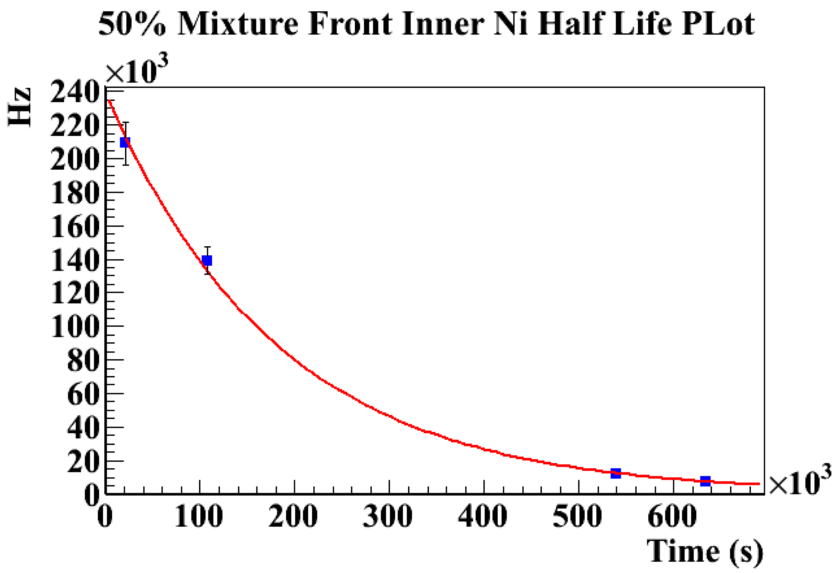

FIGURE B.17: 50% mixture front inner nickel foil half life plot.

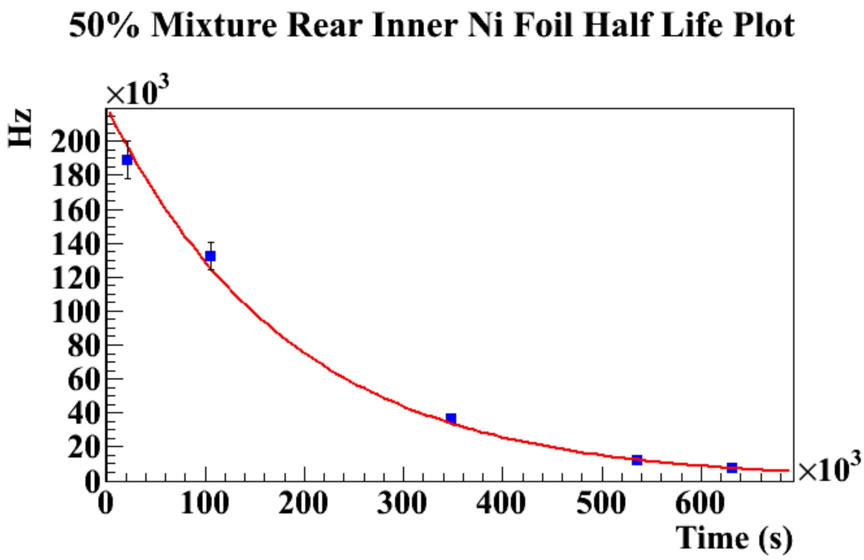

FIGURE B.18: 50% mixture rear inner nickel foil half life plot.

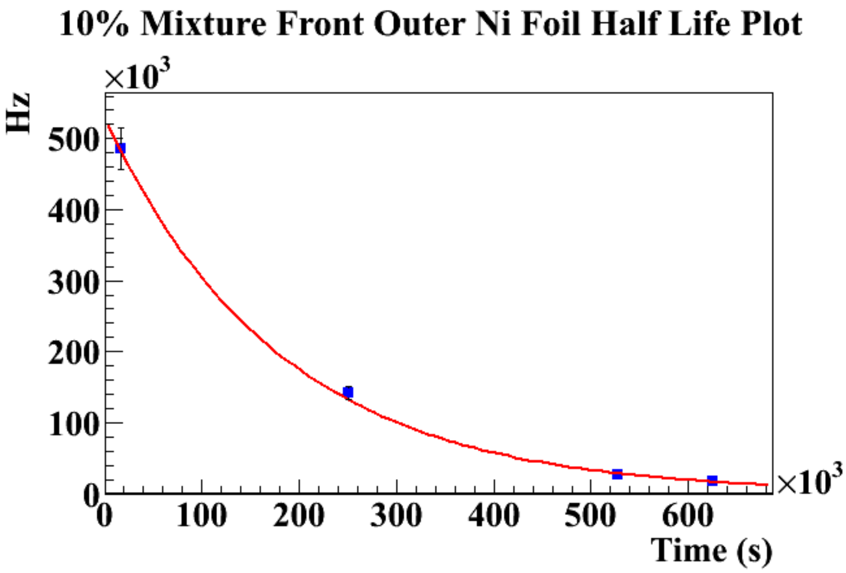

FIGURE B.19: 10% mixture front outer nickel foil half life plot.

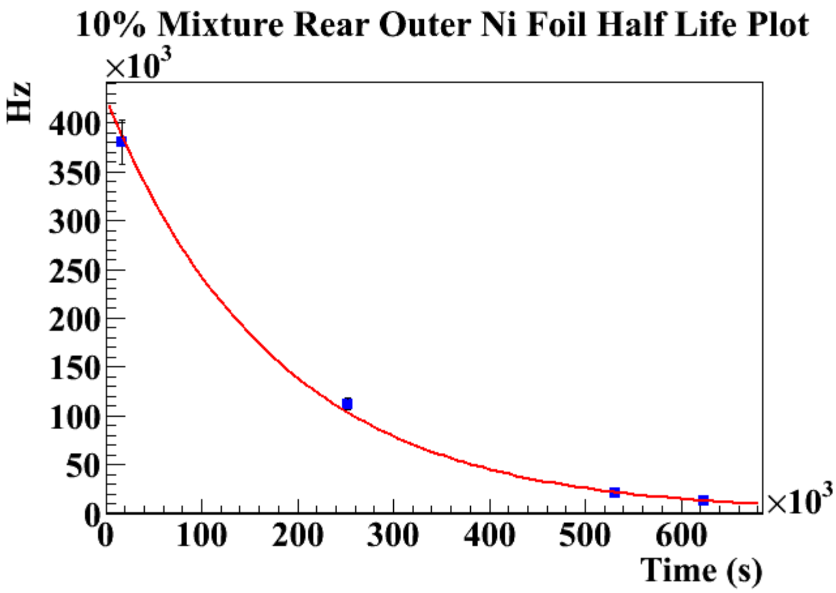

FIGURE B.20: 10% mixture rear outer nickel foil half life plot.

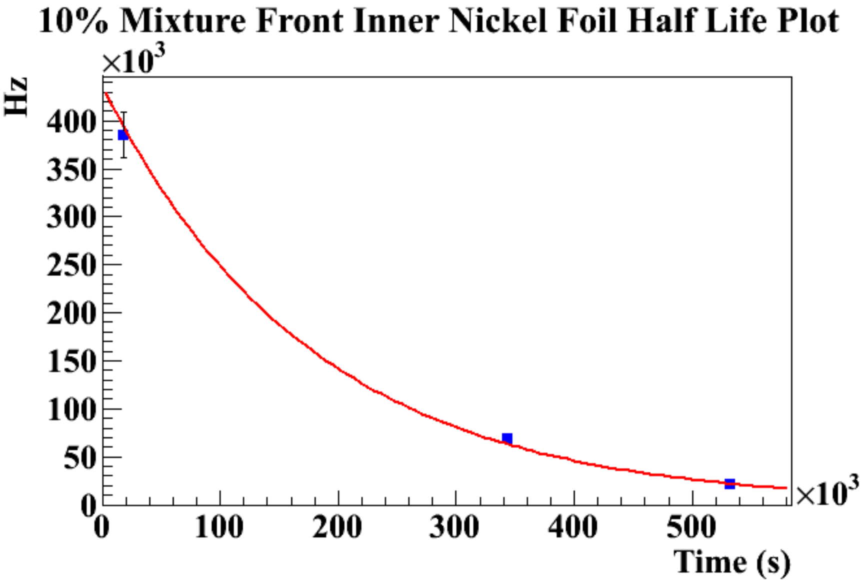

FIGURE B.21: 10% mixture front inner nickel foil half life plot.

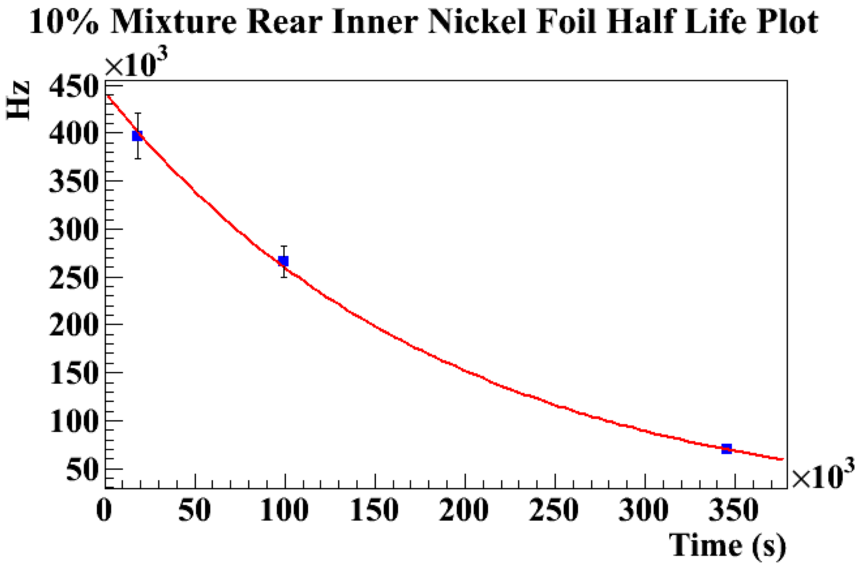

FIGURE B.22: 10% mixture rear inner nickel foil half life plot.

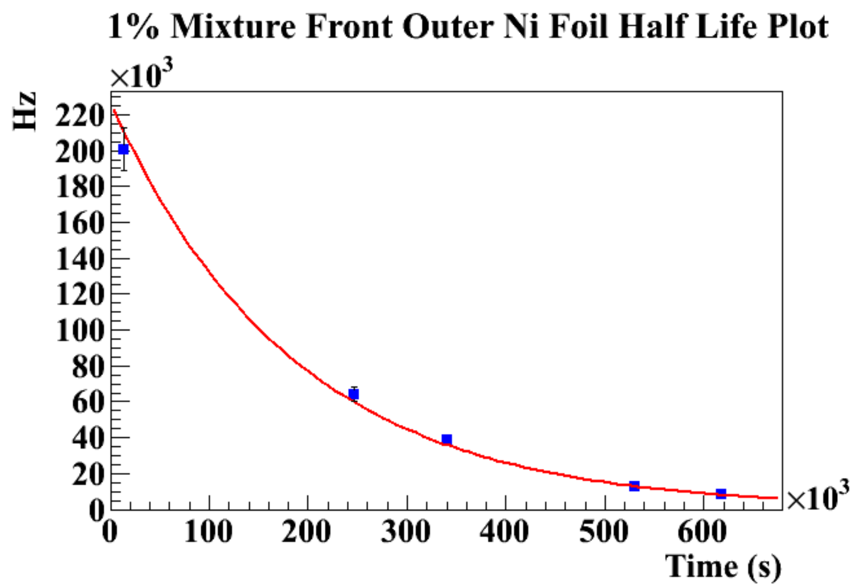

FIGURE B.23: 1% mixture front outer nickel foil half life plot.

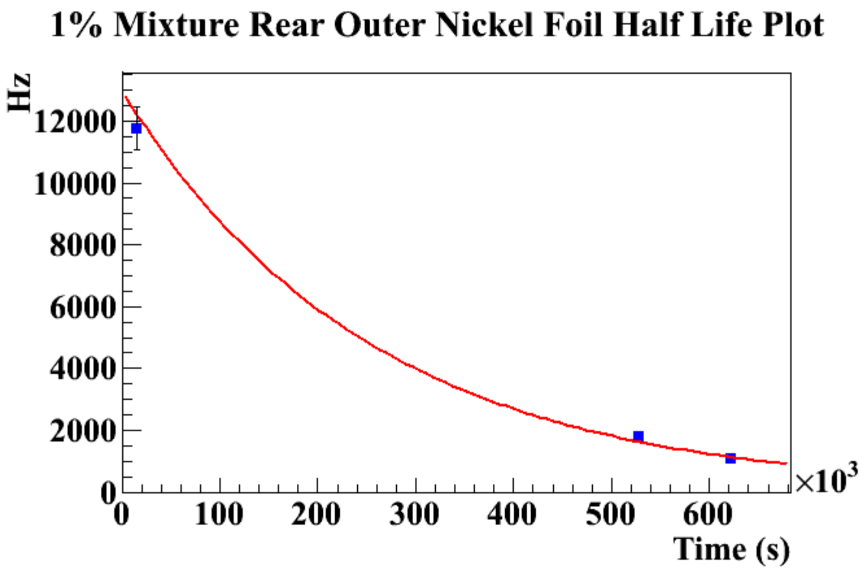

FIGURE B.24: 1% mixture rear outer nickel foil half life plot.

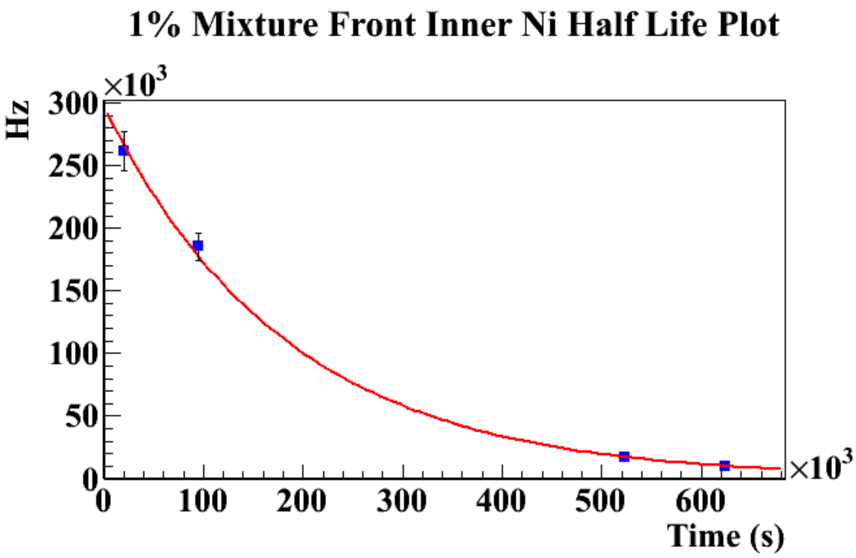

FIGURE B.25: 1% mixture front inner nickel foil half life plot.

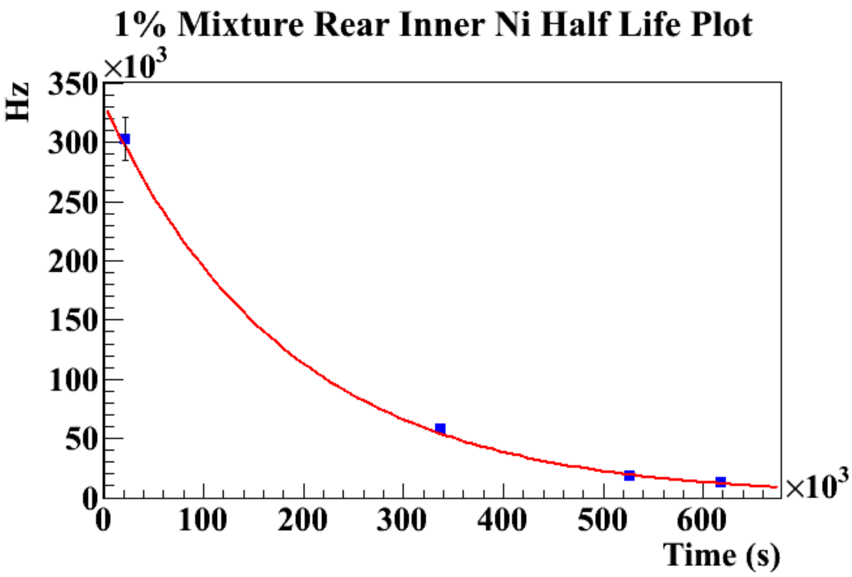

FIGURE B.26: 1% mixture rear inner nickel foil half life plot.

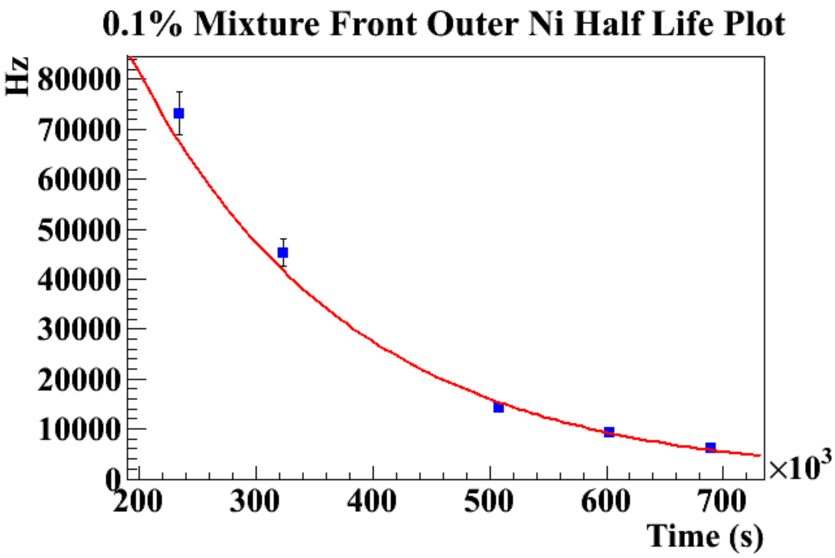

FIGURE B.27: 0.1% mixture front outer nickel foil half life plot.

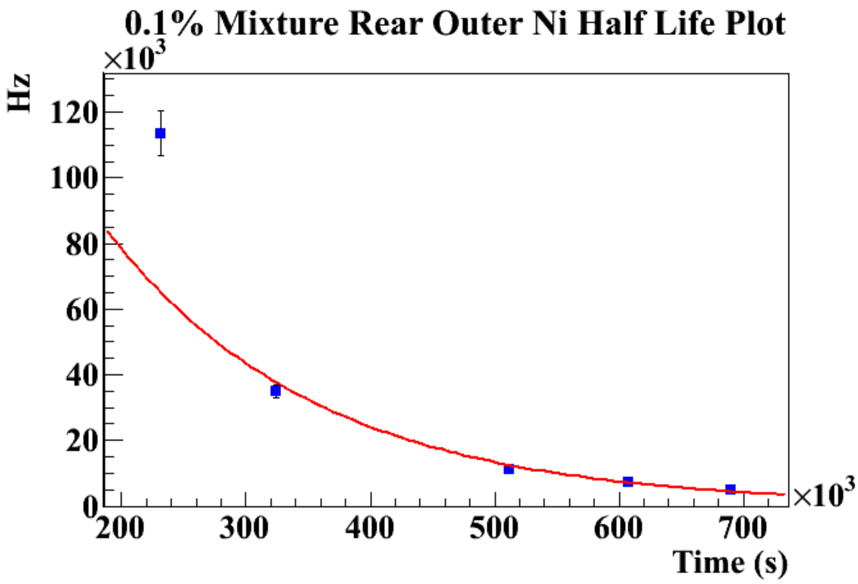

FIGURE B.28: 0.1% mixture rear outer nickel foil half life plot.

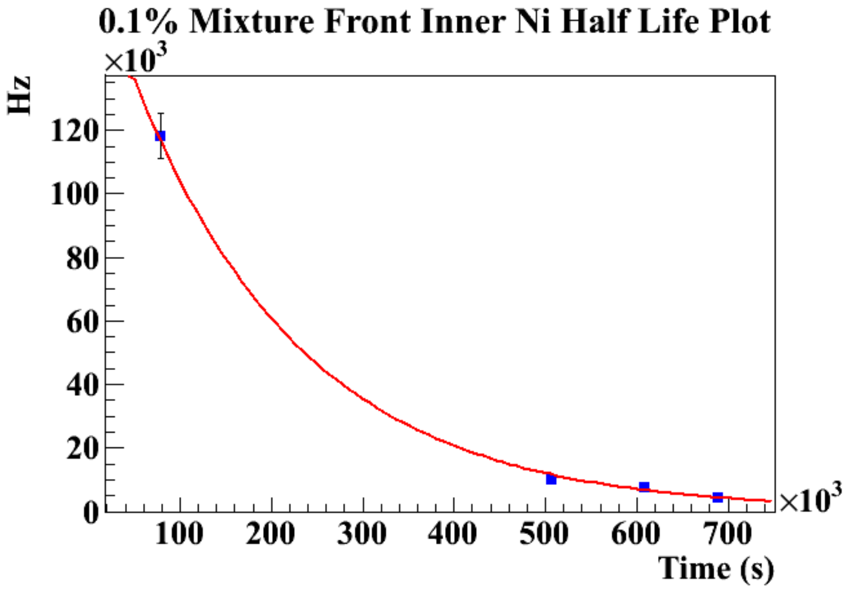

FIGURE B.29: 0.1% mixture front inner nickel foil half life plot.

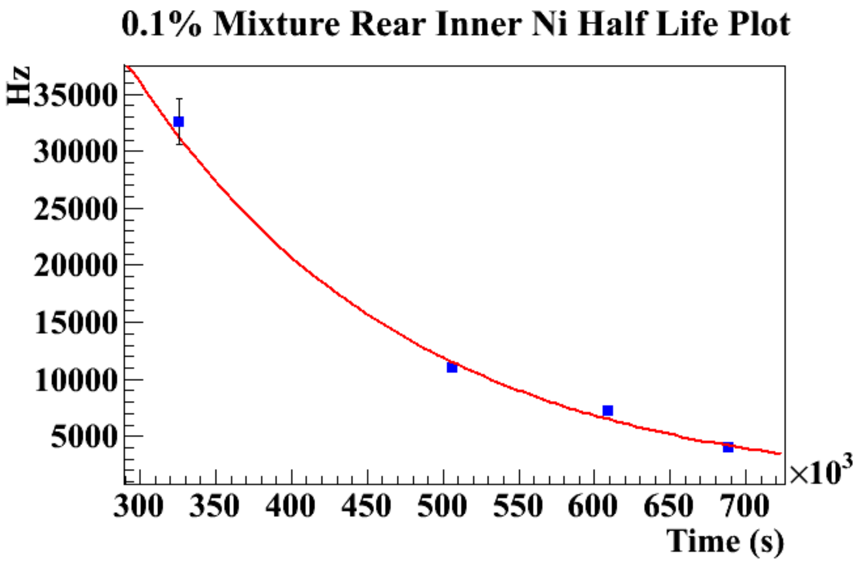

FIGURE B.30: 0.1% mixture rear inner nickel foil half life plot.

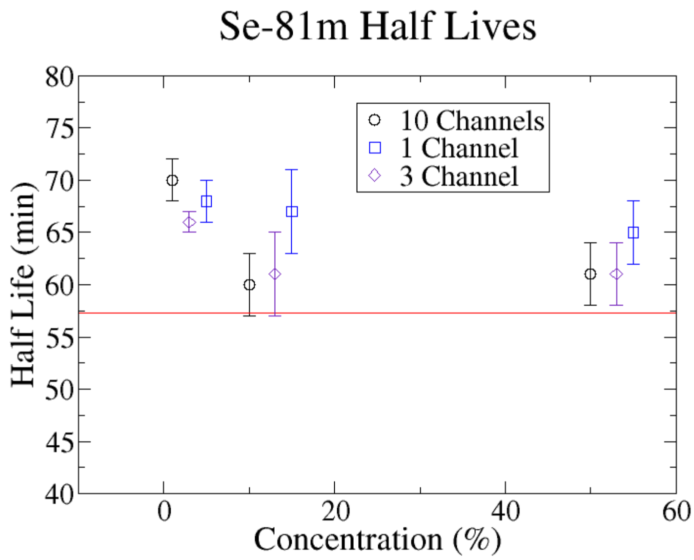

FIGURE B.31: Se-81m mixture half lives.

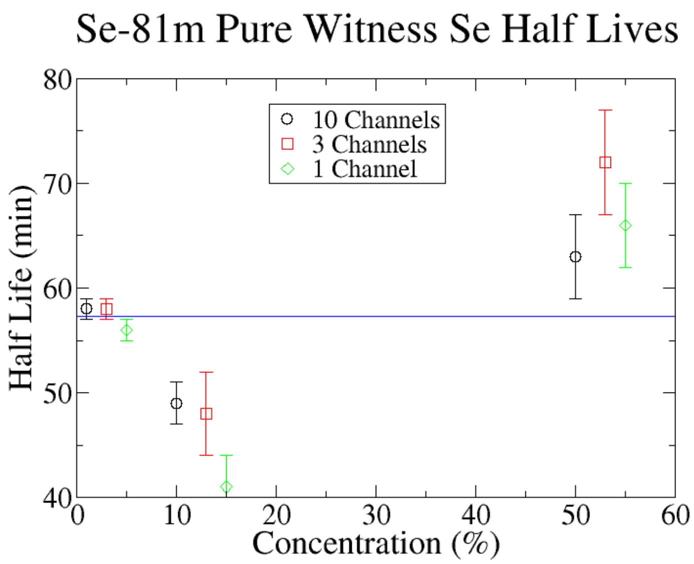

FIGURE B.32: Se-81m pure witness Se half lives.

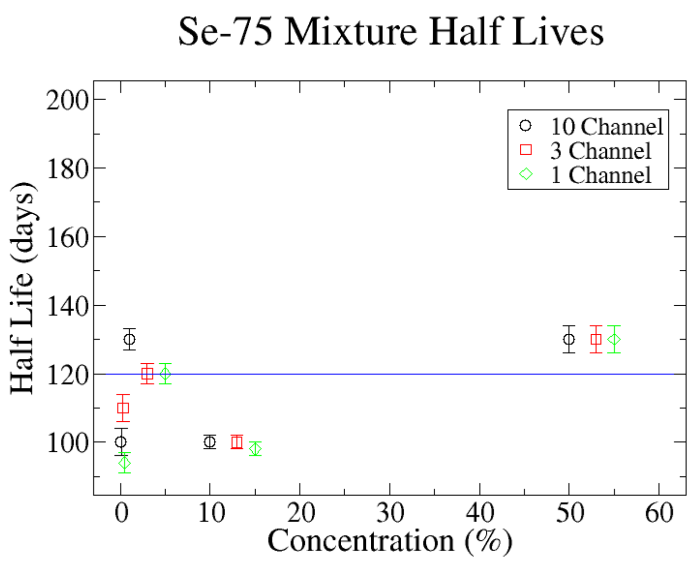

FIGURE B.33: Se-75 mixture half lives.

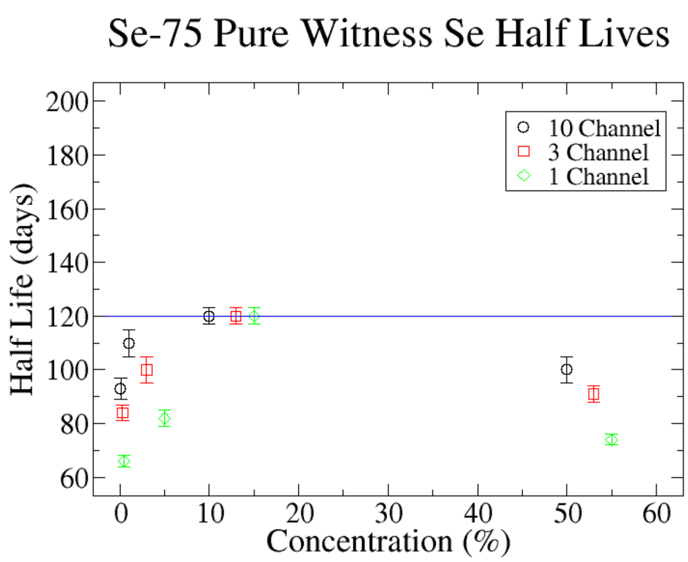

FIGURE B.34: Se-75 pure witness Se half lives.

B.3 Fit Result Tables

	1 Channel	3 Channel	10 Channel
$\ln A_0$ (Hz)	$9.0 \pm 0.3 \times 10^4$	$1.4 \pm 0.04 \times 10^5$	$1.4 \pm 0.04 \times 10^5$
$t_{\frac{1}{2}}$ (min)	65 ± 3	61 ± 3	61 ± 3
p-value	0.07	0.10	0.10

Table B.71: 50% mixture Se-81m parameters.

	1 Channel	3 Channel	10 Channel
$\ln A_0$ (Hz)	$7.8 \pm 0.4 \times 10^4$	$1.0 \pm 0.05 \times 10^5$	$1.1 \pm 0.05 \times 10^5$
$t_{\frac{1}{2}}$ (min)	66 ± 4	72 ± 5	63 ± 4
p-value	0.15	<0.01	<0.01

Table B.72: 50% mixture pure selenium Se-81m parameters.

	1 Channel	3 Channel	10 Channel
$\ln A_0$ (Hz)	$2.0 \pm 0.08 \times 10^5$	$3.2 \pm 0.13 \times 10^5$	$3.4 \pm 0.14 \times 10^5$
$t_{\frac{1}{2}}$ (min)	67 ± 4	61 ± 4	60 ± 3
p-value	0.03	0.19	0.35

Table B.73: 10% mixture Se-81m parameters.

	1 Channel	3 Channel	10 Channel
lnA_0 (Hz)	$7.1 \pm 0.43 \times 10^5$	$9.4 \pm 0.56 \times 10^5$	$9.4 \pm 0.56 \times 10^5$
$t_{\frac{1}{2}}$ (min)	41 ± 3	48 ± 4	49 ± 2
p-value	0.14	0.19	0.86

Table B.74: 10% mixture pure selenium Se-81m parameters.

	1 Channel	3 Channel	10 Channel
$\ln A_0$ (Hz)	$2.7 \pm 0.05 \times 10^5$	$4.3 \pm 0.09 \times 10^5$	$4.0 \pm 0.08 \times 10^5$
$t_{\frac{1}{2}}$ (min)	68 ± 2	66 ± 1	70 ± 2
p-value	<0.01	0.02	0.41

Table B.75: 1% mixture Se-81m parameters.

	1 Channel	3 Channel	10 Channel
$\ln A_0$ (Hz)	$6.8 \pm 0.14 \times 10^5$	$9.7 \pm 0.19 \times 10^5$	$1.0 \pm 0.02 \times 10^6$
$t_{\frac{1}{2}}$ (min)	56 ± 1	58 ± 1	58 ± 1
p-value	0.09	0.60	0.64

Table B.76: 1% mixture pure selenium Se-81m parameters.

	1 Channel	3 Channel	10 Channel
$\ln A_0$ (Hz)	$1.3 \pm 0.04 \times 10^3$	$2.0 \pm 0.06 \times 10^3$	$2.2 \pm 0.07 \times 10^3$
$t_{\frac{1}{2}}$ (min)	130 ± 4	130 ± 4	130 ± 4
p-value	< 0.01	< 0.01	< 0.01

Table B.77: 50% mixture Se-75 parameters.

	1 Channel	3 Channel	10 Channel
$\ln A_0$ (Hz)	$3.6 \pm 0.18 \times 10^3$	$4.5 \pm 0.23 \times 10^3$	$4.4 \pm 0.22 \times 10^3$
$t_{\frac{1}{2}}$ (min)	74 ± 2	91 ± 3	100 ± 5
p-value	0.01	0.03	0.01

Table B.78: 50% mixture pure selenium Se-75 parameters.

	1 Channel	3 Channel	10 Channel
$\ln A_0$ (Hz)	$2.7 \pm 0.08 \times 10^3$	$4.1 \pm 0.12 \times 10^3$	$4.5 \pm 0.13 \times 10^3$
$t_{\frac{1}{2}}$ (min)	98 ± 2	100 ± 2	100 ± 2
p-value	< 0.01	< 0.01	< 0.01

Table B.79: 10% mixture Se-75 parameters.

	1 Channel	3 Channel	10 Channel
$\ln A_0$ (Hz)	$3.6 \pm 0.11 \times 10^3$	$6.0 \pm 0.18 \times 10^3$	$6.6 \pm 0.20 \times 10^3$
$t_{\frac{1}{2}}$ (min)	120 ± 3	120 ± 3	120 ± 3
p-value	< 0.01	0.45	0.60

Table B.80: 10% mixture pure selenium Se-75 parameters.

	1 Channel	3 Channel	10 Channel
$\ln A_0$ (Hz)	$1.6 \pm 0.05 \times 10^3$	$2.5 \pm 0.08 \times 10^3$	$2.6 \pm 0.08 \times 10^3$
$t_{\frac{1}{2}}$ (min)	120 ± 3	120 ± 3	130 ± 3
p-value	< 0.01	< 0.01	<0.01

Table B.81: 1% mixture Se-75 parameters.

	1 Channel	3 Channel	10 Channel
$\ln A_0$ (Hz)	$4.1 \pm 0.16 \times 10^3$	$5.5 \pm 0.22 \times 10^3$	$5.9 \pm 0.24 \times 10^3$
$t_{\frac{1}{2}}$ (min)	82 ± 3	100 ± 5	110 ± 5
p-value	0.03	0.01	< 0.01

Table B.82: 1% mixture pure selenium Se-75 parameters.

	1 Channel	3 Channel	10 Channel
$\ln A_0$ (Hz)	$6.9 \pm 0.20 \times 10^2$	$9.9 \pm 0.30 \times 10^2$	$1.1 \pm 0.03 \times 10^3$
$t_{\frac{1}{2}}$ (min)	94 ± 3	110 ± 4	100 ± 4
p-value	0.14	0.02	< 0.01

Table B.83: 0.1% mixture Se-75 parameters.

	1 Channel	3 Channel	10 Channel
$\ln A_0$ (Hz)	$1.1 \pm 0.06 \times 10^3$	$1.4 \pm 0.07 \times 10^3$	$1.5 \pm 0.07 \times 10^3$
$t_{\frac{1}{2}}$ (min)	66 ± 2	84 ± 3	93 ± 4
p-value	< 0.01	< 0.01	0.32

Table B.84: 0.1% mixture pure selenium Se-75 parameters.

	$\ln A_0$ (Hz)	$t_{\frac{1}{2}}$ (h)	p-value
170047-003	$2.1 \pm 0.12 \times 10^5$	35 ± 1	0.75
170047-004	$1.6 \pm 0.11 \times 10^5$	35 ± 1	0.01
170047-005	$2.4 \pm 0.12 \times 10^5$	35 ± 1	0.55
170047-006	$2.2 \pm 0.09 \times 10^5$	36 ± 1	0.09
170048-003	$5.3 \pm 0.27 \times 10^5$	35 ± 1	< 0.01
170048-004	$4.3 \pm 0.21 \times 10^5$	34 ± 1	0.63
170048-005	$4.4 \pm 0.22 \times 10^5$	34 ± 1	0.13
170048-006	$4.4 \pm 0.22 \times 10^5$	36 ± 2	0.68
170049-003	$2.3 \pm 0.11 \times 10^5$	35 ± 1	0.18
170049-004	$1.7 \pm 0.10 \times 10^5$	35 ± 1	0.01
170049-005	$3.0 \pm 0.15 \times 10^5$	35 ± 1	0.54
170049-006	$3.3 \pm 0.20 \times 10^5$	36 ± 1	< 0.01
170050-003	$2.4 \pm 0.17 \times 10^5$	35 ± 1	0.01
170050-004	$3.3 \pm 0.23 \times 10^5$	31 ± 1	<0.01
170050-005	$1.8 \pm 0.13 \times 10^5$	36 ± 1	< 0.01
170050-006	$1.9 \pm 0.19 \times 10^5$	35 ± 1	< 0.01

Table B.85: 10 channel nickel foil parameters.